In presenting the dissertation as a partial fulfillment of the requirements for an advanced degree from the Georgia Institute of Technology, I agree that the Library of the Institute shall make it available for inspection and circulation in accordance with its regulations governing materials of this type. I agree that permission to copy from, or to publish from, this dissertation may be granted by the professor under whose direction it was written, or, in his absence, by the Dean of the Graduate Division when such copying or publication is solely for scholarly purposes and does not involve potential financial gain. It is understood that any copying from, or publication of, this dissertation which involves potential financial gain will not be allowed without written permission.

3/17/65
b

THE EFFECT OF TURBULENCE IN GENERATING THREE DIMENSIONAL MEAN FLOW OF AN INCOMPRESSIBLE FLUID

A THESIS

Presented to

The Faculty of the Graduate Division

by

William Baxter Swim

In Partial Fulfillment

of the Requirements for the Degree

Doctor of Philosophy in the

School of Mechanical Engineering

Georgia Institute of Technology

June, 1966

THE EFFECT OF TURBULENCE

IN GENERATING THREE DIMENSIONAL MEAN FLOW

OF AN INCOMPRESSIBLE FLUID

Approved: R. A.

Chairman

Date approved by Chairman May 16 1966

ACKNOWLEDGMENTS

The author is indebted to many individuals who contributed to the opportunity of preparing this study and to the successful completion of it. Special thanks are due to his thesis advisor, Dr. A. W. Marris, who suggested the problem and gave council and guidance during the course of the work. The participation and interest of the thesis committee members, Dr. S. C. Barnett and Dr. Dar-Veig Ho are appreciated. The encouragement and helpfulness of Dr. K. G. Picha during the program of study is gratefully acknowledged. Thanks are due Dr. K. G. Purdy for his helpfulness with the experimental program.

Special gratitude is also due Dr. Clark A. Dunn for his encouragement and guidance in continuing the author's graduate study and to the writer's wife and children for their understanding and helpfulness during the course of the graduate program.

Finally the author is indebted to the Ford Foundation for a fellowship that made the advanced study program possible.

TABLE OF CONTENTS

TABLE OF CONTENTS (Continued)

LIST OF TABLES

LIST OF ILLUSTRATIONS

LIST OF ILLUSTRATIONS (Continued)

SUMMARY

The generation of secondary flows was investigated analytically and experimentally. The analytical portion of the study dealt with the influence of turbulence on the initiation and growth of three dimensionality in a steady time-mean flow. The experimental portion was concerned with the generation of streamwise vorticity in smooth laminar flow through a curved channel.

Available theoretical work on secondary flow generation (see Square and Winter (2), Hawthorne (3) and Marris (4)) has in general been limited to laminar flow. Brundrett and Baines (1) studied secondary flow generation in turbulent flow through a rectangular duct and presented some analytical results on the effects of turbulence in generating secondary flow, but limited to planes normal to the mean-stream direction. No analysis has yet provided information on the effects of turbulence in streamwise generation of secondary flow.

The interest in secondary flow stems from the need of further refinements in design methods and further improvements in performance of fluid machinery and fluid systems. Secondary flows, in addition to changing the stream patterns, increase the transport of momentum, heat and mass. Higher pressure drops occur due to increased frictional dissipation accompanying the additional velocity gradients produced by secondary flows. Greater fluid mixing gives rise to higher apparent thermal conductivities and mass diffusivities. Violent secondary flows also account for noise generation in many fluid systems, notably pumps,

blowers and compressors. The use of secondary flow analysis in turbomachinery design is illustrated by the work of Smith (21) and Ellis (22). They used laminar secondary flow results to explain the existence of secondary flows found experimentally in the impellers of centrifugal compressors. The understanding gained led to recommendations on design changes that ultimately should lead to improved machine performance.

The analytical study presented is developed from general vector equations, applicable to any type of continuous, single-valued solenoidal vector field. These general vector equations may have applications outside the field of fluid mechanics, such as in electric field theory. The general analysis is specialized to the turbulent flow situation by using the fact that the time mean velocity vector of turbulent flow is solenoidal. An equation is derived for the streamwise generation of streamwise vorticity in terms of the kinematics of the velocity and the vorticity fields, all on a time average basis. A similar result is also presented for the generation of a vortex directed component of velocity with displacement along a vortex line. These relations can be used to ascertain the likelihood of secondary flow generation in the presence of a specific set of kinematic conditions. As the relations are based strictly on kinematic quantities, the result is not limited to any particular type of fluid model.

Kinetic conditions are introduced into the kinematic results through the use of the time averaged Navier-Stokes equation. An expression for the generation of mean secondary vorticity along a mean streamline is developed in terms of the mean Bernoulli head, the viscous stresses and the Reynolds' stresses. It is shown that mean secondary

vorticity can be developed in a stream in the absence of a binormal gradient of the mean total head through the action of a binormal component of the vector $\nabla \cdot \underset{\approx}{\sigma}$ or a tangential component of the vector $\nabla \times (\nabla \times \underset{\approx}{\sigma})$. These terms contain the Reynolds' stresses themselves as well as their first and second spatial derivatives. The analysis also shows that secondary mean vorticity can be generated in purely rectilinear flow only if the turbulence is anisotropic.

The kinetic results for the generation of mean secondary velocity along a mean vortex line shows three factors important in the secondary velocity production: the vortex directed component of the vector $\nabla \times (\nabla \cdot \underset{\approx}{\sigma})$, the component of the Bernoulli head gradient normal to the vortex lines, and the two normal components of the vector $\nabla \cdot \underset{\approx}{\sigma}$ and the interaction of the binormal component with vortex line curvature. Isotropic turbulence is shown to influence the mean flow patterns only when vortex line curvature is present.

Use of the results obtained are illustrated by selected examples of simple flow models. Kinetic effects that contribute to the generation of secondary flow are identified for: rectilinear flow, plane circular flow, turbulent boundary layer flow, flow in a pipe bend and flow in a rectangular section curved channel.

A flow visualization study of laminar flow in a curved channel was carried out using the hydrogen bubble visualization technique. It was shown that streamwise vorticity does occur in curved channel flow with a smooth, laminar inlet stream. The vortex cells were generated in the outer portion of the channel as predicted by Reid (12), but the position and size of the cells appeared to vary. Photographic records

are presented to illustrate the type of flow patterns observed. Application of the secondary flow analysis, simplified to laminar flow, shows secondary flow generation in the center portion of the channel must be driven by effects originating at the end plates. It is suggested that vortex cells are formed in succession starting at the end plates and extending into the center of the channel. Thus, as was observed, the entire channel, from top to bottom, is filled with vortex cells.

NOMENCLATURE

Symbol		Units
$\underset{\sim}{a}$	Unit vectors in w-line system	
$\underset{\sim}{A}$	Acceleration vector	
A	Crossection area	
$\underset{\sim}{b}$	Binormal unit vector in streamline coordinate system	
C	Constant	
$\underset{\approx}{d}$	Deformation tensor	
D	Diameter of bubble generating wire	
$\mathfrak{D}$	Substantial derivative	
$\underset{\sim}{e}$	Unit vectors in vortex line or cylindrical coordinate system	
g	Acceleration due to gravity	32.2 ft/sec^2
$\underset{\sim}{g}_c$	Gravitational constant	32.2 $\frac{lbm\ ft.}{lb_f\ sec.^2}$
$\underset{\sim}{g}$	Gravity vector	
$\underset{\sim}{F}_B$	Body force vector	
h	Coordinate scale factors	
$\underset{\sim}{i}$	General unit vectors	
$\underset{\sim}{L}$	Lamb vector = $\underset{\sim}{V} \times \underset{\sim}{\Omega}$	
ℓ	Arc lengths in w-line coordinate system	
m	The absolute magnitude of $\underset{\sim}{W}$	
$\underset{\sim}{M}$	The curl of vector $\underset{\sim}{W}$	
M	Pendulum constant = g/length	
p	Pressure	
P	Arbitrary point in space	

q	Velocity magnitude
Q	Volume flow rate
r	Radius of curvature of streamline
R	General geometric radius
S	Arc lengths in m-line coordinate system
$\underset{\sim}{S}$	Unit vectors in m-line coordinate system
$\underset{\sim}{t}$	Tangential unit vector in streamline coordinate system
t	Tangential arc length in streamline coordinate system
T	Time
u_B	Blade velocity
u_T	Terminal rise velocity of hydrogen bubbles
U	Bernoulli head
$\underset{\sim}{V}'$	Instantaneous vector velocity
$\underset{\sim}{V}$	Time mean vector velocity
V	Velocity components
$\underset{\sim}{v}'$	Flucutating vector velocity
x	Arc distances along vortex line coordinate system

Greek Symbols

α	Angle measure
Γ	Circulation
δ	Edge of boundary layer
θ	Angle measure
Θ	Period of oscillation of secondary flow measured in angular displacement through a bend
κ	Curvature of vortex line
λ	Second coefficient of viscosity

μ	Absolute viscosity
ν	Kinematic viscosity
ρ	Density
$\underset{\approx}{\sigma}$	Reynolds stress tensor
σ^*	Isotropic turbulence intensity
φ	Angle measure
ω	Magnitude of vorticity
$\underset{\sim}{\Omega}$	Vector vorticity = $\nabla \times \underset{\sim}{V}$
Ω	Components of vorticity

Subscripts

0	Stagnation state
1	Tangential direction in vortex line or w-line coordinate system
2	Principal normal direction in vortex line or w-line coordinate system
3	Binormal direction in vortex lin or w-line coordinate system
t	Tangential direction in streamline coordinate system
n	Principal normal direction in streamline coordinate system
b	Binormal direction in streamline coordinate system
r	Radial direction in cylindrical coordinate system
θ	Tangential direction in cylindrical coordinate system
z	Axial direction in cylindrical coordinate system
α	Unspecified coordinate axis or component
β	Unspecified coordinate axis or component
γ	Unspecified coordinate axis or component
s	Secondary flow quantity

$(\overline{\ })$	Time average of ( ) quantity
∇	Vector differential operator $\equiv \underset{\sim}{e}_1 \frac{\partial}{\partial x_1} + \underset{\sim}{e}_2 \frac{\partial}{\partial x_2} + \underset{\sim}{e}_3 \frac{\partial}{\partial x_3}$

CHAPTER I

INTRODUCTION

Statement of Problem

Little analysis has yet been made of the influence of turbulence in the generation of three dimensional flows. Brundrett and Baines (1) studied experimentally the secondary flow generated by turbulent flow in a rectangular duct. They also proposed some theoretical considerations to support their experimental findings. Analytical study of the initiation of three dimensionality in flow (2,3,4,5), sometimes referred to as secondary flow, has largely been confined to the laminar* flow of inviscid and viscous fluids. Experimental evidence (1,6,7,8,9) shows turbulence to have a marked influence on the formation of mean secondary flows.

Secondary flow can be envisioned as a departure from the general flow situation. This concept leads to a definition of secondary flow formulated from a two part approximation of the actual flow. The first approximation, a description selected to fit the actual flow with reasonable accuracy, is called the "primary flow." The difference between this first approximation and the actual flow is defined as the "secondary flow."

Two general results will be derived analytically to show the effect of the Reynolds stresses of turbulence on the generation of secondary

---

*Present results could be interpreted as applying to instantaneous flow parameters, but this is of no practical value.

flow in a homogeneous incompressible fluid. The usefulness of these results as techniques for investigating the initiation of three dimensional flow will be demonstrated in several examples.

Method of Analysis

Three dimensional mean flow generation is characterized by the appearance of circulation about streamlines. The tendency to form the spiraling motion associated with secondary flow may be detected through two indicators. One is the flow-wise component of vorticity, which will be termed "secondary vorticity." The other is the vortex-directed component of velocity, herein called "secondary velocity."

The first part of the analysis will be concerned with developing intermediate results of a purely kinematical nature and applicable to any continuous vector field. The derivation, using vorticity as a solenoidal vector field, will then be specialized to relate the generation of secondary vorticity along a streamline to the kinematics of the flow. The expression for the spatial rate of generation of secondary vorticity will be developed in terms of the geometry of both the velocity and the vorticity fields. A similar analysis using the velocity vector will lead to the dual of the vorticity result, that is an expression for the generation of secondary velocity along a vortex line.

The motivation for keeping the kinematic derivations free from dynamic effects is stated by Truesdell in the introduction of Kinematics of Vorticity (10).

> All dynamical statements I have relegated to parenthetical sections, appendices, or footnotes, not in a foolish attempt to diminish their physical importance, but rather to let the argument course freely, uninterrupted by merely inter-

> pretative remarks, and to leave the propositions free for application to such special dynamical situations as may be of interest either now or in the future - for I cannot too strongly urge that a kinematical result is a result valid forever, no matter how time and fashion may change the "laws" of physics.

The kinematic analysis, when completed, will be combined with dynamic considerations to introduce the effects of the forces, real and apparent, on the motion. The link between the kinematic and the dynamic equations will be the Lamb vector $\underset{\sim}{L} = \underset{\sim}{V} \times \underset{\sim}{\Omega}$. The resulting kinematic-kinetic equations, which without boundary conditions, comprise an underdetermined system*; will be used to establish the necessary conditions for the generation of three dimensional flow.

This use of an underdetermined system stands in contrast to the approach of hydrodynamic stability theory. Stability theory (11, 12, 13, 14) is concerned with computing the eigen values of the boundary value problem formed by the governing equations and a complete set of boundary conditions. The kinematic-kinetic approach used in this study does not use boundary conditions directly, but rather makes interpretation based on the nature of the flow at the point in question. The boundary conditions are thus introduced indirectly, through their influence on the flow parameters, i.e., velocity profiles, Bernoulli head variations, etc.

Vector methods will be used in deriving the necessary equations, thereby keeping the general results independent of coordinate systems.

---

*The term "underdetermined system" is used here to denote that the equations are used without boundary conditions. Such a system is contrary to a differential system, i.e. one in which the equations and boundary conditions together yield a unique solution, as the undetermined system will admit a variety of solutions.

This approach will also provide a simpler analysis and greater clarity of the physical phenomena than the corresponding scalar equations. The results will be presented in intrinsic coordinates defined by the streamlines or by the vortex lines. Use of the intrinsic unit vectors; in the tangential, principal normal and binormal directions to the stream or vortex lines; facilitates interpretation and application of the results.

CHAPTER II

KINEMATICS

Background

The basic ingredients of the kinematic analysis are the velocity vector and its curl, defined as the vorticity vector. The analysis is applied at an arbitrary point P in the flow region and will yield information on the tendency towards three dimensionality of the flow in terms of the field behavior of velocity and vorticity in the neighborhood of the point P.

As mentioned earlier, one of the strengths of the kinematic analysis is its independence of dynamic effects. Maintaining this independence allows one to apply the results to any fluid and to any type of motion. Neither the choice of constitutive equation of the fluid, relating stress to rate of strain, nor the type of force fields controlling the flow, will invalidate or even alter the kinematic formulations.

Kinematic analysis applied to secondary flow had its beginning in the work of Hawthorne (3). He made only limited use of pure kinematics in studying the generation of secondary vorticity in an incompressible steady laminar flow. His early introduction of the additional stipulation of inviscid flow causes a deviation from pure kinematics and a subsequent loss of generality.

Hawthorne gives a result

$$\underset{\sim}{V} \cdot \nabla \left(\frac{\Omega_t}{q}\right) = \frac{-2[\underset{\sim}{V} \times (\underset{\sim}{V} \times \Omega)] \cdot [(\underset{\sim}{V} \cdot \nabla)\underset{\sim}{V}]}{q^4} \qquad (2.1)$$

which is applicable to any steady circulation preserving motion, a special case of which is inviscid flow. Though equation 2.1 appears as a true kinematic result, the elimination of a term containing the curl of the Lamb vector was based on the equality of the Lamb vector with the gradient of the Bernoulli head. This equality, a dynamic condition, is a general truth only for inviscid fluids as can be seen from equation 3.9. Hawthorne's work however was an improvement, from the view of kinematic generality, of the earlier work of Squire and Winter (2). Their analysis was predicated entirely on the dynamically based Helmholtz equation. This earlier work did make use of some kinematic relations, but the broad generality available was already lost.

The power and extent of the kinematic approach is illustrated by the work of Marris (4). He generalized Hawthorne's analysis by dropping the inviscid flow restriction, and obtained

$$\underset{\sim}{V} \cdot \nabla \left(\frac{\Omega_t}{q}\right) = -\frac{2}{q^4}\left[\left(\underset{\sim}{V} \times \left[\underset{\sim}{V} \times \underset{\sim}{\Omega}\right]\right) \cdot (\underset{\sim}{V} \cdot \nabla)\underset{\sim}{V}\right] - \frac{\underset{\sim}{V}}{q^2} \nabla \times (\underset{\sim}{V} \times \underset{\sim}{\Omega}) \quad (2.2)$$

applicable to any laminar incompressible flow. In a companion paper (15), Marris developed the dual to the above. Using a similar technique, he arrived at the following equation for generation of secondary velocity along a vortex line

$$\underset{\sim}{\Omega} \cdot \nabla\left(\frac{V_1}{\omega}\right) = -(\underset{\sim}{V} \times \underset{\sim}{\Omega}) \cdot \nabla \times \frac{\underset{\sim}{\Omega}}{\omega^2} + \frac{\underset{\sim}{\Omega}}{\omega^2} \cdot \nabla \times (\underset{\sim}{V} \times \underset{\sim}{\Omega}) \quad (2.3)$$

General Kinematic Derivation

It will now be shown that the kinematic analysis performed by

Hawthorne and by Marris with reference to laminar incompressible flow is part of a more general kinematic analysis applicable to any vector $\underset{\sim}{W}$. This method of analysis and result may prove to be useful in disciplines other than fluid dynamics, e.g. $\underset{\sim}{W}$ could be the electric intensity of an electrostatic field or the magnetic intensity of a magnetic field. In those situations where the intensity vector, electrostatic or magnetic, were solenoidal, that is $\nabla \cdot \underset{\sim}{W} = 0$, the theory following could be applied in a manner similar to that for incompressible flow.

The vector derivation will be carried out for any vector $\underset{\sim}{W}$, not necessarily solenoidal, to make the result applicable to compressible as well as incompressible flow. By applying the restriction $\nabla \cdot \underset{\sim}{W} = 0$, the result desired for incompressible flow can easily be obtained.

Let $\underset{\sim}{W}$ represent a vector of a continuous field and let $\underset{\sim}{M}$ be its curl, then

$$\nabla \times \underset{\sim}{W} \equiv \underset{\sim}{M} \neq 0 \tag{2.4}$$

$$\nabla \cdot \underset{\sim}{M} = \nabla \cdot (\nabla \times \underset{\sim}{W}) = 0 \tag{2.5}$$

$$|\underset{\sim}{W}| \equiv w \tag{2.6}$$

$$|\underset{\sim}{M}| \equiv m \tag{2.7}$$

The solenoidal vector $\underset{\sim}{M}$ can be resolved into two components, one along and one perpendicular to $\underset{\sim}{W}$ as illustrated in Figure 1 and presented vectorially as

$$\underset{\sim}{M} = \frac{(\underset{\sim}{M} \cdot \underset{\sim}{W})\underset{\sim}{W}}{w^2} + \frac{\underset{\sim}{W} \times (\underset{\sim}{M} \times \underset{\sim}{W})}{w^2} \tag{2.8}$$

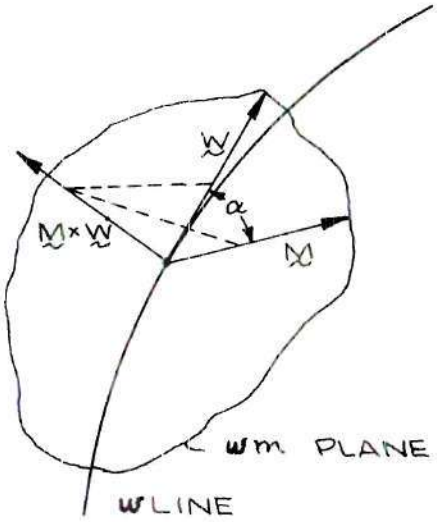

Figure 1. Resolution of Vector $\underset{\sim}{M}$.

The first term on the right is the component of $\underset{\sim}{M}$ parallel to $\underset{\sim}{W}$ as can be noted by recognizing the scalar $\underset{\sim}{M} \cdot \underset{\sim}{W}/w$ as the projection of $\underset{\sim}{M}$ onto $\underset{\sim}{W}$ and the vector $\underset{\sim}{W}/w$ as a unit vector in the direction of $\underset{\sim}{W}$. The second term can be verified as the component of $\underset{\sim}{M}$ perpendicular to $\underset{\sim}{W}$ through the definition of cross, or vector, product. $\underset{\sim}{M} \times \underset{\sim}{W}/w$ is a vector perpendicular to the plane containing both $\underset{\sim}{M}$ and $\underset{\sim}{W}$ with magnitude of $|\underset{\sim}{M}| \sin \alpha$, where α is the angle between $\underset{\sim}{M}$ and $\underset{\sim}{W}$. This vector has the desired magnitude, the projection of $\underset{\sim}{M}$ onto the normal to $\underset{\sim}{W}$ contained in the mw plane, but its direction is perpendicular to this plane. However by crossing this vector with the unit vector $\underset{\sim}{W}/w$, $\underset{\sim}{M} \times \underset{\sim}{W}/w$ is rotated 90° into the mw plane, producing the desired vector component of $\underset{\sim}{M}$. That $\underset{\sim}{W} \times (\underset{\sim}{M} \times \underset{\sim}{W})$ has the correct sense may be verified by applying the right hand rule.

The divergence of the resolution of $\underset{\sim}{M}$, equation 2.8, together with the solenoidal property of $\underset{\sim}{M}$ yields

$$\nabla \cdot \left(\frac{\underset{\sim}{M} \cdot \underset{\sim}{W}}{w^2} \underset{\sim}{W} \right) = -\nabla \cdot \left(\frac{\underset{\sim}{W} \times (\underset{\sim}{M} \times \underset{\sim}{W})}{w^2} \right) \tag{2.9}$$

Both terms in this equation can be regarded as the product of a scalar Ψ and a vector $\underset{\sim}{B}$. Application of the identity (see (16) p.114) $\nabla \cdot \psi \underset{\sim}{B} = \psi \nabla \cdot \underset{\sim}{B} + \underset{\sim}{B} \cdot \nabla \Psi$ to equation 2.9, one obtains

$$\underset{\sim}{W} \cdot \nabla \left(\frac{\underset{\sim}{M} \cdot \underset{\sim}{W}}{w^2} \right) = - \frac{\underset{\sim}{M} \cdot \underset{\sim}{W}}{w^2} \nabla \cdot \underset{\sim}{W} - \frac{1}{w^2} \nabla \cdot [\underset{\sim}{W} \times (\underset{\sim}{M} \times \underset{\sim}{W})] - [\underset{\sim}{W} \times (\underset{\sim}{M} \times \underset{\sim}{W})] \cdot \nabla \frac{1}{w^2} \tag{2.10}$$

The following intermediate steps are needed in simplifying equation 2.10 (see (16), p. 114, 115)

$$-\nabla \frac{1}{w^2} = + \frac{\nabla w^2}{w^4} = + \frac{\nabla (\underset{\sim}{W} \cdot \underset{\sim}{W})}{w^4} \tag{2.11}$$

$$\frac{\nabla (\underset{\sim}{W} \cdot \underset{\sim}{W})}{w^4} = \frac{2[\underset{\sim}{W} \cdot \nabla \underset{\sim}{W} + \underset{\sim}{W} \times (\nabla \times \underset{\sim}{W})]}{w^4} = \frac{2(\underset{\sim}{W} \cdot \nabla \underset{\sim}{W} + \underset{\sim}{W} \times \underset{\sim}{M})}{w^4} \tag{2.12}$$

$$-\nabla \cdot [\underset{\sim}{W} \times (\underset{\sim}{M} \times \underset{\sim}{W})] = -(\underset{\sim}{M} \times \underset{\sim}{W}) \cdot (\nabla \times \underset{\sim}{W}) + \underset{\sim}{W} \cdot \nabla \times (\underset{\sim}{M} \times \underset{\sim}{W}) \tag{2.13}$$

$$-\nabla \cdot [\underset{\sim}{W} \times (\underset{\sim}{M} \times \underset{\sim}{W})] = -(\underset{\sim}{M} \times \underset{\sim}{W}) \cdot \underset{\sim}{M} + \underset{\sim}{W} \cdot \nabla \times (\underset{\sim}{M} \times \underset{\sim}{W}) = \underset{\sim}{W} \cdot \nabla \times (\underset{\sim}{M} \times \underset{\sim}{W}) \tag{2.14}$$

Using the intermediate steps outlined above and with M_1 defined as the component of $\underset{\sim}{M}$ along $\underset{\sim}{W}$, equation 2.10 can be put into the form

$$\underset{\sim}{W} \cdot \nabla \left(\frac{M_1}{w} \right) = \frac{-M_1}{w} \nabla \cdot \underset{\sim}{W} + \frac{1}{w^2} \underset{\sim}{W} \cdot \nabla \times (\underset{\sim}{M} \times \underset{\sim}{W}) + \frac{2}{w^4} [\underset{\sim}{W} \times (\underset{\sim}{M} \times \underset{\sim}{W}) \cdot (\underset{\sim}{W} \cdot \nabla) \underset{\sim}{W}] + \frac{2}{w^4} [\underset{\sim}{W} \times (\underset{\sim}{M} \times \underset{\sim}{W}) \cdot (\underset{\sim}{W} \times \underset{\sim}{M})] \tag{2.15}$$

The last term on the right is zero as it is a scalar, or box, product contains 2 parallel vectors, $(\underset{\sim}{M} \times \underset{\sim}{W})$ and $(\underset{\sim}{W} \times \underset{\sim}{M})$. Dropping this term and effecting a sign change by changing the order in the vector product $(\underset{\sim}{M} \times \underset{\sim}{W})$, i.e. $\underset{\sim}{M} \times \underset{\sim}{W} = - \underset{\sim}{W} \times \underset{\sim}{M}$ equation 2.15 becomes

$$- \underset{\sim}{W} \cdot \nabla\left(\frac{M_1}{w}\right) = - \frac{M_1}{w} \nabla \cdot \underset{\sim}{W} + \frac{1}{w^2} \underset{\sim}{W} \cdot \nabla \times (\underset{\sim}{W} \times \underset{\sim}{M})$$

$$+ \frac{2}{w^4} [\underset{\sim}{W} \times (\underset{\sim}{W} \times \underset{\sim}{M}) \cdot (\underset{\sim}{W} \cdot \nabla)\underset{\sim}{W}] \qquad (2.16)$$

The equation above is a general kinematic result that can be applied to compressible as well as incompressible flow. Restricting the $\underset{\sim}{W}$ field to being solenoidal, analogous to introducing fluid incompressibility in steady flow, equation 2.16 simplifies to

$$- \underset{\sim}{W} \cdot \nabla\left(\frac{M_1}{w}\right) = \frac{1}{w^2} \underset{\sim}{W} \cdot \nabla \times (\underset{\sim}{W} \times \underset{\sim}{M}) + \frac{2}{w^4} [\underset{\sim}{W} \times (\underset{\sim}{W} \times \underset{\sim}{M}) \cdot (\underset{\sim}{W} \cdot \nabla)\underset{\sim}{W}] \qquad (2.17)$$

Comparison of this kinematic result with equation 2.2, derived by Marris (4) for steady laminar flow of an incompressible fluid, reveals the identical nature of these equations. The only restriction used in 2.17 is that the vector $\underset{\sim}{W}$ be solenoidal, so this result can be applied to vectors meeting this one requirement. Equation 2.16 can be applied to any continuous vector field. Since the time mean velocity vector of turbulent flow is solenoidal, as will be shown later, equation 2.17 will be utilized in the secondary vorticity derivation of turbulent flow.

A further general reduction of 2.17 may be obtained by introducing the intrinsic coordinates of the w-lines, lines tangent to the $\underset{\sim}{W}$

vector throughout the field. The tangential, principal normal and binormal directions of these w-lines will be designated by the unit vectors $\underset{\sim}{a}_1$, $\underset{\sim}{a}_2$, and $\underset{\sim}{a}_3$ respectively. The arc distances in these directions will be denoted by ℓ_1, ℓ_2 and ℓ_3. Using this notation

$$\underset{\sim}{W} \cdot \nabla\left(\frac{\underset{\sim}{M} \cdot \underset{\sim}{W}}{W^2}\right) = \underset{\sim}{W} \cdot \nabla\left(\frac{M_1}{w}\right) = w \frac{\partial}{\partial \ell_1}\left(\frac{M_1}{w}\right) \tag{2.18}$$

Equation 2.17 can now be put in the alternate form

$$\frac{\partial}{\partial \ell_1}\left(\frac{M_1}{w}\right) = -\frac{1}{w^2}\,\underset{\sim}{a}_1 \cdot \nabla \times (\underset{\sim}{W} \times \underset{\sim}{M}) - \frac{2}{w^5}\left[\underset{\sim}{W} \times (\underset{\sim}{W} \times \underset{\sim}{M}) \cdot (\underset{\sim}{W} \cdot \nabla)\underset{\sim}{W}\right] \tag{2.19}$$

This equation expresses the spatial rate of change of the ratio of the $\underset{\sim}{W}$ directed component of $\underset{\sim}{M}$ to the magnitude of $\underset{\sim}{W}$ with displacement along the w-line. Two terms are seen to influence the spatial growth of this ratio, both of which involve the geometry of the composite vector field formed by the cross product of $\underset{\sim}{W}$ with its curl.

A result analogous to equation 2.19 can be obtained through the interchange of role of $\underset{\sim}{M}$ and $\underset{\sim}{W}$ in the preceding development. This alternate development will be used in the secondary velocity analysis of Chapter II. A one to one interchange of symbols in equation 2.19 is not possible as the simplification $\nabla \times \underset{\sim}{W} = \underset{\sim}{M}$ used above will not now be available, i.e. $\nabla \times \underset{\sim}{M} \neq \underset{\sim}{W}$. The comparable result, as shown in Appendix A, is

$$\frac{\partial}{\partial S_1}\left(\frac{W_1}{m}\right) = \frac{1}{m}\left[\frac{\underset{\sim}{S}_1 \cdot \nabla \times (\underset{\sim}{W} \times \underset{\sim}{M})}{m} - (\underset{\sim}{W} \times \underset{\sim}{M}) \cdot \nabla \times \left(\frac{\underset{\sim}{M}}{m^2}\right)\right] \tag{2.20}$$

Equation 2.20 can rearranged using the following kinematic results:

$$\nabla \times \left(\frac{\underset{\sim}{M}}{m^2}\right) = \frac{1}{m^2} \underset{\sim}{S}_1 \times \nabla m + \frac{1}{m} \nabla \times \underset{\sim}{S}_1 \tag{2.21}$$

and, from Truesdell (10),

$$\nabla \times \underset{\sim}{S}_1 = (\underset{\sim}{S}_1 \cdot \nabla \times \underset{\sim}{S}_1)\underset{\sim}{S}_1 + \kappa \underset{\sim}{S}_3 \tag{2.22}$$

together with

$$(\underset{\sim}{W} \times \underset{\sim}{M}) \cdot \underset{\sim}{S}_1 = 0 \tag{2.23}$$

and

$$\underset{\sim}{S}_1 \times \nabla = \underset{\sim}{S}_3 \frac{\partial}{\partial S_2} - \underset{\sim}{S}_2 \frac{\partial}{\partial S_3} \tag{2.24}$$

In the above κ is the curvature of the $\underset{\sim}{M}$ vector line, $\underset{\sim}{S}_1$, $\underset{\sim}{S}_2$, $\underset{\sim}{S}_3$ is the right handed system of unit vectors in the tangential, principal normal and binormal directions to the m-lines and S_1, S_2, S_3, are the arc distances in these directions. Using the simplifications above, the second general kinematic result becomes

$$\frac{\partial}{\partial S_1}\left(\frac{W_1}{m}\right) = \frac{1}{m^3}\left[m\underset{\sim}{S}_1 \cdot \nabla \times (\underset{\sim}{W} \times \underset{\sim}{M}) - \left(\frac{\partial m}{\partial S_2} + m\kappa\right) \underset{\sim}{S}_3 \cdot (\underset{\sim}{W} \times \underset{\sim}{M}) \right.$$

$$\left. + \frac{\partial m}{\partial S_3} \underset{\sim}{S}_2 \cdot (\underset{\sim}{W} \times \underset{\sim}{M}) \right] \tag{2.25}$$

This identity expresses the growth of the $\underset{\sim}{M}$ directed component of $\underset{\sim}{W}$ with displacement along the m vector line in terms of the geometries of both the $\underset{\sim}{W}$ and $\underset{\sim}{M}$ fields.

Further vector manipulations could be carried out on equations

2.19 and 2.25, but no improvement would be obtained with respect to the problem at hand, that is describing the generation of secondary currents in a turbulent fluid stream. It is with the flow problem in mind that leads one to preserve the vector form $\underset{\sim}{W} \times \underset{\sim}{M}$. This vector is analogous to the Lamb vector, $\underset{\sim}{V} \times \underset{\sim}{\Omega}$, which will provide a convenient means of introducing kinetic effects into the kinematic results.

Secondary Vorticity Analysis

The kinematic generalization of Marris, equation 2.2, which includes, as special cases the results of the other workers, applies only to laminar flow or to the instantaneous flow parameters of turbulent flow. Though this result, and similar ones, has had extensive application to laminar flow, it has not, nor can it be successfully applied to turbulent flow. These existing methods become unmanageable for turbulent flow due to the random variation of the flow parameters with time. Averaging the flow parameters over time and introducing the Reynolds stresses into the kinematic generalization will lead to useful new results.

The instantaneous flow parameters of a turbulent flow field can be expressed as the sum of a time average component and a fluctuating component. For the vector velocity, this sum may be expressed as

$$\underset{\sim}{V}' = \underset{\sim}{V} + \underset{\sim}{v}' \qquad (2.26)$$

The notation used here departs from customary practice for convenience in this work. Primed upper case letters will be used herein to represent instantaneous parameters while the corresponding unprimed upper case

letters will denote time averaged parameters. The primed lower case letter v' will be used for the fluctuating velocity. Using this notation, the time average velocity $\underset{\sim}{V}$, defined in the usual manner, is

$$\underset{\sim}{V} = \frac{1}{\Delta T}\int_{T_o}^{T_o+\Delta T} \underset{\sim}{V}'(T)\, dT \tag{2.27}$$

where the time interval, ΔT, of the averaging process is taken to be large compared to the time scale of turbulence.

Restricting the analysis to incompressible fluids and applying the time average to the instantaneous continuity equation yields

$$\overline{\rho\nabla \cdot \underset{\sim}{V}'} = \rho\overline{\nabla \cdot (\underset{\sim}{V}+\underset{\sim}{v}')} = \rho(\overline{\nabla \cdot \underset{\sim}{V}}+\overline{\nabla \cdot \underset{\sim}{v}'}) = 0 \tag{2.28}$$

Since the time average of the fluctuating component is, by definition, zero ($\overline{\underset{\sim}{v}'} \equiv 0$),

$$\overline{\nabla \cdot \underset{\sim}{v}'} = \nabla \cdot \overline{\underset{\sim}{v}}' = 0 \tag{2.29}$$

The above equation shows that conservation of mass must be satisfied on the time average as well as instantaneously, and, equally important to this analysis, that the time average velocity vector is solenoidal.

$$\nabla \cdot \underset{\sim}{V} = 0 \tag{2.30}$$

Due to this solenoidal nature of the time mean velocity vector for a turbulent flow field, the kinematic results of the previous section apply without any restriction. $\underset{\sim}{V}$ is used in place of $\underset{\sim}{W}$ in equation 2.19 and it follows that $\underset{\sim}{\Omega}$ must replace $\underset{\sim}{M}$. The general kinematic result for secondary vorticity becomes

$$q \frac{\partial}{\partial t} \left(\frac{\Omega_t}{q}\right) = -\frac{1}{q^2} \underset{\sim}{V} \cdot \nabla \times (\underset{\sim}{V} \times \underset{\sim}{\Omega}) - \frac{2}{q^4} [\underset{\sim}{V} \times (\underset{\sim}{V} \times \underset{\sim}{\Omega}) \cdot (\underset{\sim}{V} \cdot \nabla) \underset{\sim}{V}] \qquad (2.31)$$

The curl of the time average velocity vector, symbolized by

$$\underset{\sim}{\Omega} = \nabla \times \underset{\sim}{V} \qquad (2.32)$$

is the time average vector vorticity. This same form for the time average vorticity is obtained by taking the time average of the equation defining the instantaneous vorticity

$$\underset{\sim}{\Omega}' = \nabla \times \underset{\sim}{V}' = \nabla \times (\underset{\sim}{V} + \underset{\sim}{v}') \qquad (2.33)$$

The usefulness of equation 2.31 stems from the physical interpretation of the derivative of the ratio Ω_t/q, along a streamline as the circulation around a stream tube. The basis of this interpretation as outlined by Hawthorne (3) for laminar flow and equally true for turbulent flow, is as follows: given an elemental stream tube of cross-section A, with a circulation Γ about it and carrying a mass flow rate ρQ. Since the mass flow rate is constant at all points along a stream tube, the volume flow rate Q will also be constant for an incompressible fluid. Thus

$$\frac{\partial}{\partial t} \left(\frac{\Gamma}{Q}\right) = \frac{1}{Q} \frac{\partial}{\partial t} (\Gamma) \qquad (2.34)$$

Substituting $\Omega_t A$ for Γ and qA for Q gives

$$\frac{1}{Q} \frac{\partial \Gamma}{\partial t} = \frac{\partial}{\partial t} \left(\frac{\Omega_t}{q}\right) \qquad (2.35)$$

The rate of increase of Ω_t/q, the ratio of the flow directed

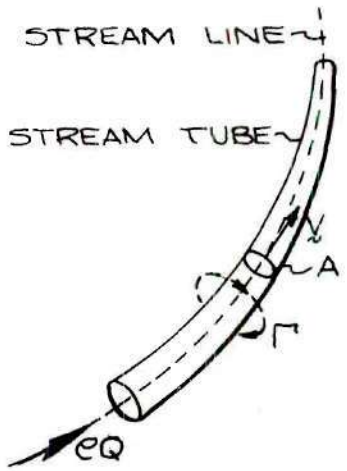

Figure 2. Element of a Stream Tube.

component of vorticity to the local velocity, is directly proportional to the rate of increase of circulation about the stream tube. The velocity in the denominator has the effect of "normalizing" the streamwise vorticity to a reference area, thus eliminating the streamtube flow area effect in determining the net rate of increase in secondary vorticity along the tube.

The general kinematic result of equation 2.31 sets forth the generation of streamwise vorticity, or circulation about a stream tube, with displacement along a streamline in terms of the nature of both the velocity and the vorticity fields. The terms on the right can be rearranged for easier interpretation.

The first term on the right of equation 2.31 can be reduced by noting $\underset{\sim}{V} = q\underset{\sim}{t}$, thus this term is rewritten as

$$- \frac{1}{q^2} \underset{\sim}{V} \cdot \nabla \times (\underset{\sim}{V} \times \underset{\sim}{\Omega}) = - \frac{\underset{\sim}{t}}{q} \cdot \nabla \times (\underset{\sim}{V} \times \underset{\sim}{\Omega}) \qquad (2.36)$$

The second term on the right side of equation 2.31 can be simplified first by recognizing $(\underset{\sim}{V} \cdot \nabla)\ \underset{\sim}{V}$ as the steady state acceleration vector and second by resolving this vector into two components, one along and one normal to the streamlines. Thus for steady flow

$$(\underset{\sim}{V} \cdot \nabla \underset{\sim}{V}) = \frac{d}{dt} \underset{\sim}{V} = \underset{\sim}{A} \qquad (2.37)$$

and

$$\underset{\sim}{A} = A_t \underset{\sim}{t} + A_n \underset{\sim}{n} \qquad (2.38)$$

Substituting the resolved form of the spatial acceleration into the second right-hand term of equation 2.31 yields

$$\frac{2}{q^4} [\underset{\sim}{V} \times (\underset{\sim}{V} \times \underset{\sim}{\Omega}) \cdot \{(\underset{\sim}{V} \cdot \nabla)\underset{\sim}{V}\}] = \frac{2}{q^4} [\underset{\sim}{V} \times (\underset{\sim}{V} \times \underset{\sim}{\Omega}) \cdot A_n \underset{\sim}{n}] \qquad (2.39)$$

The tangential acceleration component term is eliminated as the box product $\underset{\sim}{V} \times (\underset{\sim}{V} \times \underset{\sim}{\Omega}) \cdot A_t \underset{\sim}{t}$ is zero since $\underset{\sim}{V}$ and $\underset{\sim}{t}$ are parallel vectors.

The magnitude of the normal or centripetal component of acceleration is q^2/r, where r is the local radius of curvature of the streamline at the point in question. Using these simplifications of the right hand side, equation 2.31 may be rewritten as

$$q \frac{\partial}{\partial t} \left(\frac{\Omega_t}{q}\right) = - \frac{\underset{\sim}{t}}{q} \cdot \nabla \times (\underset{\sim}{V} \times \underset{\sim}{\Omega}) - \frac{2}{rq^2} \underset{\sim}{n} \cdot \underset{\sim}{V} \times (\underset{\sim}{V} \times \underset{\sim}{\Omega}) \qquad (2.40)$$

Interchanging the dot and cross in the box product of the equation above allows a further simplification.

$$-\frac{2}{q^2 r}\,\underset{\sim}{n}\cdot\underset{\sim}{V}\times(\underset{\sim}{V}\times\underset{\sim}{\Omega})=\frac{-2}{q^2 r}\,\underset{\sim}{n}\times\underset{\sim}{V}\cdot(\underset{\sim}{V}\times\underset{\sim}{\Omega})=-\frac{2}{qr}\,\underset{\sim}{n}\times\underset{\sim}{t}\cdot(\underset{\sim}{V}\times\underset{\sim}{\Omega}) \quad (2.41)$$

Since $\underset{\sim}{t}$, $\underset{\sim}{n}$ and $\underset{\sim}{b}$ form a right hand triad,

$$\underset{\sim}{n}\times\underset{\sim}{t}=-\underset{\sim}{b} \quad (2.42)$$

equation 2.40 may now be rewritten as

$$\frac{\partial}{\partial t}\left(\frac{\Omega_t}{q}\right)=-\frac{\underset{\sim}{t}\cdot\nabla\times(\underset{\sim}{L})}{q^2}+\frac{2\underset{\sim}{b}\cdot\underset{\sim}{L}}{q^2 r} \quad (2.43)$$

The rate of increase of secondary circulation, Ω_t/q with displacement along a streamline is now seen to be dependent on the geometry of the field defined by the Lamb vector L, in particular the streamwise component of the curl of the Lamb vector, $\underset{\sim}{t}\cdot\nabla\times\underset{\sim}{L}/q^2$ term; and the binormal component of the Lamb vector from the $\underset{\sim}{b}\cdot\underset{\sim}{L}$ term. This binormal component of the Lamb vector term can now be reduced to the apparently simpler expression

$$\frac{2}{q^2 r}\,\underset{\sim}{b}\cdot(\underset{\sim}{V}\times\underset{\sim}{\Omega})=\frac{2}{qr}\,\underset{\sim}{n}\cdot\underset{\sim}{\Omega}=\frac{2\Omega_n}{qr} \quad (2.44)$$

However this reduction is not fruitful for the present purpose since it destroys the Lamb vector, the link to be used to the dynamic equations. Other simplifications might also be possible, however the form above seems to be the most advantageous for the present use. When no

direct introduction of dynamics is intended, reduced forms of equation 2.43 may prove useful.

The general result, given in equation 2.43 is restricted by only two assumptions:

1) The fluid is incompressible, and

2) the motion is steady with respect to the time average.

In its present form, this result is applicable to any incompressible fluid, no matter what form its constitutive equation may take.

Secondary Velocity Analysis

An analogous geometric result can be obtained for secondary velocity generation along a vortex line from the general relations obtained for a solenoidal vector. This second kinematic result, similar in form to equation 2.31, will give the spatial rate of generation of the ratio - the tangential component of the mean velocity to the magnitude of the mean vorticity - with displacement along the vortex line.

The ratio V_1/ω can be interpreted as the secondary flow, i.e. the flow associated with the vortex component of the mean velocity. To illustrate this interpretation, the vortex component of the velocity can be expressed as

$$V_1 = Q_s/A \tag{2.45}$$

the ratio of the secondary volume flow rate Q_s to the cross-sectional area A of a vortex tube or filament. The magnitude of the vorticity is related to the constant circulation, Γ about the vortex tube by

$$\omega = \Gamma/A \tag{2.46}$$

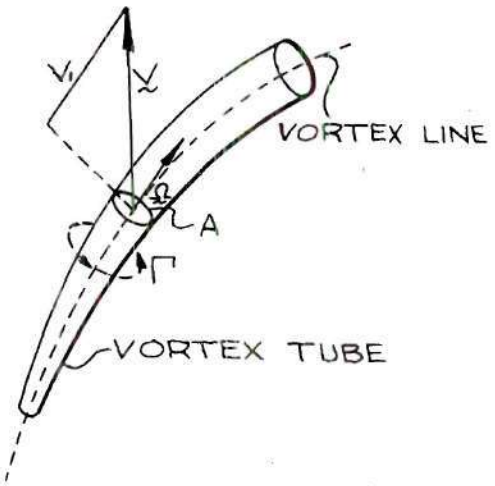

Figure 3. Element of a Vortex Tube.

The ratio $\frac{V_1}{\omega}$ becomes

$$\frac{V_1}{\omega} = \frac{Q_s}{\Gamma} \propto Q_s \tag{2.47}$$

which shows V_1/ω is directly proportional to the magnitude of the secondary flow rate. This interpretation was prompted by Hawthorne's use of secondary circulation to replace the ratio Ω_t/q. To the writer's knowledge the secondary flow rate interpretation has not been previously presented.

The second general kinematic result, equation 2.25 provides the vehicle to determine the expression for the generation of secondary flow. Replacing $\underset{\sim}{M}$ by the vorticity vector $\underset{\sim}{\Omega}$ requires $\underset{\sim}{W}$ to be replaced by $\underset{\sim}{V}$. Making these changes in equation 2.25, one obtains

$$\frac{\partial}{\partial x_1}\left(\frac{V_1}{\omega}\right) = \frac{1}{\omega^3}\left[\omega \underset{\sim}{e}_1 \cdot \nabla \times (\underset{\sim}{V} \times \underset{\sim}{\Omega}) - \left(\frac{\partial \omega}{\partial x_2} + \omega K\right) \underset{\sim}{e}_3 \cdot (\underset{\sim}{V} \times \underset{\sim}{\Omega}) + \frac{\partial \omega}{\partial x_3} \underset{\sim}{e}_2 \cdot (\underset{\sim}{V} \times \underset{\sim}{\Omega})\right] \qquad (2.48)$$

This result expresses the rate of growth of mean secondary flow with displacement along a vortex line in terms of:

1. The interaction of the mean Lamb vector with the two $\underset{\sim}{e}_1$ components of the vorticity gradient,*

2. the interaction of the mean Lamb vector with the curvature of the vortex lines, and

3. the vortex directed component of the curl of the Lamb vector.

Equation 2.48, applicable to incompressible steady-time-mean turbulent flow, can be reduced to the same form Marris (15) obtained for laminar flow.

The above geometrical result has only the same two restrictions that apply to the secondary circulation result, i.e.

1. The fluid is incompressible, and

2. the motion is steady on the time average.

Also, like the secondary circulation result, equation 2.48 can be applied to any type of incompressible fluid, without regard to the form of the fluid's constitutive equation.

Both these general results, derived on the basis of kinematics

---

*The $\underset{\sim}{e}_1$ components of the vorticity gradient are obtained from

$$\underset{\sim}{e}_1 \times \nabla\omega = \underset{\sim}{e}_3 \frac{\partial \omega}{\partial x_2} - \underset{\sim}{e}_2 \frac{\partial \omega}{\partial x_3}$$

alone, will be combined with dynamic considerations in Chapter III to obtain more useful results, but applicable only to a particular fluid model, that is a Newtonian fluid.

Special Cases

Portions of the above outlined analysis, but applied only to laminar flow have appeared frequently in the published literature, notably in the work of Squire and Winter (2), Hawthorne (3, 18, 19) and Marris (4, 15, 17, 20), as well as in the work of Scorer and Wilson (5), A. G. Smith (21) and Ellis (22).

Squire and Winter were among the earlier workers to employ a quasi-kinematic analysis to secondary flow. They dealt with the generation of secondary flow - occurring in turning vane passages - created by velocity gradient in the spanwise direction and presented usable results. However, though they used some kinematic manipulations, from the view of kinematic generality it was unfortunate that the starting point was a dynamic equation, Helmholtz's equation of motion. The simplification $\nabla \times (\underset{\sim}{L}) = 0$ for an inviscid, incompressible fluid, was also utilized.

Hawthorne's work was more general than that of Squire and Winter, and it contained their result as a special case. Hawthorne used geometrical conditions, similar to the approach used in this study, to develop a result for the generation of secondary circulation in terms of the flowwise component of the vorticity vector. His work is applicable to an incompressible, quasi-inviscid model. The term "quasi-inviscid" is used here to convey the use of the inviscid equations of motion together with

the actual velocity fields created by viscous action, i.e. a linear velocity gradient produced by viscous forces or by screens inserted in the flow. In terms of the notation used in this paper, Hawthorne's "kinematic" result can be stated as

$$\frac{\partial}{\partial t}\left(\frac{\Omega_t}{q}\right) = 2\,\frac{\Omega_n}{qr} \tag{2.49}$$

This same result can be obtained from the vector equation 2.19 if the equivalent of the inviscid flow restriction, a dynamic consideration, is applied. An easier comparison, however, can be made from the turbulent flow result since both the laminar flow velocity and the time-mean turbulent flow velocity are solenoidal and both are similarly related to the kinematics of their particular flow fields. Thus, the result of this analysis, applying the restriction curl $\underset{\sim}{L} = 0$ to equation 2.43 is

$$\frac{\partial}{\partial t}\left(\frac{\Omega_t}{q}\right) = \frac{2\underset{\sim}{b} \cdot \underset{\sim}{L}}{q^2 r} \tag{2.50}$$

which reduces directly to Hawthorne's result through the use of equation 2.44. Hawthorne's result is actually only semi-kinematic since the simplification $\nabla \times \underset{\sim}{L} = 0$ was based on equating grad U with $\underset{\sim}{L}$, a dynamical consideration.

Marris (4,15) generalized and extended Hawthorne's result for laminar flow while pointing out the utility of keeping the kinematic analysis separate from kinetic considerations. In the first paper, Marris applied Hawthorne's analysis to viscous flow, which required

retaining the term $\nabla \times \underset{\sim}{L}$. His result, applicable to laminar flow, is

$$\frac{\partial}{\partial t}\left(\frac{\Omega_t}{q}\right) = \frac{2\Omega_b}{q^2 r} - \frac{\underset{\sim}{t} \cdot \nabla \times (\underset{\sim}{V} \times \underset{\sim}{\Omega})}{q^2} \qquad (2.51)$$

This equation, containing Hawthorne's result and the added term containing the viscous effect $\underset{\sim}{t} \cdot \nabla \times \underset{\sim}{L}$, can also be obtained from the result derived on the basis of the solenoidal vector $\underset{\sim}{W}$. As pointed out by Marris, the admission of viscosity relaxes Hawthorne's restriction that a binormal gradient of total head, p_o, is the only influence on the generation of secondary vorticity.

Marris (15) applied a similar kinematic approach to secondary flow analysis in laminar flow in which the velocity vector was resolved instead of the vorticity vector. An expression was developed for the generation of the vortex directed component of velocity with displacement along a vortex line. For steady incompressible laminar flow, it was shown that

$$\frac{\partial}{\partial x_1}\left(\frac{V_1}{\omega}\right) = -\frac{1}{\omega}\left[(\underset{\sim}{V} \times \underset{\sim}{\Omega}) \cdot \nabla \times \frac{\underset{\sim}{\Omega}}{\omega^2} - \frac{\underset{\sim}{\Omega}}{\omega^2} \cdot \nabla \times (\underset{\sim}{V} \times \underset{\sim}{\Omega})\right] \qquad (2.52)$$

The general vector derivation, equation 2.20 also yields this same result.

Scorer and Wilson (5) developed an inviscid but compressible form of Hawthorne's analysis (3). Starting from Eulers equation, their analysis lead to the equation

$$\frac{\partial}{\partial t}\left(\frac{\Omega_t}{q}\right) = \frac{2\Omega_n}{qr} + \frac{K}{\rho}\,\underset{\sim}{t} \times \text{grad}\,\rho \cdot \underset{\sim}{g} - \frac{\Omega_t}{q}\nabla \cdot \underset{\sim}{V} \qquad (2.53)$$

This equation was used to illustrate the secondary flow generation due to curved streamlines in a steady stratified - density decreasing with elevation - inviscid fluid. They predicted the onset of Gŏrtler type instability when atmospheric air streams are bent by flow over an obstacle such as a mountain range. This secondary flow phenomenon was offered as one cause of "clear-air turbulence" in mountain waves.

Application of the kinematic analysis to laminar secondary flow in centrifugal compressors has been made by A. G. Smith (21) and G. O. Ellis (22). It was shown that $I(=p + \frac{1}{2}\rho q^2 - \frac{1}{2}\rho u_B^2)$ plays the same role in generation of secondary circulation in rotating passages as p_o, the total pressure, does in a stationary passage. Both I and p_o come from the $\underset{\sim}{b} \cdot \underset{\sim}{L}$ term of equation 2.43 specialized for application to an inviscid fluid. Radial flow passages were shown to produce secondary circulation without the necessity of passage curvature. Ellis demonstrates that the existence of a large secondary flow eddy found experimentally in the flow passage near the tip of a centrifugal compressor impeller - can be understood through an analysis similar to Hawthorne's. The secondary flow is explained by reference to the existence of an energy gradient between the hub and shroud.

Other applications of the laminar flow results have been made, but to date no published work provides the basis for dealing with turbulent flow as the references cited do for laminar flow. Brundrett and Baines (1) have performed a limited analytical study of secondary flow generation by Reynolds stresses to complement an extensive experimental study. In their analysis, the curl of the Navier-Stokes equation for mean quantities was used to develop a relation between streamwise vorticity and

Reynolds stresses. In the notation of this study, their expression is

$$\rho\left(V_n \frac{\partial \Omega_t}{\partial n} + V_b \frac{\partial \Omega_t}{\partial b}\right) = \frac{\partial^2}{\partial n \partial b}\left(\rho\sigma_{nn} - \rho\sigma_{bb}\right) - \left(\frac{\partial^2}{\partial b^2} - \frac{\partial^2}{\partial n^2}\right)\rho\sigma_{nb} + \mu\left(\frac{\partial^2 \Omega_t}{\partial n^2} + \frac{\partial^2 \Omega_t}{\partial b^2}\right) \qquad (2.54)$$

This equation relates the rate of growth of streamwise vorticity along a secondary streamline to transverse gradients of the Reynolds stress components. The principal normal and binormal derivatives of Ω_t in equation 2.54 limit the application of this result to planes perpendicular to the mean flow direction. It is not possible to follow the flow-wise development of secondary flow using this expression.

The influence of the Reynolds stresses in producing streamwise generation of secondary flow has only been inferred to date. Chapter III will develop the required relations needed to analyze the mean secondary flow generation due to the presence of turbulence.

CHAPTER III

KINETICS

Use of Reynolds Equations to Express Lamb Vector

The full utilization of the kinematic results obtained in Chapter II requires the kinematics to be combined with dynamical considerations. In this manner, the influences of surface and body forces - both real and apparent - on the time mean motion of fluids can be ascertained. As stated previously, the development to this point is restricted only by the assumptions of incompressibility and time average steadiness, so no a priori restrictions are placed on the fluid model to be used in the equations of motion. The Lamb vector $\underset{\sim}{L}$ provides the bridge between the kinematics and the kinetics as both equations will yield an expression for $\underset{\sim}{V} \times \underset{\sim}{\Omega}$. Eliminating $\underset{\sim}{V} \times \underset{\sim}{\Omega}$ between them will thus provide the desired relation between the steady motion of a fluid particle and the force fields acting on the flow.

To obtain the dynamical expression for the Lamb vector, one may start with the general dynamical equation resulting from Newton's second law of motion. This equation, expressing the acceleration of an element of fluid in terms of the stresses acting on it, may be written as

$$\rho \frac{D\underset{\sim}{V}'}{DT} = \nabla \cdot \underset{\approx}{\tau} + \underset{\sim}{F}_B \qquad (3.1)$$

Several manipulations must be made on this equation to obtain the results desired. The stress tensor $\underset{\approx}{\tau}$ must be expressed in terms of

the deformation tensor $\underset{\approx}{d}\left(=\frac{\nabla\underset{\sim}{V}+\nabla\underset{\sim}{V}^{T}}{2}\right)$. The functional relation between these two tensors

$$\underset{\approx}{\tau} = f(\underset{\approx}{d}) \tag{3.2}$$

is called the constitutive equation of the fluid. Continuum mechanics - see Eringen (23) - affirms through Stokes hypothesis that $\underset{\approx}{\tau}$ can always be expressed in terms of the second and lower powers of $\underset{\approx}{d}$. However for most applications a linear relation between stress and deformation is sufficient. Using this simplification and introducing the Newtonian fluid assumption

$$\lambda = -2/3\,\mu \tag{3.3}$$

leads to the Navier-Stokes equations of motion.

$$\rho\frac{D\underset{\sim}{V}'}{DT} = -\nabla p' + \nabla\cdot\mu\nabla\underset{\sim}{V}' + \nabla\frac{\mu}{3}(\nabla\cdot\underset{\sim}{V}') - \nabla\left(\frac{\varphi'}{\rho^{-1}}\right) \tag{3.4}$$

Upon assumption of constant viscosity, incompressibility, and steady flow, this equation reduces

$$\underset{\sim}{V}'\cdot\nabla\underset{\sim}{V}' = -\nabla\left(\frac{p'}{\rho}+\varphi'\right) + \nu\nabla^{2}\underset{\sim}{V}' \tag{3.5}$$

Since

$$\underset{\sim}{V}'\cdot\nabla\underset{\sim}{V}' = \frac{\nabla\,\underset{\sim}{V}'\cdot\underset{\sim}{V}'}{2} - \underset{\sim}{V}'\times(\nabla\times\underset{\sim}{V}') \tag{3.6}$$

the equation of motion yields for the instantaneous Lamb vector

$$\underset{\sim}{V}' \times \underset{\approx}{\Omega}' = \nabla\left(\frac{p'}{\rho} + \varphi' + \frac{q'^2}{2}\right) - \nu \nabla^2 \underset{\sim}{V}' \tag{3.7}$$

In terms of the Bernoulli head,

$$U' = \frac{p'}{\rho} + \frac{q'^2}{2} + \varphi' \tag{3.8}$$

this expression is

$$\underset{\sim}{V}' \times \underset{\approx}{\Omega}' = \nabla U' - \nu \nabla^2 \underset{\sim}{V}' \tag{3.9}$$

Replacing the instantaneous flow parameters with the sum of the time average plus the fluctuating component and reducing, we get

$$\underset{\sim}{V} \times \underset{\approx}{\Omega} = \nabla U - \nabla \cdot \underset{\approx}{\sigma} - \nu \nabla^2 \underset{\sim}{V} \tag{3.10}$$

The symmetric dyad $\underset{\approx}{\sigma}$ of the Reynolds stresses can be represented as

$$\sigma = -\left[\begin{array}{l} \overline{v_t' v_t'}\ \underset{\sim}{t}\,\underset{\sim}{t} + \overline{v_t' v_n'}\ \underset{\sim}{t}\,\underset{\sim}{n} + \overline{v_t' v_b'}\ \underset{\sim}{t}\,\underset{\sim}{b} \\ + \overline{v_n' v_t'}\ \underset{\sim}{n}\,\underset{\sim}{t} + \overline{v_n' v_n'}\ \underset{\sim}{n}\,\underset{\sim}{n} + \overline{v_n' v_b'}\ \underset{\sim}{n}\,\underset{\sim}{b} \\ + \overline{v_b' v_t'}\ \underset{\sim}{b}\,\underset{\sim}{t} + \overline{v_b' v_n'}\ \underset{\sim}{b}\,\underset{\sim}{n} + \overline{v_b' v_b'}\ \underset{\sim}{b}\,\underset{\sim}{b} \end{array}\right] \tag{3.11}$$

or

$$\begin{array}{l} \underset{\approx}{\sigma} = + \sigma_{tt}\ \underset{\sim}{t}\,\underset{\sim}{t} + \sigma_{tn}\ \underset{\sim}{t}\,\underset{\sim}{n} + \sigma_{tb}\ \underset{\sim}{t}\,\underset{\sim}{b} \\ \qquad + \sigma_{nt}\ \underset{\sim}{n}\,\underset{\sim}{t} + \sigma_{nn}\ \underset{\sim}{n}\,\underset{\sim}{n} + \sigma_{nb}\ \underset{\sim}{n}\,\underset{\sim}{b} \\ \qquad + \sigma_{bt}\ \underset{\sim}{b}\,\underset{\sim}{t} + \sigma_{bn}\ \underset{\sim}{b}\,\underset{\sim}{n} + \sigma_{bb}\ \underset{\sim}{b}\,\underset{\sim}{b} \end{array} \tag{3.12}$$

where $\sigma_{\alpha\beta} = \sigma_{\beta\alpha}$ or in terms of fluctuating velocity components as $\overline{v'_\alpha v'_\beta} = \overline{v'_\beta v'_\alpha}$. The terms $\overline{v'_\alpha v'_\beta}$ are the time average of the product of v'_α and v'_β components of the fluctuating velocity vector.

The special case of isotropic turbulence leads to the simplification

$$\nabla \cdot \underset{\approx}{\sigma} = \nabla \sigma^* \tag{3.13}$$

in which σ^* is the intensity of isotropic turbulence. In this case therefore, the Reynolds stresses have the same influence on the Lamb vector as the Bernoulli head. This is confirmed by the following equation for an inviscid fluid

$$\underset{\sim}{V} \times \underset{\approx}{\Omega} = \nabla U - \nabla \sigma^* = \nabla(p_o + \varphi + \sigma^*) \tag{3.14}$$

The addition of U and σ^* produces a modified Bernoulli head $U^* = (p_o + \varphi - \sigma^*)$. The net effect of isotropic Reynolds stresses can be viewed as simply adding to the pressure.

For inviscid turbulent flow, contrary to the inviscid laminar case, see Marris (4), the Lamb vector and the normal to the Bernoulli surface are no longer parallel due to the presence of the Reynolds stresses. The surface, U = constant, will not, in general contain the mean streamlines and mean vortex lines because of the vector $\nabla \cdot \underset{\approx}{\sigma}$.

Equation 3.10 can now be used to eliminate the Lamb vector from either equation 2.43 for the secondary circulation result or equation 2.48 for the secondary velocity result. Setting $\nu = 0$ will simplify the results to the inviscid flow case. The generality of the vector

equations is evident here, for only one dynamical equation is needed even though it must be applied to two different coordinate systems; the intrinsic coordinates associated with either the streamlines or the vortex lines. Thus in the former, the α and β subscripts will select the components in the streamline system while in the latter, they will select components in the vortex line system.

Secondary Vorticity Equation

The formal expression for the generation of mean secondary vorticity along a mean streamline, in terms of the mean Bernoulli head, the viscous stresses and the Reynolds stresses is obtained by eliminating the Lamb vector between equations 2.43 and 3.10. In terms of the coordinate system defined by the streamlines this procedure yields

$$\frac{\partial}{\partial t}\left(\frac{\Omega_t}{q}\right) = \frac{2}{q^2 r}\left(\frac{\partial U}{\partial b} - \underset{\sim}{b} \cdot \left[\nabla \cdot \underset{\approx}{\sigma} + \nu\nabla^2 \underset{\sim}{V}\right]\right)$$

$$+ \frac{1}{q^2}\,\underset{\sim}{t} \cdot \nabla \times \left[\nabla \cdot \underset{\approx}{\sigma} + \nu\nabla^2 \underset{\sim}{V}\right] \qquad (3.15)$$

As the viscous terms act primarily as a damping factor, Marris (4), the direct effect of viscosity on the secondary flow generation will be neglected. Setting $\nu = 0$, one obtains

$$\frac{\partial}{\partial t}\left(\frac{\Omega_t}{q}\right) = \frac{2}{q^2 r}\left(\frac{\partial U}{\partial b} - \underset{\sim}{b} \cdot \nabla \cdot \underset{\approx}{\sigma}\right) + \frac{1}{q^2}\,\underset{\sim}{t} \cdot \nabla \times \left(\nabla \cdot \underset{\approx}{\sigma}\right) \qquad (3.16)$$

Equation 3.16 represents the generation of secondary mean vorticity as an inviscid process. It must be emphasized, however that

only the direct effect of viscosity on the mean secondary vorticity generation process itself has been discounted. The indirect effect of viscosity, which would appear directly merely as a dissipative factor, is twofold. Viscous effects could generate the binormal gradient of the mean Bernoulli head $\partial U/\partial b$ as well as influence the gradients of the Reynolds stresses contained in the $\nabla \cdot \underset{\approx}{\sigma}$ terms. In this sense the effect of viscosity is included in the analysis.

A significant fact disclosed by equation 3.16 is that mean secondary vorticity can be developed in a stream in the absence of a binormal gradient of mean total head through the action of

1. A bi-normal component of the vector $\nabla \cdot \underset{\approx}{\sigma}$. Due to the spatial variation of the orientation of the vectors $\underset{\sim}{t}$, $\underset{\sim}{n}$ and $\underset{\sim}{b}$ for the mean streamline, the scalar $\underset{\sim}{b} \cdot \nabla \cdot \underset{\approx}{\sigma}$ will involve not only the spatial derivatives of the Reynolds stresses, but also the Reynolds stresses themselves.

2. A tangential component of the vector $\nabla \cdot (\nabla \cdot \underset{\approx}{\sigma})$. This

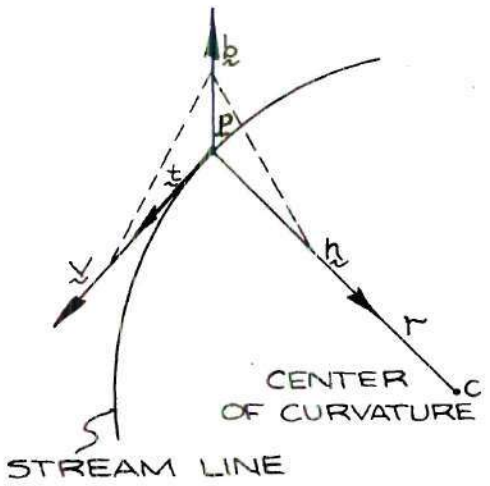

Figure 4. Intrinsic Coordinate System Defined by Streamline.

term likewise contains the Reynolds stresses themselves and their first spatial derivatives and, in addition, the second spatial derivatives of the Reynolds stresses.

Another important fact can be noted from equation 3.16. Secondary mean vorticity can be generated in the mean streamline direction of purely reclilinear flow due to the turbulence. Thus for reclilinear flow, $r = \infty$, equation 2.43 becomes

$$\frac{\partial}{\partial t}\left(\frac{\Omega_t}{q}\right) = \frac{1}{q^2}\,\underset{\sim}{t} \cdot \nabla \times (\nabla \cdot \underset{\approx}{\sigma}) \tag{3.17}$$

A flow-wise generation of mean flow-wise vorticity will occur if the Reynolds stress distribution is such that the vector $\nabla \cdot \underset{\approx}{\sigma}$ possesses a solenoidal component, and if $\nabla \times \nabla \cdot \underset{\approx}{\sigma}$ has a component in the direction of the mean streamline. For the case of isotropic turbulence, curl $\nabla \cdot \underset{\approx}{\sigma}$ is zero and no secondary flow should occur. This conclusion is supported by the velocity measurements of Brundrett and Baines (1) for turbulent flow in a straight rectangular duct. Though strong secondary flows were measured, no secondary flow generation was detected along lines of symmetry. The lines of symmetry would also correspond to near isotropic turbulence.

As the result of rectilinear flow would imply, streamline curvature is required for isotopic Reynolds stresses to become effective in secondary vorticity generation. This conclusion is verified by noting that the divergence of the Reynolds stress is irrotational for any isotropic turbulent flow. With this simplification equation 3.16 reduces to

$$\frac{\partial}{\partial t}\left(\frac{\Omega_t}{q}\right) = \frac{2}{q^2 r}\left[\frac{\partial}{\partial b}\left(U - \sigma^*\right)\right] = \frac{2}{q^2 r}\frac{\partial U^*}{\partial b} \tag{3.18}$$

This equation shows that secondary vorticity can be generated by isotropic turbulence only when a binormal gradient of the Reynolds stress occurs together with mean streamline curvature.

For unspecified types of flow the relative effects of the elements of $\underset{\approx}{\sigma}$ and their first and second spatial derivatives can be assessed by maintaining the intrinsic unit vectors $\underset{\sim}{t}$, $\underset{\sim}{n}$ and $\underset{\sim}{b}$ for the streamlines. These unit vectors will themselves be functions of position.

The symmetric Reynolds stress tensor is a function of spatial position in the flow field and of time. It may be regarded as a linear transformation which converts the unit normal vector of a given surface element to the Reynolds stress vector acting upon that surface element. The turbulent stresses on these surface elements are given by

$$\underset{\sim}{\sigma}_t = \underset{\approx}{\sigma} \cdot \underset{\sim}{t} = \underset{\sim}{t} \cdot \underset{\approx}{\sigma} = \sigma_{tt}\underset{\sim}{t} + \sigma_{tn}\underset{\sim}{n} + \sigma_{tb}\underset{\sim}{b} \tag{3.19}$$

$$\underset{\sim}{\sigma}_n = \underset{\approx}{\sigma} \cdot \underset{\sim}{n} = \underset{\sim}{n} \cdot \underset{\approx}{\sigma} = \sigma_{nt}\underset{\sim}{t} + \sigma_{nn}\underset{\sim}{n} + \sigma_{nb}\underset{\sim}{b} \tag{3.20}$$

$$\underset{\sim}{\sigma}_b = \underset{\approx}{\sigma} \cdot \underset{\sim}{b} = \underset{\sim}{b} \cdot \underset{\approx}{\sigma} = \sigma_{bt}\underset{\sim}{t} + \sigma_{bn}\underset{\sim}{n} + \sigma_{bb}\underset{\sim}{b} \tag{3.21}$$

Unlike the Reynolds stress tensor which depends only upon time and spatial position, the Reynolds stress vectors $\underset{\sim}{\sigma}_t$, $\underset{\sim}{\sigma}_n$ and $\underset{\sim}{\sigma}_b$ depend upon time, spatial position and in addition, upon the orientation of the surface elements.

Using the comma to denote partial differentiation* with respect to all coordinates following it, e.g.

$$\sigma_{bt,tn} = \frac{\partial^2}{\partial t \partial n} \sigma_{bt} \tag{3.22}$$

The first scalar product on the right side equation 3.16, as shown in Appendix C, can be expressed as

$$\underset{\sim}{b} \cdot (\nabla \cdot \underset{\approx}{\sigma}) = \nabla \cdot \underset{\sim}{\sigma}_b + \underset{\sim}{b} \cdot (\underset{\sim}{\sigma}_\varepsilon \cdot \nabla \underset{\sim}{e}_\varepsilon) \tag{3.23}$$

or in terms of t,n and b

$$\begin{aligned} \underset{\sim}{b} \cdot (\nabla \cdot \underset{\approx}{\sigma}) = {} & (\sigma_{bt,t} + \sigma_{bn,n} + \sigma_{bb,b}) \\ & + (\sigma_{bt} \nabla \cdot \underset{\sim}{t} + \sigma_{bn} \nabla \cdot \underset{\sim}{n} + \sigma_{bb} \nabla \cdot \underset{\sim}{b}) \\ & + b \cdot (\underset{\sim}{\sigma}_t \cdot \nabla \underset{\sim}{t} + \underset{\sim}{\sigma}_n \cdot \nabla \underset{\sim}{n} + \underset{\sim}{\sigma}_b \cdot \nabla \underset{\sim}{b}) \end{aligned} \tag{3.24}$$

Note that the sum of the first six terms on the right of equation 3.24 are $\nabla \cdot \underset{\sim}{\sigma}_b$. The second scalar product is

---

*Some caution must be exercised in performing differentiation when using intrinsic coordinates. As pointed out by Bjørgum (24), the order of differentiation is not necessarily commutative, i.e.

$$\frac{\partial^2}{\partial t \partial n} \neq \frac{\partial^2}{\partial n \partial t}$$

as intrinsic coordinates do not in general constitute an ordinary system of coordinates. In some cases orthogonal surfaces to $\underset{\sim}{t}$, $\underset{\sim}{n}$ and $\underset{\sim}{b}$ do not exist. The system fails if either the vector lines defining the natural coordinates have zero curvature or the vector magnitude goes to zero.

$$\begin{aligned}
\underset{\sim}{t} \cdot \nabla \times (\nabla \cdot \underset{\approx}{\sigma}) &= (\sigma_{bt,tn} + \sigma_{bn,nn} + \sigma_{bb,bn}) \\
&+ (\sigma_{bt} \nabla \cdot \underset{\sim}{t} + \sigma_{bn} \nabla \cdot \underset{\sim}{n} + \sigma_{bb} \nabla \cdot \underset{\sim}{b})_{,n} \\
&- (\sigma_{nt} \nabla \cdot \underset{\sim}{t} + \sigma_{nn} \nabla \cdot \underset{\sim}{n} + \sigma_{nb} \nabla \cdot \underset{\sim}{b})_{,b} \\
&- (\sigma_{nt,tb} + \sigma_{nn,nb} + \sigma_{nb,bb}) \\
&+ \underset{\sim}{t} \cdot \nabla \times (\underset{\approx}{\sigma}_t \cdot \nabla \underset{\sim}{t} + \sigma_{\underset{\sim}{n}} \cdot \nabla \underset{\sim}{n} + \sigma_{\underset{\sim}{b}} \cdot \nabla \underset{\sim}{b}) \qquad (3.25) \\
&+ \nabla \cdot \underset{\approx}{\sigma}_t (\underset{\sim}{t} \cdot \nabla \times \underset{\sim}{t}) + \nabla \cdot \underset{\approx}{\sigma}_n (\underset{\sim}{t} \cdot \nabla \times \underset{\sim}{n}) + \nabla \cdot \underset{\approx}{\sigma}_b (\underset{\sim}{t} \cdot \nabla \times \underset{\sim}{b})
\end{aligned}$$

as is shown in Appendix D.

The complete expression for the flow-wise generation of mean vorticity is thus

$$\frac{\partial}{\partial t}\left(\frac{\Omega_t}{q}\right) = \frac{2}{q^2_r} \frac{\partial U}{\partial b} \qquad (3.26a)$$

due to the interaction of mean streamline curvature and the binormal gradient of the mean Bernoulli head

$$\begin{aligned}
- \frac{2}{q^2_r} [&\sigma_{bt,t} + \sigma_{bn,n} + \sigma_{bb,b} + \sigma_{bt} \nabla \cdot \underset{\sim}{t} + \sigma_{bn} \nabla \cdot \underset{\sim}{n} \\
&+ \sigma_{bb} \nabla \cdot \underset{\sim}{b} + \underset{\sim}{b} \cdot (\underset{\approx}{\sigma}_t \cdot \nabla \underset{\sim}{t} + \underset{\approx}{\sigma}_n \cdot \nabla \underset{\sim}{n} + \underset{\approx}{\sigma}_b \cdot \nabla \underset{\sim}{b})] \qquad (3.26b)
\end{aligned}$$

due to interaction of the mean streamline curvature and the Reynolds stress gradients, Reynolds stresses and spatial variation of intrinsic unit vectors of the mean streamline

$$+\frac{1}{q^2}\Big[-\Big\{\sigma_{nt,tb}+\sigma_{nn,nb}+\sigma_{nb,bb}+(\sigma_{nt}\nabla\cdot\underset{\sim}{t}+\sigma_{nn}\nabla\cdot\underset{\sim}{n}+\sigma_{nb}\nabla\cdot\underset{\sim}{b})_{,b}\Big\}$$

$$+\Big\{\sigma_{bt,tn}+\sigma_{bn,nn}+\sigma_{bb,bn}+(\sigma_{bt}\nabla\cdot\underset{\sim}{t}+\sigma_{bn}\nabla\cdot\underset{\sim}{n}+\sigma_{bb}\nabla\cdot\underset{\sim}{b})_{,n}\Big\}$$

$$+\ \underset{\sim}{t}\cdot\nabla\times(\underset{\sim}{\sigma}_t\cdot\nabla\underset{\sim}{t}+\underset{\sim}{\sigma}_n\cdot\nabla\underset{\sim}{n}+\underset{\sim}{\sigma}_b\cdot\nabla\underset{\sim}{b}) \qquad (3.26c)$$

$$+\Big\{\nabla\cdot\underset{\sim}{\sigma}_t(\underset{\sim}{t}\cdot\nabla\times\underset{\sim}{t})+\nabla\cdot\underset{\sim}{\sigma}_n(\underset{\sim}{t}\cdot\nabla\times\underset{\sim}{n})+\nabla\cdot\underset{\sim}{\sigma}_b(\underset{\sim}{t}\cdot\nabla\times\underset{\sim}{b})\Big\}\Big]$$

representing the effect of second gradients of the Reynolds stress elements on rectilinear streamlines; the interaction of the Reynolds stress elements with the first and second spatial derivatives of the intrinsic unit vectors; and the interaction of the first derivatives of the Reynolds stresses with the first spatial variations of the unit vectors. The vector operator form of equation 3.26 can be written as

$$\frac{\partial}{\partial t}\left(\frac{\Omega_t}{q}\right)=\frac{2}{q^2r}\frac{\partial U}{\partial b}-\frac{2}{q^2r}\left[\nabla\cdot\underset{\sim}{\sigma}_b+\underset{\sim}{b}\cdot(\underset{\sim}{\sigma}_\epsilon\cdot\nabla\underset{\sim}{i}_\epsilon)\right]$$

$$+\frac{1}{q^2}\Big[(\underset{\sim}{t}\cdot\nabla\times\underset{\sim}{t})\nabla\cdot\underset{\sim}{\sigma}_t+(\underset{\sim}{t}\cdot\nabla\times\underset{\sim}{n})\nabla\cdot\underset{\sim}{\sigma}_n+(\underset{\sim}{t}\cdot\nabla\times\underset{\sim}{b})\nabla\cdot\underset{\sim}{\sigma}_b$$

$$+\ \underset{\sim}{t}\cdot\nabla\times(\underset{\sim}{\sigma}_t\cdot\nabla\underset{\sim}{t}+\underset{\sim}{\sigma}_n\cdot\nabla\underset{\sim}{n}+\underset{\sim}{\sigma}_b\cdot\nabla\underset{\sim}{b})$$

$$+\ \underset{\sim}{n}\cdot\nabla(\nabla\cdot\underset{\sim}{\sigma}_b)-\underset{\sim}{b}\cdot\nabla(\nabla\cdot\underset{\sim}{\sigma}_n)\ \Big] \qquad (3.27)$$

which is a more convenient form from which to effect coordinate transformations.

The above general result, equations 3.26 or 3.27 can be applied to particular cases to determine if secondary circulation generation will occur at a selected point P. The use of this equation, illustrated by

several examples in Chapter IV, required knowledge of the geometry of the streamlines — to work out the geometric terms such as $\underset{\sim}{t} \cdot \nabla \times \underset{\sim}{t}$ — and an assumption about the nature of the Reynolds stress distribution at the point in question. As secondary flow would alter the velocity and vorticity fields by convection, in general the equation would have to be applied iteratively to follow the progressive changes of the flow pattern. If the assumption of small disturbances, as outlined by Hawthorne (21), is applicable, it is possible to assume the velocity field to be convected with the secondary flow. Using this technique the flow may be followed over a finite path length, e.g. flow through a bend as illustrated in the example on pages 52 - 54.

Secondary Velocity Equation

The time mean Lamb vector $\underset{\sim}{V} \times \underset{\sim}{\Omega}$ of equation 2.48 will now be eliminated — as in the previous section — by introducing the selected equation of motion. The behavior of the secondary velocity generation under the influence of the force fields and the elements of the Reynolds stresses will then be revealed.

Restricting the analysis, as before, to steady-time-mean flow of an inviscid incompressible fluid, the Lamb vector as given in equation 3.10 is directly applicable here. Paralleling the procedure for the secondary vorticity result, the symmetric tensor of the Reynolds stress is expressed in terms of the unit vectors, $\underset{\sim}{e}_1$, $\underset{\sim}{e}_2$ and $\underset{\sim}{e}_3$ defined by tangent, principal normal and binormal to the vortex line passing through the point under study. In this coordinate system, see Figure 5, the Reynolds stress dyad is

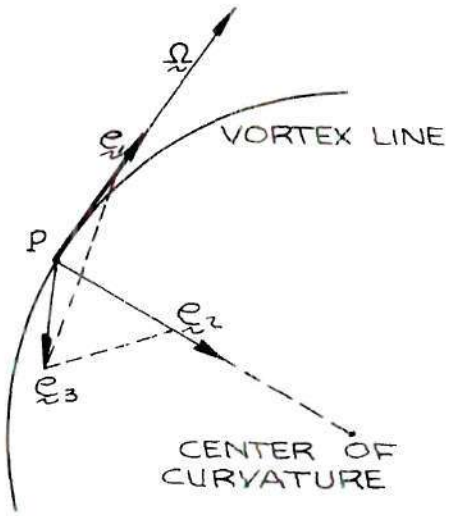

Figure 5. Intrinsic Coordinates Defined by Vortex Line.

$$\sigma = -\rho\left[\begin{array}{l} \overline{v_1'v_1'}\ \underset{\sim}{e}_1\underset{\sim}{e}_1 + \overline{v_1'v_2'}\ \underset{\sim}{e}_1\underset{\sim}{e}_2 + \overline{v_1'v_3'}\ \underset{\sim}{e}_1\underset{\sim}{e}_3 \\ + \overline{v_2'v_1'}\ \underset{\sim}{e}_2\underset{\sim}{e}_1 + \overline{v_2'v_2'}\ \underset{\sim}{e}_2\underset{\sim}{e}_2 + \overline{v_2'v_3'}\ \underset{\sim}{e}_2\underset{\sim}{e}_3 \\ + \overline{v_3'v_1'}\ \underset{\sim}{e}_3\underset{\sim}{e}_1 + \overline{v_3'v_2'}\ \underset{\sim}{e}_3\underset{\sim}{e}_2 + \overline{v_3'v_3'}\ \underset{\sim}{e}_3\underset{\sim}{e}_3 \end{array}\right] \tag{3.28}$$

or

$$\begin{aligned} \underset{\approx}{\sigma} = {} & \sigma_{11}\underset{\sim}{e}_1\underset{\sim}{e}_1 + \sigma_{12}\,\underset{\sim}{e}_1\underset{\sim}{e}_2 + \sigma_{13}\underset{\sim}{e}_1\underset{\sim}{e}_3 \\ & + \sigma_{21}\underset{\sim}{e}_2\underset{\sim}{e}_1 + \sigma_{22}\underset{\sim}{e}_2\underset{\sim}{e}_2 + \sigma_{23}\underset{\sim}{e}_2\underset{\sim}{e}_3 \\ & + \sigma_{31}\underset{\sim}{e}_3\underset{\sim}{e}_1 + \sigma_{32}\underset{\sim}{e}_3\underset{\sim}{e}_2 + \sigma_{33}\underset{\sim}{e}_3\underset{\sim}{e}_3 \end{aligned} \tag{3.29}$$

where as before $\sigma_{\alpha\beta} = \sigma_{\beta\alpha}$ are the scalar components of the stress, but now in the x_1, x_2, x_3 coordinate system.

The Lamb vector is eliminated between equations 2.48 and 3.10, to obtain an expression for the generation of a secondary flow

rate in terms of the dynamical effects. This combination can be expressed as

$$\frac{\partial}{\partial x_1}\left(\frac{V_1}{\omega}\right) = \frac{1}{\omega^3}\left[-\omega\, \underset{\sim}{e}_1 \cdot \nabla \times (\nabla \cdot \underset{\approx}{\sigma}) - \left([\omega K + \frac{\partial \omega}{\partial x_2}]\underset{\sim}{e}_3 - \frac{\partial \omega}{\partial x_1}\underset{\sim}{e}_3\right) \cdot (\nabla U - \nabla \cdot \underset{\approx}{\sigma})\right] \quad (3.30)$$

for $\nabla \times \nabla U = 0$ Upon rearrangement, equation 3.30 can be presented as

$$\frac{\partial V_1}{\partial x_1} = \frac{V_1}{\omega}\frac{\partial \omega}{\partial x_1} + \frac{1}{\omega^2}\frac{\partial(U,\omega)}{\partial(x_2,x_3)} - \frac{K}{\omega}\frac{\partial U}{\partial x_3} - \frac{1}{\omega}\underset{\sim}{e}_1 \cdot \nabla \times (\nabla \cdot \underset{\approx}{\sigma})$$

$$+ \frac{1}{\omega}\left[\left(\frac{1}{\omega}\frac{\partial \omega}{\partial x_2} + K\right)\underset{\sim}{e}_3 - \frac{1}{\omega}\frac{\partial \omega}{\partial x_3}\underset{\sim}{e}_2\right] \cdot (\nabla \cdot \underset{\approx}{\sigma}) \quad (3.31)$$

where

$$\frac{\partial(U,\omega)}{\partial(x_2,x_3)} = \frac{\partial U}{\partial x_2}\frac{\partial \omega}{\partial x_3} - \frac{\partial U}{\partial x_3}\frac{\partial \omega}{\partial x_2} \quad (3.32)$$

is a Jacobian representation first given by Marris (17).

The vector $\nabla \cdot \underset{\approx}{\sigma}$, has the same general form as shown in equations B.14 and B.16. In the vortex line coordinate system, it may be expressed as

$$\nabla \cdot \underset{\approx}{\sigma} = \underset{\sim}{e}_1(\nabla \cdot \underset{\sim}{\sigma}_1) + \underset{\sim}{e}_2(\nabla \cdot \underset{\sim}{\sigma}_2) + \underset{\sim}{e}_3(\nabla \cdot \underset{\sim}{\sigma}_3)$$

$$+ \underset{\sim}{\sigma}_1 \cdot \nabla \underset{\sim}{e}_1 + \underset{\sim}{\sigma}_2 \cdot \nabla \underset{\sim}{e}_2 + \underset{\sim}{\sigma}_3 \cdot \nabla \underset{\sim}{e}_3 \quad (3.33)$$

in which

$$\underset{\sim}{\sigma}_\alpha = \underset{\approx}{\sigma} \cdot \underset{\sim}{e}_\alpha = \underset{\sim}{e}_\alpha \cdot \underset{\approx}{\sigma} = \sigma_{\alpha 1}\underset{\sim}{e}_1 + \sigma_{\alpha 2}\underset{\sim}{e}_2 + \sigma_{\alpha 3}\underset{\sim}{e}_3 \quad (3.34)$$

for $\alpha = 1, 2, 3$.

The complete expansion of the vector $\nabla \cdot \underset{\approx}{\sigma}$ is shown in Appendix B.

The two scalars resulting from dot products with $\nabla \cdot \underset{\approx}{\sigma}$ in equation 3.31 can be expanded, as shown in Appendix C, into the following forms:

$$\underset{\sim}{e}_2 \cdot (\nabla \cdot \underset{\approx}{\sigma}) = \sigma_{21,1} + \sigma_{22,2} + \sigma_{23,3} + \sigma_{21} \nabla \cdot \underset{\sim}{e}_1 + \sigma_{22} \nabla \cdot \underset{\sim}{e}_2 \qquad (3.35)$$
$$+ \sigma_{23} \nabla \cdot \underset{\sim}{e}_3 + \underset{\sim}{e}_2 \cdot (\underset{\sim}{\sigma}_1 \cdot \nabla \underset{\sim}{e}_1 + \underset{\sim}{\sigma}_2 \cdot \nabla \underset{\sim}{e}_2 + \underset{\sim}{\sigma}_3 \cdot \nabla \underset{\sim}{e}_3)$$

$$\underset{\sim}{e}_3 \cdot (\nabla \cdot \underset{\approx}{\sigma}) = \sigma_{31,1} + \sigma_{32,2} + \sigma_{33,3} + \sigma_{31} \nabla \cdot \underset{\sim}{e}_1 \qquad (3.36)$$
$$+ \sigma_{32} \nabla \cdot \underset{\sim}{e}_2 + \sigma_{33} \nabla \cdot \underset{\sim}{e}_3 + \underset{\sim}{e}_3 \cdot (\underset{\sim}{\sigma}_1 \cdot \nabla \underset{\sim}{e}_1$$
$$+ \underset{\sim}{\sigma}_2 \cdot \nabla \underset{\sim}{e}_2 + \underset{\sim}{\sigma}_3 \cdot \nabla \underset{\sim}{e}_3)$$

The vortex directed component of curl of $\nabla \cdot \underset{\approx}{\sigma}$, derived in Appendix D, can be expressed as

$$\underset{\sim}{e}_1 \cdot \nabla \times (\nabla \cdot \underset{\approx}{\sigma}) = (\sigma_{31,12} + \sigma_{32,22} + \sigma_{33,32}) - (\sigma_{21,13} \qquad (3.37)$$
$$+ \sigma_{22,23} + \sigma_{23,33}) + (\sigma_{31} \nabla \cdot \underset{\sim}{e}_1 + \sigma_{32} \nabla \cdot \underset{\sim}{e}_2 + \sigma_{33} \nabla \cdot \underset{\sim}{e}_3)_{,2}$$
$$- (\sigma_{21} \nabla \cdot \underset{\sim}{e}_1 + \sigma_{22} \nabla \cdot \underset{\sim}{e}_2 + \sigma_{23} \nabla \cdot \underset{\sim}{e}_3)_{,3}$$
$$+ \underset{\sim}{e}_1 \cdot \nabla \times (\underset{\sim}{\sigma}_1 \cdot \nabla \underset{\sim}{e}_1 + \underset{\sim}{\sigma}_2 \cdot \nabla \underset{\sim}{e}_2 + \underset{\sim}{\sigma}_3 \cdot \nabla \underset{\sim}{e}_3)$$
$$+ \nabla \cdot \underset{\sim}{\sigma}_1 (\underset{\sim}{e}_1 \cdot \nabla \times \underset{\sim}{e}_1) + \nabla \cdot \underset{\sim}{\sigma}_2 (\underset{\sim}{e}_1 \cdot \nabla \times \underset{\sim}{e}_2) + \nabla \cdot \underset{\sim}{\sigma}_3 (\underset{\sim}{e}_1 \cdot \nabla \times \underset{\sim}{e}_3)$$

Substituting the results given in equations 3.35, 3.36 and 3.37 into equation 3.31 yields

$$\omega^2 \frac{\partial}{\partial x_1}\left(\frac{V_1}{\omega}\right) = \frac{1}{\omega}\frac{\partial(U,\omega)}{\partial(x_2,x_3)} - \kappa\frac{\partial U}{\partial x_3} - (\underset{\sim}{e}_2\cdot\nabla)(\nabla\cdot\underset{\sim}{\sigma}_3) + (\underset{\sim}{e}_3\cdot\nabla)(\nabla\cdot\underset{\sim}{\sigma}_2)$$

$$+ \left(-\underset{\sim}{e}_1\cdot\nabla\times\left[-\frac{1}{\omega}\frac{\partial\omega}{\partial x_3}\underset{\sim}{e}_2\cdot + \left[\kappa+\frac{1}{\omega}\frac{\partial\omega}{\partial x_2}\right]\underset{\sim}{e}_3\cdot\right)(\underset{\sim}{\sigma}_1\cdot\nabla\underset{\sim}{e}_1 +$$

$$+ \underset{\sim}{\sigma}_2\cdot\nabla\underset{\sim}{e}_2 + \underset{\sim}{\sigma}_2\cdot\nabla\underset{\sim}{e}_3) - (\underset{\sim}{e}_1\cdot\nabla\times\underset{\sim}{e}_1)\nabla\cdot\underset{\sim}{\sigma}_1 +$$

$$+ \left(-\underset{\sim}{e}_1\cdot\nabla\times\underset{\sim}{e}_2 - \frac{1}{\omega}\frac{\partial\omega}{\partial x_3}\right)\nabla\cdot\underset{\sim}{\sigma}_2 + \left(-\underset{\sim}{e}_1\cdot\nabla\times\underset{\sim}{e}_3 + \kappa + \frac{1}{\omega}\frac{\partial\omega}{\partial x_2}\right)\nabla\cdot\underset{\sim}{\sigma}_3 \qquad (3.38)$$

In the $\underset{\sim}{e}_1$, $\underset{\sim}{e}_2$, $\underset{\sim}{e}_3$ coordinate system, equation 3.38 can be expanded into the following form.

$$\left(\frac{\partial V_1}{\partial x_1} - \frac{V_1}{\omega}\frac{\partial\omega}{\partial x_1}\right) = \frac{1}{\omega}\left[\frac{1}{\omega}\left(\frac{\partial U}{\partial x_2}\frac{\partial\omega}{\partial x_3} - \frac{\partial U}{\partial x_3}\frac{\partial\omega}{\partial x_2}\right) - \kappa\frac{\partial U}{\partial x_3}\right.$$

$$- (\sigma_{31,12}+\sigma_{32,22}+\sigma_{33,32}) + (\sigma_{21,13}+\sigma_{22,23}+\sigma_{23,33})$$

$$- \frac{\partial}{\partial x_2}(\sigma_{31}\nabla\cdot\underset{\sim}{e}_1 + \sigma_{32}\nabla\cdot\underset{\sim}{e}_2 + \sigma_{33}\nabla\cdot\underset{\sim}{e}_3) + \frac{\partial}{\partial x_3}(\sigma_{21}\nabla\cdot\underset{\sim}{e}_1$$

$$+ \sigma_{22}\nabla\cdot\underset{\sim}{e}_2 + \sigma_{23}\nabla\cdot\underset{\sim}{e}_3) - \nabla\cdot\underset{\sim}{\sigma}_1(\underset{\sim}{e}_1\cdot\nabla\times\underset{\sim}{e}_1) - \nabla\cdot\underset{\sim}{\sigma}_2(\underset{\sim}{e}_1\cdot\nabla\times\underset{\sim}{e}_2$$

$$+ \frac{1}{\omega}\frac{\partial\omega}{\partial x_3}) - \nabla\cdot\underset{\sim}{\sigma}_3(\underset{\sim}{e}_1\cdot\nabla\times\underset{\sim}{e}_3 - \kappa - \frac{1}{\omega}\frac{\partial\omega}{\partial x_2}) - [\underset{\sim}{e}_1\cdot\nabla\times\left[+\frac{1}{\omega}\frac{\partial\omega}{\partial x_3}\underset{\sim}{e}_2\cdot\right.$$

$$\left.\left.-(\kappa+\frac{1}{\omega}\frac{\partial\omega}{\partial x_2})\underset{\sim}{e}_3\cdot\right][\underset{\sim}{\sigma}_1\cdot\nabla\underset{\sim}{e}_1 + \underset{\sim}{\sigma}_2\cdot\nabla\underset{\sim}{e}_2 + \underset{\sim}{\sigma}_3\cdot\nabla\underset{\sim}{e}_3]\right] \qquad (3.39)$$

Equations 3.38 and 3.39 give a method to predict the secondary flow generation with displacement along a vortex line. In cases of weak or zero secondary vorticity, the vortex lines will lie in a plane normal to the mean velocity vector. The vorticity of the flow will be confined

to the boundary layer region, where the vorticity magnitude and direction is determined by the boundary layer velocity gradient.

As the vortex lines generally exist in planes normal to the mean flow direction, the predicting equation 3.38 can not follow the flow but rather gives information on the relative secondary velocity generation tendency at any point in a plane normal to the mean flow.

Equation 3.39 shows three factors important in secondary flow production along a vortex line. These are

1. The vortex directed component of the curl of div $\underset{\approx}{\sigma}$

2. The components of the Bernoulli head gradient normal to the vortex line plus the interaction of the binormal component of ∇U with the curvature of the vortex lines and

3. The two normal components of the divergence of the Reynolds stress tensor plus the interaction of $\underset{\sim}{e}_3 \cdot (\nabla \cdot \underset{\approx}{\sigma})$ with K.

All three effects are amplified by small vorticity magnitudes as shown by the $\frac{1}{\omega^2}$ and $\frac{1}{\omega^3}$ multipliers present in the right hand side of equation 3.39. The influence of small values of ω is mitigated though by the tendency of the vorticity gradients to diminish with diminishing vorticity magnitude.

The relation for production of secondary velocity in isotropic turbulence can be obtained from equation 3.38; however it is much easier to introduce the isotropic specialization into equation 2.48. Using equation 3.14, the Lamb vector for isotropic turbulence, to eliminate $\underset{\sim}{V} \times \underset{\approx}{\Omega}$ in equation 2.48 leads to

$$\frac{\partial}{\partial x_1}\left(\frac{V_1}{\omega}\right) = \frac{1}{\omega^3}\left[-\left(\frac{\partial \omega}{\partial x_2} + \omega K\right)\frac{\partial (U+\sigma^*)}{\partial x_3} + \frac{\partial \omega}{\partial x_3}\frac{\partial (U+\sigma^*)}{\partial x^2}\right] \qquad (3.40)$$

This equation shows, as was found in the secondary vorticity case, that the Reynolds stress has exactly the same type of influence on secondary velocity generation as the Bernoulli head.

CHAPTER IV

GENERAL APPLICATIONS

The application of the results presented in Chapter III to particular coordinate systems must account for the scale factors required by the coordinate system selected. The scale factors, h_α, responsible for changes in linear dimensions from a rectangular Cartesian to another system; are related to the length of a line element ds by

$$ds^2 = h_\alpha^2 \, dx_\alpha^2 \tag{4.1}$$

The intrinsic coordinate systems, $\underset{\sim}{t}$, $\underset{\sim}{n}$, $\underset{\sim}{b}$ and $\underset{\sim}{e}_1$, $\underset{\sim}{e}_2$, $\underset{\sim}{e}_3$ used in the development are based on linear measures along the coordinate axis. Therefore the scale factors for these two systems are all unity. Cylindrical and spherical coordinate systems, the most convenient for some applications, use angular measures as a space variable which introduces non unity scale factors. Due to the problem one might have in converting from a form of an equation to a system involving non unity scale factors, it is recommended that the transformation of coordinates proceed from the vector form of the desired expressions. Thus to convert $\nabla \cdot \underset{\approx}{a}$ into cylindrical coordinates, one should start with the equation B.14 rather than B.16.

The vector forms can then be reduced using standard differential operators applicable to the coordinate system selected. Morse and Feshback (16), pages 114 to 117, provides a very convenient source of the vector

and dyadic operators applicable to any orthogonal curvilinear coordinate system.

Secondary Vorticity Generation in Rectilinear Flow

For rectilinear and spatially constant mean flow in which case $\underset{\sim}{t}$, $\underset{\sim}{n}$ and $\underset{\sim}{b}$ become spatially constant Cartesian unit vectors, equation 3.26 reduces to

$$\frac{\partial \Omega_t}{\partial t} = \frac{1}{q}\left[(\sigma_{bt,tn} + \sigma_{bn,nn} + \sigma_{bb,bn}) - (\sigma_{nt,tb} + \sigma_{nn,nb} + \sigma_{nb,bb})\right] \quad (4.2)$$

A case of practical interest for rectilinear mean flow in which mean secondary vorticity is developed due to anisotropy in the turbulence is that of mean flow along a corner of a channel. For an internal corner, the measurements of Brundrett and Baines show that a secondary flow exists, with flow into the corner along the bisector of the corner angle and away from the corner along the side walls. Secondary flow streamlines for flow in a square duct are illustrated in Figure 6. Prandtl (26) gave an empirical explanation for this phenomenon on the basis that the turbulent fluctuating velocity components were greater in the direction of the tangent to the curves of constant mean velocity than in the normal direction to the curves. This correlation has been confirmed by experiments of Gessner and Jones (8) and Brundrett and Baines.

However, the foregoing analysis indicates that this difference in turbulent velocity components represents only a part of the secondary flow generation process. For the complete cause of secondary flow developed by the action of anisotropic turbulence, the second spatial gradients of the elements of the Reynolds stress tensor, as indicated by equation

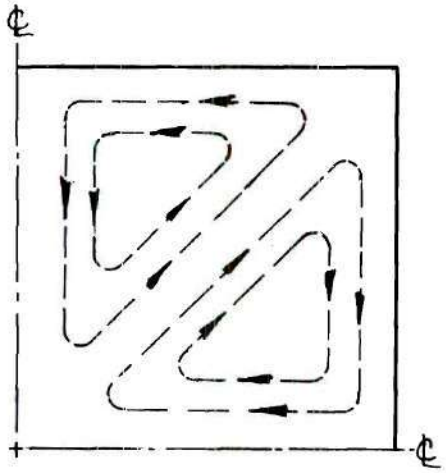

Figure 6. Secondary Flow Pattern, Turbulent Flow in a Square Duct.

4.2, must be considered. This conclusion is substantiated by Brundrett and Baines's measurements. They show the production of secondary vorticity is concentrated near the corners, as shown in Figure 7, the region where the greatest Reynolds stress gradients occur.

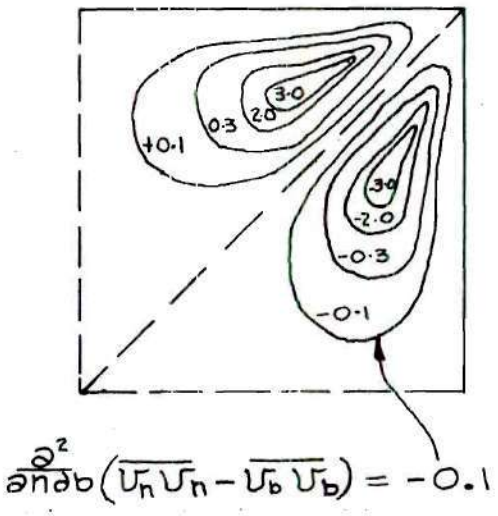

Figure 7. Production of Vorticity (Dimensionless) in a Square Duct. After Brundrett and Baines.

Correlations with flow-wise velocity fluctuations play a part in the generation of secondary mean vorticity through the presence of the terms

$$\frac{1}{q}\left[\sigma_{nt,tb} - \sigma_{bt,tn}\right] \tag{4.3}$$

If these terms can be ignored and we consider only the Reynolds stresses and their second gradients in the plane normal to the mean flow then one would have

$$\frac{\partial \Omega_t}{\partial t} = \frac{-1}{q}\left[\frac{\partial^2}{\partial n \partial b}\left(\sigma_{nn} - \sigma_{bb}\right) + \left(\frac{\partial^2}{\partial b^2} - \frac{\partial^2}{\partial n^2}\right)\sigma_{nb}\right] \tag{4.4}$$

since $\sigma_{nb} = \sigma_{bn}$.

For rectilinear streamlines the directions n and b are any perpendicular directions forming a right handed system $\underset{\sim}{t}$, $\underset{\sim}{n}$, $\underset{\sim}{b}$ with the mean flow direction t.

Secondary Vorticity Generation in Plane Circular Flow

A plane circular streamline (r = const) will be assumed for the mean flow. The secondary-vorticity generating effect of a mean velocity or total head gradient in the direction perpendicular to the plane of the streamline (binormal direction) being well established (2,3), this effect will be excluded, and attention will be concentrated specifically on the effects of the Reynolds stresses.

A physical situation approaching this flow model may be that of fully developed turbulent flow in the passage between two concentric cylinders of small width to radius ratio and of very large depth to width

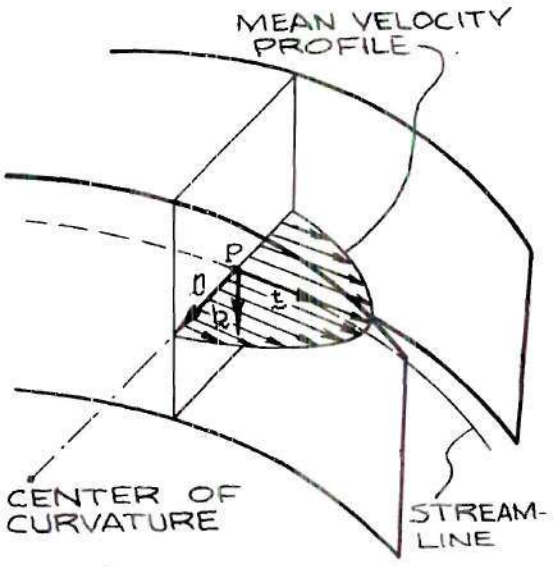

Figure 8. Streamline Coordinate System for Curved Channel Flow.

ratio. For such a channel, illustrated in Figure 8, the mean velocity gradients from the boundary layers of the curved walls are in the plane containing the mean streamline and the radius of curvature of the mean streamline and will therefore play little or no part in creating secondary flow. The turbulence characteristics of this system were studied experimentally by Eskinazi and Yeh (7). They discovered that the radial component of $\overline{v_r'v_r'}$ turbulent intensity tends to be suppressed at the inner (convex-to-flow) wall of the channel, "by Reynolds stresses working on the mean momentum gradient," while amplified at the outer wall.

The cylindrical coordinate system, shown in Figure 8, is a convenient one for use with plane circular streamlines. In this coordinate system, $\underset{\sim}{t}$ corresponds to $\underset{\sim}{e}_\theta$, $\underset{\sim}{n}$ to $-\underset{\sim}{e}_n$ and $\underset{\sim}{b}$ to $-\underset{\sim}{e}_z$. The development of the secondary vorticity expression will proceed from equation

3.27*, using the following geometric conditions

$$\nabla \underset{\sim}{t} = \nabla \underset{\sim}{e}_\theta = -\frac{1}{r} \underset{\sim}{e}_\theta \underset{\sim}{e}_r \tag{4.5}$$

$$\nabla \underset{\sim}{n} = -\nabla \underset{\sim}{e}_r = -\frac{\underset{\sim}{e}_\theta \underset{\sim}{e}_\theta}{r} \tag{4.6}$$

$$\nabla \underset{\sim}{b} = \nabla \underset{\sim}{e}_3 = 0 \tag{4.7}$$

$$\nabla \times \underset{\sim}{t} = \nabla \times \underset{\sim}{e}_\theta = \frac{1}{r} \underset{\sim}{e}_z \tag{4.8}$$

$$\nabla \times \underset{\sim}{n} = -\nabla \times \underset{\sim}{e}_r = 0 \tag{4.9}$$

$$\nabla \times \underset{\sim}{b} = \nabla \times \underset{\sim}{e}_z = 0 \tag{4.10}$$

$$\underset{\sim}{t} \cdot \nabla \times \underset{\sim}{t} = \underset{\sim}{t} \cdot \nabla \times \underset{\sim}{n} = \underset{\sim}{t} \cdot \nabla \times \underset{\sim}{b} = 0 \tag{4.11,4.12,4.13}$$

$$\underset{\sim}{n} \cdot \nabla = -\underset{\sim}{e}_r \cdot \nabla = -\frac{\partial}{\partial r} \tag{4.14}$$

$$\underset{\sim}{b} \cdot \nabla = \underset{\sim}{e}_z \cdot \nabla = \frac{\partial}{\partial z} \tag{4.15}$$

Using the above geometric conditions and neglecting the binormal Bernoulli head gradient, equation 3.27 simplifies to

$$\frac{1}{r}\frac{\partial}{\partial\theta}\left(\frac{\Omega_\theta}{q}\right) = \frac{-2}{q^2 r}\left[\nabla \cdot \underset{\sim}{g}_z + \underset{\sim}{e}_z \cdot \left[\underset{\sim}{g}_\theta \cdot \left(-\frac{\underset{\sim}{e}_\theta \underset{\sim}{e}_r}{r}\right) - \underset{\sim}{g}_r \cdot \left(-\frac{\underset{\sim}{e}_\theta \underset{\sim}{e}_\theta}{r}\right)\right]\right] +$$

---

*The vector operator form of the secondary vorticity result was used because the scale factors involved in cylindrical coordinates preclude direct use of equation 3.26. If use of 3.26 is attempted, two terms in the expansion σ_{rz}/r^2 and $\sigma_{\theta z,\theta}/r$ will be missed as these terms result from a partial derivative of the scale factor, $1/r$. The first term comes from $\frac{\partial}{\partial r}\frac{1}{r}\frac{\partial}{\partial r}(r\sigma_{rz})$ while the second is obtained from $\frac{\partial}{\partial r}\frac{1}{r}\frac{\partial}{\partial\theta}\sigma_{\theta z}$.

$$+ \frac{1}{q^2}\left[\underset{\sim}{e}_\theta \cdot \nabla \times \left[\underset{\sim}{\sigma}_\theta \cdot \left(-\frac{\underset{\sim}{e}_\theta \underset{\sim}{e}_r}{r}\right) - \underset{\sim}{\sigma}_r \cdot \left(-\frac{\underset{\sim}{e}_\theta \underset{\sim}{e}_\theta}{r}\right)\right.\right.$$

$$\left.\left. - \frac{\partial}{\partial r}(\nabla \cdot \underset{\sim}{\sigma}_z) - \frac{\partial}{\partial z}(-\nabla \cdot \underset{\sim}{\sigma}_r)\right]\right] \qquad (4.16)$$

which on expansion, as shown in Appendix E, reduces to

$$\frac{\partial}{\partial\theta}\left(\frac{\Omega_\theta}{q}\right) = \frac{-2}{q^2}\left[\sigma_{zr,r} + \frac{\sigma_{zr}}{r} + \frac{\sigma_{z\theta,\theta}}{r} + \sigma_{zz,z}\right]$$

$$+ \frac{r}{q^2}\left[-\sigma_{\theta\theta,z} - \sigma_{rz,rr} - \frac{\sigma_{rz,r}}{r} + \frac{\sigma_{rz}}{r^2} + \frac{\sigma_{z\theta,\theta}}{r^2} - \frac{\sigma_{z\theta,\theta r}}{r}\right.$$

$$\left. - \sigma_{zz,zr} + \sigma_{rr,rz} + \frac{\sigma_{rr,z}}{r} + \frac{\sigma_{r\theta,\theta z}}{r} + \sigma_{rz,zz}\right] \qquad (4.17)$$

As based on Eskinazi and Yeh's result on the gradient of $\overline{v_r' v_r'}$ in the radial direction, $\sigma_{rr,r}$ might be a potential contributor to secondary flow generation. Inspection of equation 4.17 however reveals this term does not directly influence the secondary flow process. One might infer that since $\sigma_{rr,r}$ is large, $\sigma_{rz,r}$ may also be large. Then $\overline{v_r v_z}$ and its radial gradient could drive the secondary flow generation process as indicated in the following expression

$$\frac{\partial}{\partial\theta}\left(\frac{\Omega_\theta}{q}\right) = -\left(\frac{3}{q^2}\sigma_{rz,r} + \frac{\sigma_{rz}}{q^2 r}\right) \qquad (4.18)$$

$$\frac{\partial}{\partial\theta}\left(\frac{\Omega_\theta}{q}\right) = +\frac{1}{q^2}\left[\left(3\frac{\partial}{\partial r} + \frac{1}{r}\right)\overline{v_r' v_z'}\right] \qquad (4.19)$$

where all second gradients and first gradients in θ and z have been

neglected. The effect of a large value of $\overline{v'_r v'_z}$ at the outer wall and a positive radial gradient of $\overline{v'_r v'_z}$ would work together in producing a positive streamwise generation of vorticity.

Oscillatory Secondary Vorticity

Turbulent flow in a pipe bend will lead to an oscillating secondary circulation if a binormal gradient of the normal Reynolds stresses, $\sigma_{rr,z}$ exists at the bend inlet. It will be assumed that the Reynolds stresses will be convected, without distortion, by the secondary circulation. The interaction of the binormal gradient of the Reynolds stresses with the secondary flow will lead to a harmonically oscillating circulation similar to the type found by Hawthorne (3) and by Marris (4).

The secondary vorticity Ω_t is related to the circumferential velocity component V_c, as illustrated in Figure 9, by

$$\Omega_t(\pi R^2) = V_c \, 2\pi R \tag{4.20}$$

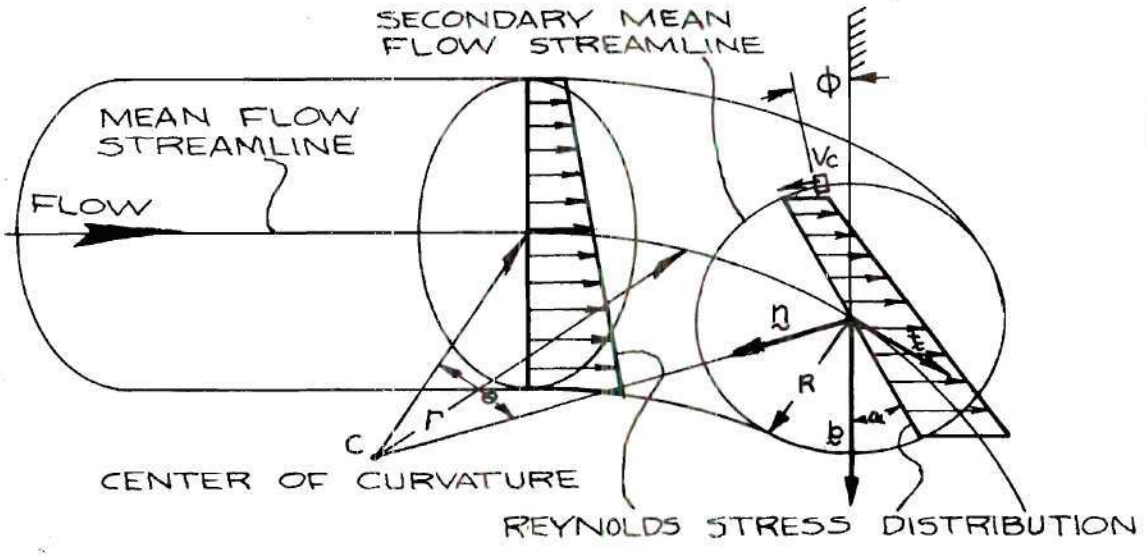

Figure 9. Secondary Vorticity in Pipe Bend.

when Ω_t is a suitable average value of the vorticity over the cross section of the pipe. Since the circumferential velocity can be related to an angular rotation rate $\dot{\phi}$, with respect to the fixed pipe walls, of the main flow, equation 4.20 leads to

$$\Omega_t = 2\dot{\phi} \tag{4.21}$$

The tangential velocity q, assumed unchanged by the small secondary flow, can be related to the angular position of an element of fluid as it moves around the bend by

$$q = r\dot{\theta} \tag{4.22}$$

Substituting equations 4.21 and 4.22 into the result for plane circular flow, yields a differential equation for the angular velocity of the secondary circulation $\dot{\phi}$ with respect to the angular velocity of the main stream $\dot{\theta}$ through the bend. The initial binormal gradient of the normal Reynolds stress, due to the convection by the secondary flow, will have $\frac{\partial \sigma}{\partial b}$ cos α component acting in the binormal direction as the flow proceeds around the bend. The differential equation is thus

$$\frac{1}{r}\frac{\partial}{\partial\theta}\left(\frac{2\dot{\phi}}{\dot{\theta}r}\right) = \frac{1}{q^2 r}\left(\frac{\partial \sigma}{\partial b}\cos\alpha\right) \tag{4.23}$$

Noting that $\varphi = \varphi_o + \alpha$ and assuming $\frac{\partial \sigma}{\partial b}$ is a constant at its initial value

$$\left.\frac{\partial \sigma}{\partial b}\right|_{\theta=0} = C \tag{4.24}$$

one obtains

$$\frac{\partial^2 \alpha}{\partial \theta^2} = \frac{C}{2\dot{\theta}^2 r}\cos\alpha \tag{4.25}$$

which is of the form of the differential equation of a pendulum making the angle α with the vertical

$$\frac{d^2\alpha}{dT^2} = M^2 \cos \alpha \tag{4.26}$$

The angular displacement through the bend for one full cycle of the secondary motion is

$$\Theta = \frac{2\pi}{\overline{M}} = 2\pi \Big/ \sqrt{\frac{(\sigma, b)\,|\theta = 0^o}{2\mathring{\theta}^2_r}} = 2\pi \sqrt{\frac{2r\mathring{\theta}^2}{C}} \tag{4.27}$$

The secondary velocity is related to the angular position in the bend by

$$V_c = \frac{-2\pi r \varphi_o}{\Theta} \sin 2\pi \frac{\theta}{\Theta} \tag{4.28}$$

This solution is based on the assumptions that the Reynolds stresses are carried along with the secondary flow and that these stresses are maintained at their initial values. Both of these assumptions are only approximations as the turbulent stresses are continually being generated by the presence of the wall and are continually being dissipated by the action of viscosity. It is felt that the assumptions would hold for short periods of time and therefore this model will give a qualitative picture of the flow behavior.

Secondary Flow Generation in a Turbulent Boundary Layer

In applying the secondary velocity result, equation 3.39, to plane, parallel turbulent boundary layer flow, the vortex-line tangent vector will be parallel to the plate and normal to the flow such that the vector $\underset{\sim}{V} \times \underset{\sim}{e}_1$ will be in the direction of the outward normal to the plate.

If the vortex lines are straight (i.e. K, the curvature, $\simeq 0$) the directions of $\underset{\sim}{e}_2$ and $\underset{\sim}{e}_3$ are arbitrary.

This would tend to introduce an ambiguity in the equations. However as the vortex lines lie in planes parallel to the plate and normal to the velocity vector, the only possible vortex line curvature would occur when the plate was bend in the direction of flow as illustrated in Figure 10. Therefore the flat plate treated in this section is a limiting case, $K \to 0$, of a curved boundary. The $\underset{\sim}{e}_2$

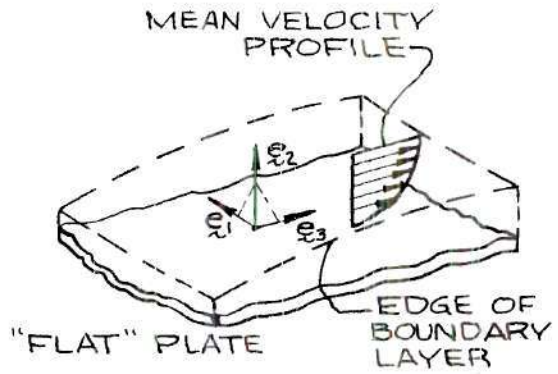

Figure 10. Secondary Velocity Coordinate System for Turbulent Boundary Layer Flow.

direction will therefore be normal to the plate, directed from the plate into the main stream. The $\underset{\sim}{e}_3$ direction, defined from $\underset{\sim}{e}_1$ and $\underset{\sim}{e}_2$ by the right hand rule, will point in the flow direction as shown in Figure 10. Using this flow model

$$\nabla \cdot \underset{\sim}{e}_1 \simeq \nabla \cdot \underset{\sim}{e}_2 \simeq \nabla \cdot \underset{\sim}{e}_3 \simeq 0 \qquad (4.29, 4.30, 4.31)$$

$$\nabla \times \underset{\sim}{e}_1 \simeq \nabla \times \underset{\sim}{e}_2 \simeq \nabla \times \underset{\sim}{e}_3 \simeq 0 \qquad (4.32, 4.33, 4.34)$$

$$\nabla \underset{\sim}{e}_1 \simeq \nabla \underset{\sim}{e}_2 \simeq \nabla \underset{\sim}{e}_3 \simeq 0 \qquad (4.35, 4.36, 4.37)$$

$$\frac{\partial U}{\partial x_3} \simeq \frac{\partial \omega}{\partial x_3} \simeq 0 \qquad (4.38, 4.39)$$

From 4.38 and 4.39 the Jacobian $\partial(U,\omega)/\partial(x_2,x_3)$ is approximately zero

$$\frac{\partial(U,\omega)}{\partial(x_2,x_3)} \simeq 0 \qquad (4.40)$$

Using the above approximations, equation 3.39 reduces to

$$\omega^2 \frac{\partial}{\partial x_1}\left(\frac{V_1}{\omega}\right) = -\sigma_{32,22} + \sigma_{32,2}\left(\frac{1}{\omega}\frac{\partial \omega}{\partial x_2}\right) \qquad (4.41)$$

Since $\omega = \partial q/\partial x_2$, the equation above may be expressed as

$$\frac{\partial}{\partial x_1}\left(\frac{V_1}{\omega}\right) = \frac{1}{\omega^2}\left[\frac{-\partial^2 \sigma_{32}}{(\partial x_2)^2} + \frac{1}{\omega}\frac{\partial \sigma_{32}}{\partial x_2}\frac{\partial^2 q}{(\partial x_2)^2}\right] \qquad (4.42)$$

The experimental measurements of P. S. Klebanoff (26) shows σ_{32}, which represents $-\overline{v_3 v_2}$, to have a positive second derivative near the wall that goes negative as the edge of the boundary layer, $x_2 = \delta$ is reached. The first derivative of σ_{32} is always positive, decreasing to zero at $x_2 = \delta$. The second derivative of q is zero very near the wall (i.e. in the viscous sublayer) and near the boundary layer edge, but it is negative through the central portion of the boundary layer.

Therefore near the wall $\frac{\partial}{\partial x_1}\left(\frac{V_1}{\omega}\right)$ will be negative and will tend to become positive with displacement toward the edge of the boundary layer. This leads one to expect the streamlines to bend towards the vortex line

near the wall and away from the vortex line near the edge of the boundary layer. Due to the opposite sense of the secondary velocities set up at different elevations within the boundary layer, the formation of a swirling or vortex type motion, as detected by S. J. Kline and P. W. Runstadler (27) could result. Similar experimental results have been reported by K. A. Meyer and S. J. Kline (28).

Secondary Flow Generation in a Curved Channel

To establish the influence of curvature on secondary velocity generation, equation 3.38 will be applied to turbulent flow in a curved channel of infinite depth. This model will approximate the flow in the central portion of a deep, narrow channel where the effects of the end plates are negligible. With increasing radius of curvature, the curved-channel result approaches the flat-plate result of the previous section.

The secondary velocity, taken to be small, is assumed to cause no appreciable distortion of the primary flow, which moves in circular paths around the channel.

The x_1, x_2, x_3 axis and unit vectors $\underset{\sim}{e}_1$, $\underset{\sim}{e}_2$, $\underset{\sim}{e}_3$ to be used are shown in Figure 11. The vector $\underset{\sim}{e}_1$ will, by definition, be parallel to the vortex vector; in this two dimensional model $\underset{\sim}{\Omega}$ will parallel the axis of curvature due to the boundary layer velocity gradient on the side walls. The vector $\underset{\sim}{e}_2$ will be chosen in the radial direction, and along the outer wall, directed towards the center of curvature. The direction of $\underset{\sim}{e}_3$ will be fixed from $\underset{\sim}{e}_1$ and $\underset{\sim}{e}_2$ by the right-hand rule. Due to the opposite direction of the vorticity vector at the outer wall from that at the inner wall, $\underset{\sim}{e}_1$, and $\underset{\sim}{e}_3$ will both undergo a change in sense from

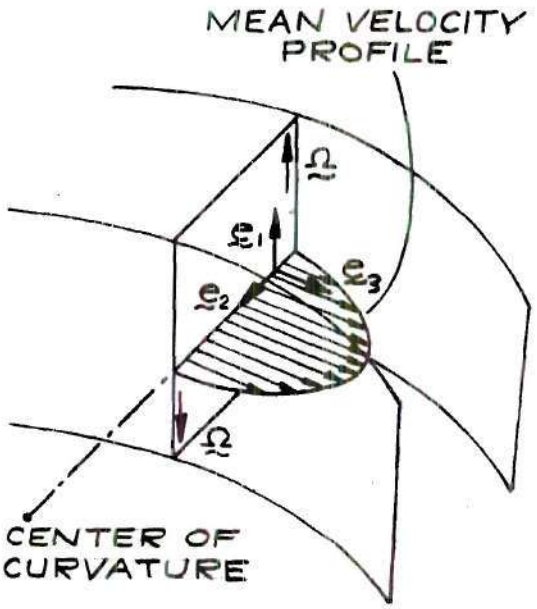

Figure 11. Vortex Line Coordinate System for Curved Channel Flow.

wall to wall.

To use standard vector operators, it will be convenient to convert the intrinsic coordinates to cylindrical coordinates. Referring to Figure 11,

$$\underset{\sim}{e}_1 = -\underset{\sim}{e}_z \tag{4.43}$$

$$\underset{\sim}{e}_2 = -\underset{\sim}{e}_r \tag{4.44}$$

$$\underset{\sim}{e}_3 = +\underset{\sim}{e}_\theta \tag{4.45}$$

Now since

$$\nabla = \underset{\sim}{e}_r \frac{\partial}{\partial r} + \frac{\underset{\sim}{e}_\theta}{r} \frac{\partial}{\partial \theta} + \underset{\sim}{e}_z \frac{\partial}{\partial z} \tag{4.46}$$

then

$$\nabla \underset{\sim}{e}_1 = -\nabla \underset{\sim}{e}_z = 0 \tag{4.47}$$

$$\nabla \cdot \underset{\sim}{e}_1 = -\nabla \cdot \underset{\sim}{e}_z = 0 \tag{4.48}$$

$$\nabla \times \underset{\sim}{e}_1 = -\nabla \times \underset{\sim}{e}_z = 0 \tag{4.49}$$

$$\nabla \underset{\sim}{e}_2 = -\nabla \underset{\sim}{e}_r = -\frac{1}{r} \underset{\sim}{e}_\theta \underset{\sim}{e}_\theta \tag{4.50}$$

$$\nabla \cdot \underset{\sim}{e}_2 = -\nabla \cdot \underset{\sim}{e}_r = -\frac{1}{r} \tag{4.51}$$

$$\nabla \times \underset{\sim}{e}_2 = -\nabla \times \underset{\sim}{e}_r = 0 \tag{4.52}$$

$$\nabla \underset{\sim}{e}_3 = \nabla \underset{\sim}{e}_\theta = -\frac{\underset{\sim}{e}_\theta \underset{\sim}{e}_r}{r} \tag{4.53}$$

$$\nabla \cdot \underset{\sim}{e}_3 = \nabla \cdot \underset{\sim}{e}_\theta = 0 \tag{4.54}$$

$$\nabla \times \underset{\sim}{e}_3 = \nabla \times \underset{\sim}{e}_\theta = \frac{\underset{\sim}{e}_z}{r} \tag{4.55}$$

In reducing equation 3.38, spatial changes with respect to z are neglected as the flow field is infinite in that direction. Spatial gradients in the flow, θ, direction are assumed small compared to gradients in the principal normal, r, direction. These simplifications, together with the above geometric conditions, lead to the following result:

$$\frac{\partial}{\partial x_1}\left(\frac{V_1}{\omega}\right) = \frac{1}{\omega^2}\left[\sigma_{\theta r,rr} - \frac{1}{\omega}\frac{\partial \omega}{\partial r}\sigma_{\theta r,rr} - \frac{2}{\omega r}\frac{\partial \omega}{\partial r}\sigma_{\theta r} + \frac{3\sigma_{\theta r,r}}{r}\right] \tag{4.56}$$

The two additional terms, $1/\omega^2\left(\frac{-2}{\omega r}\frac{\partial \omega}{\partial r}\sigma_{\theta r} + \frac{3\sigma_{\theta r,r}}{r}\right)$ represent the difference between this curved-channel result and equation 4.41 the

flat-plate result, illustrate the effect of curvature on secondary velocity generation. The sign change between these equations results from the change in coordinate system.

CHAPTER V

FLOW VISUALIZATION STUDY OF LAMINAR FLOW IN A CURVED CHANNEL

Introduction

A visual study of laminar flow in a curved channel was made to determine if streamwise vorticity was generated as has been predicted. Dean (30) and Reid (12), using stability criteria, have both shown the generation of streamwise vortex cells to be possible. Reid's analysis also yielded the size and position of the anticipated cells.

Flow between concentric rotating cylinders, the classical Taylor problem (31), gives a similar predicted secondary flow pattern. Several analytical analysis and experimental observations, reviewed by Chandrasekar (14), have been made for the concentric cylinder system. These results show that a velocity profile in which the velocity magnitude increasing radially inward, corresponding to a rotating inner cylinder and a stationary outer cylinder, leads to a streamwise component of vorticity. A similar velocity profile, velocity increasing with decreasing radius, exists in the region near the outer wall of a curved channel with stationary walls. The boundary layer velocity profile on the outer wall of a stationary curved channel should therefore lead to streamwise vorticity.

No experimental verification of Reid's analysis was available until 1958 and then only from a concentric cylinder apparatus. Brewster, Grosberg and Nissan (32) pumped glycerine-water solutions through a horizontal

concentric cylinder apparatus. Their visual results gave a tentative confirmation to the existence of streamwise vorticity. However the experimental apparatus used precluded smooth laminar flow into and out of the curved test section. Inlet and outlet pipes were connected into the concentric cylinder through a perforated rotating cylinder as shown in Figure 12. The abrupt change in flow section and the agitation supplied by the perforated cylinder could introduce large disturbances directly into the flow under study.

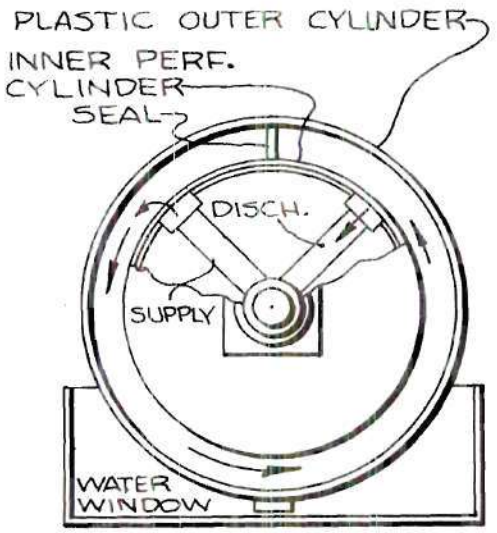

Figure 12. End View of Horizontal Concentric Cylinder Apparatus of Brewster, et al.

A laminar flow curved channel apparatus was built in this study to determine if longitudinal vortex flow could occur when the flow entered and left the test section smoothly. A second purpose for the experimental apparatus was to provide a simple flow example to which the analytical techniques of this study, simplified to laminar flow, might be applied.

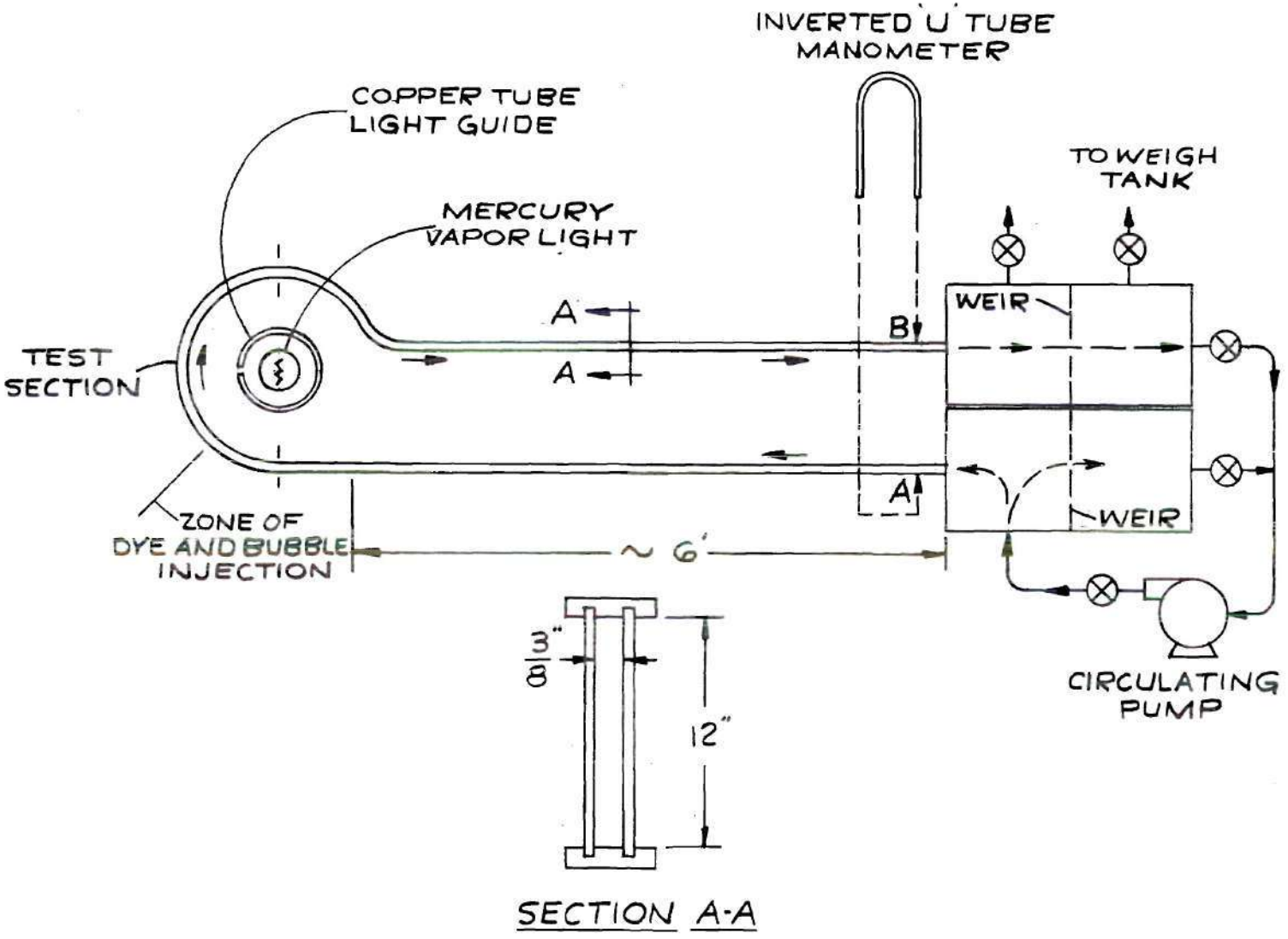

Figure 13. General Arrangement of Experimental Apparatus.

Discussion of Experimental Apparatus

The flow system used in this study is illustrated in Figures 13, 14, 15 and 16. A curved plexiglas test section, plexiglas inlet and exit ducts, a pair of constant head tanks and a circulation pump were arranged as shown in Figure 13.

The test section was a horizontal return bend with a constant radius of curvature and a rectangular flow passage 3/8 inch wide by 11-3/4 inches deep. The inner wall had a two inch of curvature. The curved walls were formed from segments of cast acrylic cylinders with 1/8 inch wall

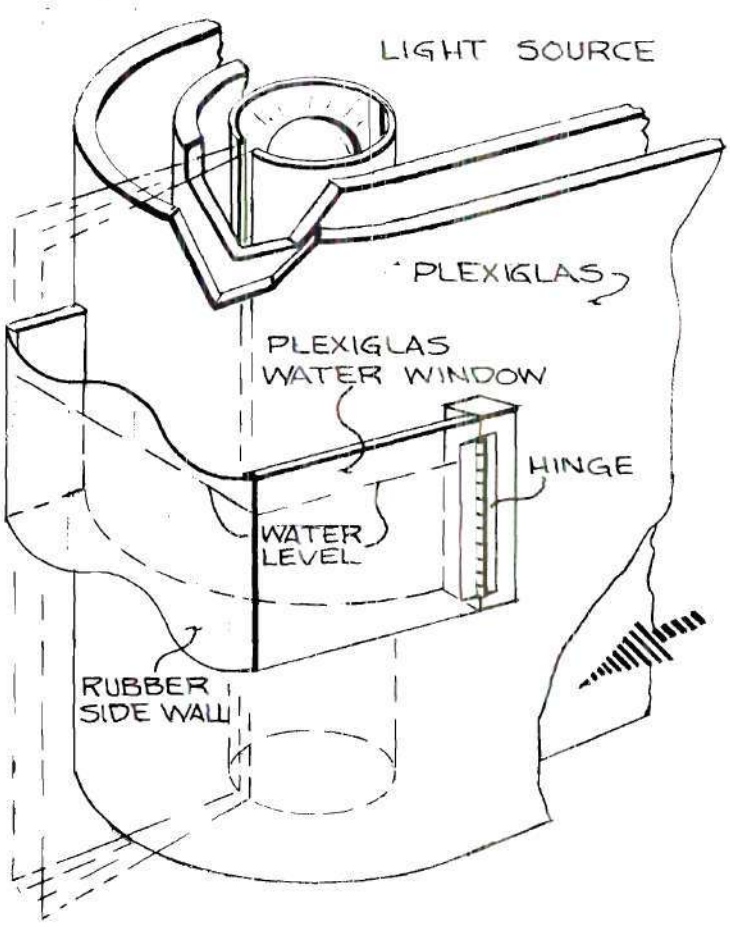

Figure 14. Sketch of Curved Channel Test Section.

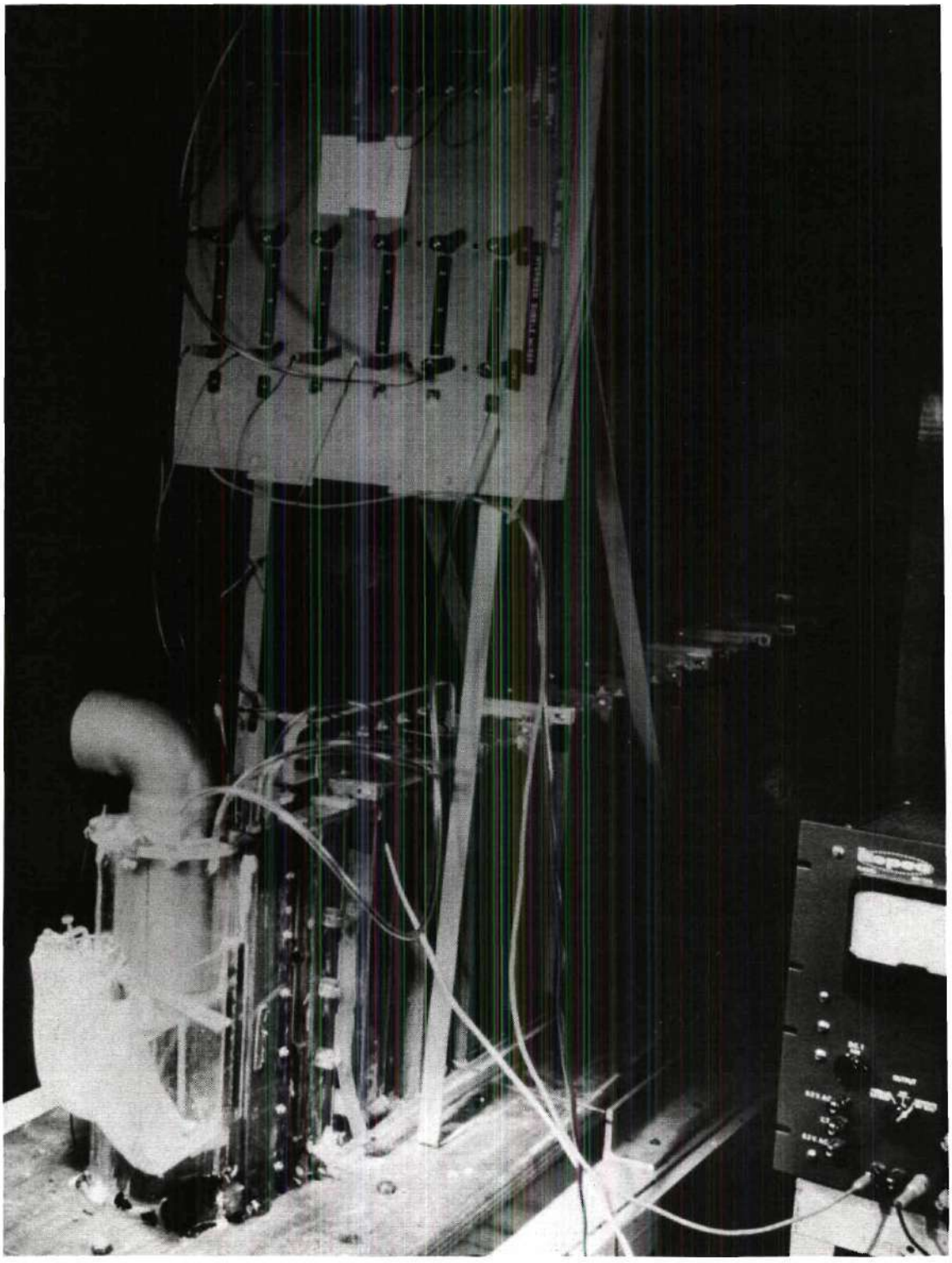

Figure 15. Experimental Apparatus, End View.

thickness. The inner wall was a section from a four inch O. D. cylinder while the outer wall was cut from a five inch O. D. cylinder.

The top and bottom plates were machined from 1/4 inch plexiglas plate. One-eighth inch slots milled into the plates permitted the cylindrical side walls to recess into these end walls. Steel thru-bolts, 13 inches long, were installed outside the side wall, extending from the top through the bottom plate and secured on the under side of a 3/4 inch plywood base. The plywood base provided structural rigidity to the plexiglas duct system.

A set of electrode holders, shown in Figure 17, were placed in a water tight box at the entrance to the curved section. The holders were accurately milled from 1/4 inch plexiglas stock to insure a smooth, flat internal surface. The holders were also carefully aligned and pinned together to eliminate any flow disturbances.

Water entered and left the test section in straight plexiglas ducts approximately six feet in length. These ducts, with 3/8 inch by 11 3/4 inch crossections to match the test section, had 1/8 inch plexiglas side walls and 1/4 inch plexiglas tops and bottoms. As in the test bend, the top and bottom plates, were slotted to permit recessing the side walls.

The straight ducts were fastened, as above, to the same plywood base as the test section. The base was fitted with leveling screws to hold the test section and ducting horizontal. It was found necessary to add vertical ribs to the side walls of the straight duct to prevent the walls from bowing under the applied pressure. Braces were also required to maintain the vertical alignment of the channel.

The flow rate was established by controlling the static head across

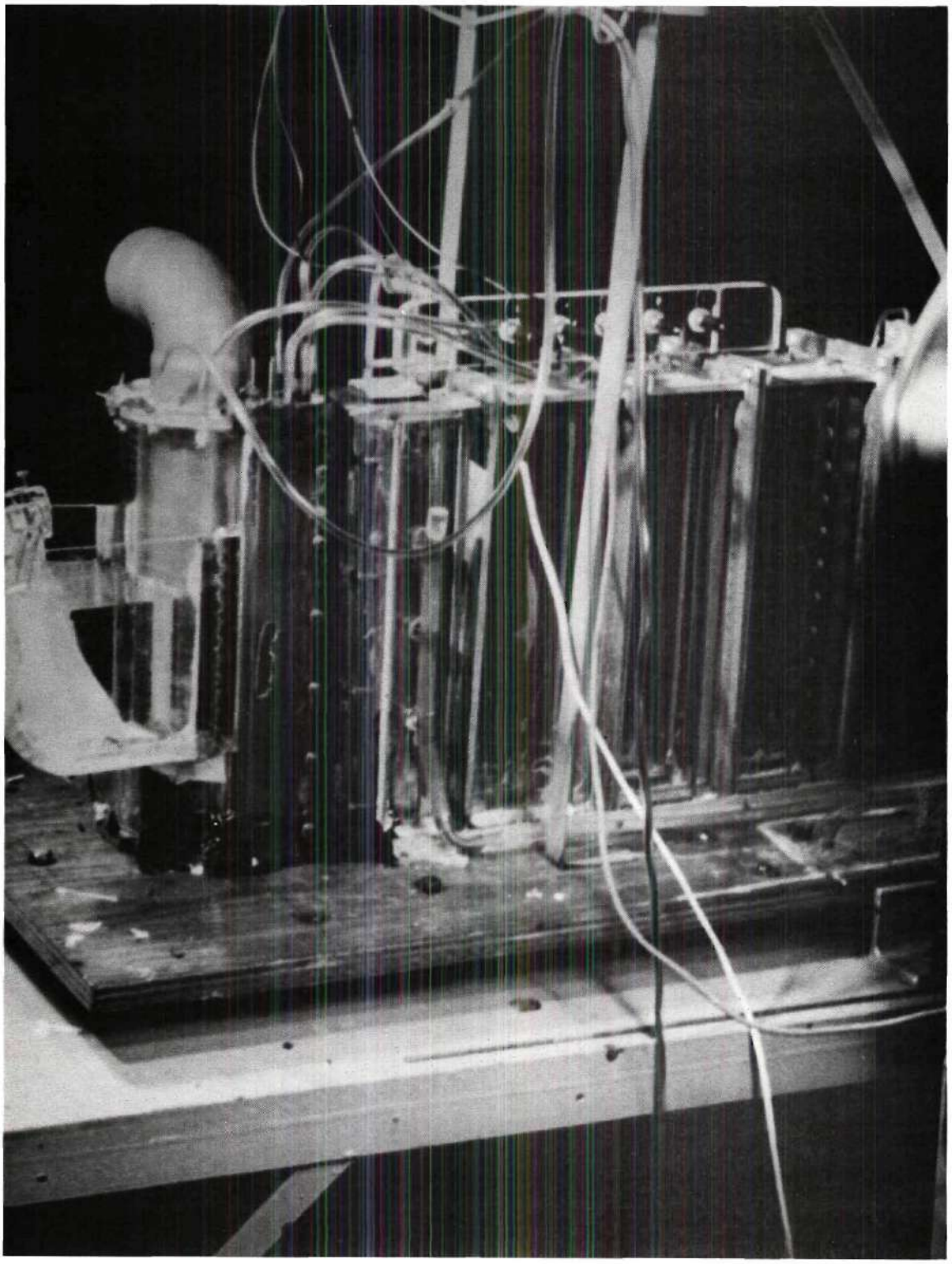

Figure 16. Experimental Apparatus, Side View.

the system. Control of the static head was maintained by using an adjustable weir in the supply and in the discharge tanks. By controlling the weir heights, the static pressure and pressure drop could be adjusted easily. The tanks and weir system used are illustrated in Figure 13.

Pressure drop was measured by an inverted, oil over water, U-tube manometer. One leg of the manometer was connected to a set of three static pressure taps spaced vertically near the entrance of the supply duct and the other leg to a similar set of taps at the exit of the discharge duct. These positions are noted A and B respectively on Figure 13. An auxiliary weight tank was used to determine the flow rate as a function of pressure drop through the duct system.

The test section and connecting ducts were made of plexiglas not only to permit visual observation but also to provide additional protection from electrical shock. The insulating property of the plastic thus provided a safety factor in using the selected visualization technique. This technique, called the hydrogen bubble method, used high voltage DC current to electrolyze the flowing water.

The hydrogen bubble technique, perfected by Geller (33) in 1954 and later refined first by Clutler and Smith (34) and then by Schraub, et al. (35), uses very small bubbles to mark the flow patterns. A brief description of this method, which appears to be the most useful and versatile available to visualize low speed flows, is given below.

Water molecules can be broken into ions of the constituent elements, H_2 and O_2, by applying an electrical power source of sufficient voltage across two immersed electrodes. The electrolysis threshold voltage is dependent on the impurities present in the water, but with only a slight

water hardness, the electrolysis was found to commence at less than 25 volts. At low voltage however, insufficient bubble generation occurred for good visual pictures. Flow studies at velocities of 0.1 to 1.0 feet per second were made using potentials of 200 to 400 volts. Some observations were made with potentials as high as 900 volts, the upper limit of the available power supply. In general it is not necessary to go to voltages above 300, and by using additives to raise the water's conductivity, this upper voltage can be reduced even further.

During the electrolysis process hydrogen ions collect at the cathode where H_2 gas is evolved. A similar process occurs at the anode with oxygen. Since the water molecule is composed of two hydrogen atoms per oxygen atom, hydrogen gas is generated at twice the rate of oxygen. The hydrogen gas is thus the better visual marker, though both H_2 and O_2 can be used together if two separate traces are desired.

The gas generated at the electrodes is swept off by the flowing stream. The buoyant force should be much smaller than the viscous drag force for a bubble to follow the stream well. Therefore very small bubble sizes are necessary. A terminal velocity due to buoyancy can be computed from Stokes equation for $N_{Re} < 1.0$. Equating the buoyant force to the Stokes drag force, the following expression is obtained relating the terminal velocity u_t in ft/sec to the bubble diameter D' in thousandths of an inch

$$u_t = \frac{D^2\left(1 - \frac{\rho_{H_2}}{\rho_{H_2O}}\right)g}{18\,\nu} \simeq \frac{D^2 g}{18\,\nu} = 0.00124\,(D')^2 \qquad (5.1)$$

For a 0.001 inch diameter bubble, $N_{Re} = 0.084 \ll 1$, the computed terminal velocity is 0.001 feet per second. Thus 0.001 inch diameter bubbles generated in a 0.25 ft/sec mean velocity stream will rise only 0.020 inch during a five inch path.

Sufficiently small bubbles can be generated by using fine wires, 5 mils or smaller, as the marking electrodes. The diameter of the bubbles generated ranges from 0.5 to 1.0 times the diameter of the wire (35), depending on the water velocity and the applied potential. Lowering the fluid velocity or raising the voltage can cause an increase in bubble size.

Stainless steel or tungsten wires, 1 to 5 mils in diameter, were used as the hydrogen generators and were installed in the flow channel upstream of the section to be studied. As only one bubble line was needed to mark the flow, the oxygen electrode was placed downstream of the test section. A vertical 80 mil stainless steel hypodermic tube was used for the anode instead of small wires because the bubble generation rate appeared to decrease with decreased anode size. This effect is thought to be caused by the reduction in conductance between the anode and the fluid accompanying a decrease in anode surface area. An anode surface greater than that of the 80 mil tube did not seem to improve the bubble generation rate significantly.

The relatively large anode tube was also much easier to handle than the fragile wires used for the cathode. Wires two mils or less in diameter proved to be very aggravating to use. Extreme care and patience had to be employed together with some special techniques. As wires were installed vertically with a 12 inch unsupported length, they had to be

placed in tension to prevent bowing. The combination of length and tension made the wires susceptible to breakage by any foreign matter entrained in the flow. The charged wire also seemed to attract and collect small pieces of scale and lint. This buildup of trash seriously interfered with the wire performance, reducing, and in extreme cases virtually eliminating the bubble generation. It was therefore found desirable to keep the water as clean as possible to minimize cleaning and periodic replacement of the bubble wires.

Electrical power was supplied to the electrodes from a Kepco regulated DC power supply, Model 430 D. It contained two independent power supplies which could be used individually, in series or in parallel; each power supply was capable of supplying 500 milliamperes current at potentials up to 450 volts.

A concentrated high-intensity light source is required for good visual results. The bubbles become brilliant spots when they enter an area of high light intensity. The incident light reflected from the liquid-gas interface gives the bubbles the appearance of small, almost point, light sources.

To detect the streamwise component of vorticity, the flow patterns in planes normal to the streamlines were selected for observation, with the line of sight being in the tangential direction as shown in Figure 17. To achieve this result, a line source of light was needed. The illumination could then be confined to the section under observation as uniform illumination of the entire test section gave poorer results. Light reflected from bubbles throughout the flow and the bubbles closest

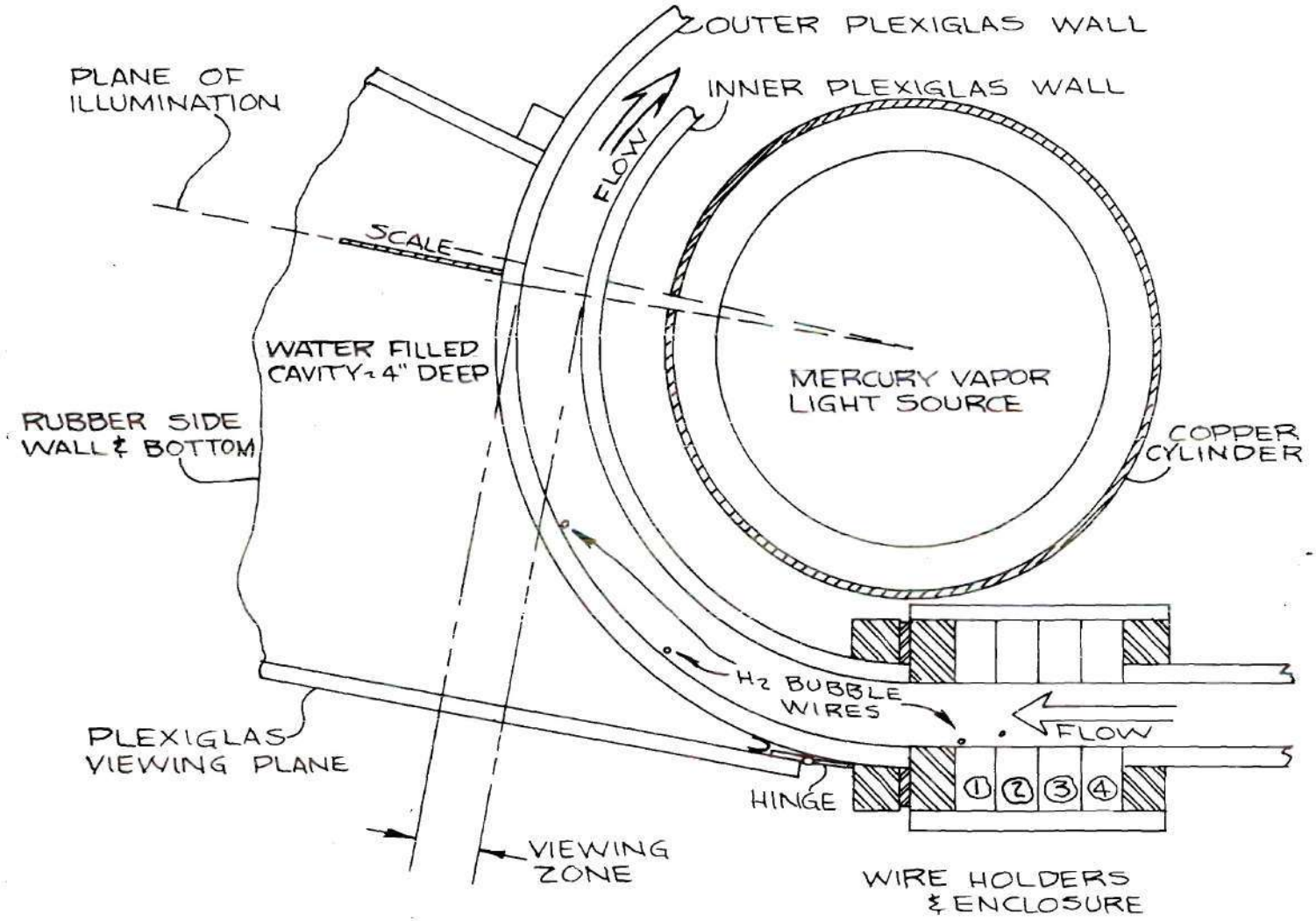

Figure 17. Detail of Lighting System and Observation Window.

to the observer effectively masked the flow in the interior of the passage. A light source, described below, was placed near the center of curvature of the test section and light was emitted radially from a vertical line. The arrangement proved very effective as maximum contrast between the bubbles and the surroundings was obtained when the line of observation was perpendicular to the plane of light. This geometry also protected the observer's eyes from direct rays of high intensity light.

The vertical plane of light also proved very advantageous in identifying or locating the flow plane selected for observation. Thus if the section 135 degrees from the inlet was to be studied, the light source could be directed to that plane. Only the bubbles passing through the illuminated band, as depicted in Figure 17, obtained the brilliance associated with good visibility.

The desired high intensity light was provided by a cylindrical mercury vapor lamp, approximately 2-1/4 inches in diameter by 11 inches long, enclosed in a section of three inch O.D. copper pipe. A 1/8 inch axial slot milled in the pipe was used to form the line source. The tube-bulb combination, when installed vertically near the center of curvature of the test section, provided a serviceable light source. Rotation of the pipe in a stationary mounting collar allowed the direction of the light to be controlled.

A small auxiliary fan forced cooling air between the lamp and the tube to keep the plexiglas test section from being damaged by the high temperature of the lamp. An elbow that was installed at the top of the tube directed extraneous light and hot air away from the observer.

Even with a very strong light source, some difficulty was encountered in visual study during the daylight hours. Much better results were obtained at night when the background light was negligible. As might be anticipated good photographic results were more difficult to obtain than good visual observations. Many flow patterns that could be interpreted by direct observation were unintelligible on film, even when the photographs were taken under ideal conditions. Because of this difficulty, some of the flow patterns to be described will not be supported by photographic records.

The curved wall of the test section with water on one side and air on the other, caused severe distortion of the visual image. This difficulty, due to the difference in coefficient of refraction between water and air, was eliminated by installing a water window on the curved channel. The window, illustrated in Figure 17 was simply a container of water, having one flat viewing surface, attached to the outside of the curved section. Using the water window, light traveling from the H_2 bubbles to the point of observation would pass through the curved wall from water into water. The passage from water to air was accomplished across the flat viewing surface, where the refraction coefficient difference would introduce no distortion.

A hinge attaching the viewing surface to the test section permitted the surface to rotate about a vertical axis. A flexible rubber membrane was used for the bottom and one side of the window section to keep the compartment water-tight while allowing movement of the viewing plane. During use, the flat viewing face of the window was aligned parallel to the flow section selected for observation. The light source was also

adjusted to illuminate the same plane of flow. Control over both the viewing face and the light source permitted selective observations to be made around the channel.

The plastic ruler appearing in the photographs of the bubble patterns was located inside the water window. Placed in the plane of observation, the ruler served a dual purpose. It provided a scale, in centimeters, to make measurements from the photographs and it served as a convenient reference on which to focus the camera.

Visual Results

Illustrated in the following photographs and sketches are the flow patterns identified by the hydrogen bubbles. The water window was attached to permit observation of the central portion of the channel, far removed from the influences of the end plates. All the patterns illustrated were marked by straight vertical wires, located along the outer channel wall, producing continuous streams of bubbles.* The size and position of the wires used is listed in Table 1. The photographs were taken with the average velocity in the channel set at 6 fpm, 15 fpm or 16-1/2 fpm. Each of these values is well above the critical velocity of 1.69 fpm, computed in Appendix F. The vortex formation appears clearer and more dramatic at the high velocities as the high velocity cells were established at smaller angles of turning, θ, through the bend.

---

*Some workers (34,35), have used kinked wires and pulsed voltages. Neither of these techniques were used in the illustrations.

Table 1. Location and Size of Vertical Hydrogen Bubble Wires

Wire Designation	Location		Wire Diameter
	t Direction	n Direction	
1	1/2" from inlet	1/8" from OD wall	0.003"
2	1/4" from inlet	1/16" from OD wall	0.001"
3	in bend, θ = 5°	1/32" from OD wall	0.003"
4	in bend, θ = 30°	1/32" from OD wall	0.001"

Well defined secondary flow patterns were observed for velocities above the critical value. Secondary flows did develop as streamwise vortex cells confirming the secondary flow type predicted by Reid (12).

At very low flows, considerably below the critical velocity, secondary flow patterns in the central section of the channel were absent. The vertical sheet of hydrogen bubbles traveled around the curve undistorted except for some minor disturbances near the end plates. Due to the method of installing the bubble wires, clear pictures of the flow in the vicinity of the end plates could not be obtained.

The general pattern of the secondary flow development was similar in all of the observed cases and is illustrated in Figure 18. The bubbles would leave the wires in a vertical sheet which appeared, in crossection, as a straight line. Portions of this straight line commenced to be displaced in the radial direction as the flow proceeded around the channel. The bending of the vertical bubble lines tended to form a modified sine wave with the amplitude extending in the principal normal direction and

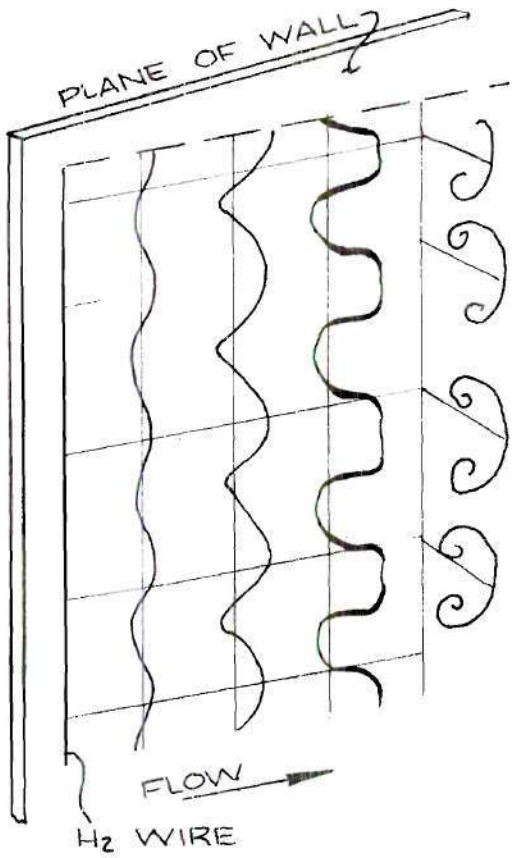

Figure 18. Transition of Straight Bubble Line into Vortex Patterns.

the wave length in the binormal direction. Photographs of the wave can be seen in Figures 20.c, 22.a, and 30.b. The wave continued to grow in amplitude but exhibited some flattening at the inward projecting crests. As the bubble lines are swept around the channel, the wave crests projecting inward start breaking over themselves as seen in Figures 20.a, 20.d, 22.a and 22.b. This rolling occurred only for the inward crests and no such behavior was observed for the crests at the outer wall. Following the breaking, the secondary flow developed into a series of streamwise vortex cells, generally consisting of vortex pairs. The cell patterns are clearly evident in Figures 26.b, and 28 through 32.

Just prior to the breaking of the wave form, the flattening and spreading of the wave crest gave rise to a striking flow pattern. The bubble density in the crests was rapidly depleted and the initial vertical bubble sheet was transformed into a series of horizontal sheets. Viewed in crossection this flow pattern gave the appearance of a ladder set into the flow passage with side walls forming the ladder rails and the bubble lines forming the rungs. The horizontal sheets, looking in the streamwise direction, appeared to curve smoothly into the vortex cells, as can be seen in the upper part of Figure 26.a. In many observations the horizontal sheets were the most dominant feature of the flow. The strong horizontal lines can be seen in Figure 27.

Some vacant spaces were noticed in the bubble patterns; e.g. Figure 26.a, and 28; however the actual secondary flow pattern should be distributed throughout the crossection. It is felt that the bubble density in these unmarked zones was too low to illustrate adequately the flow pattern.

Several different types of vortex patterns were observed, as illustrated in Figure 19. Both the radial position of the center and the diameter of individual cells varied. Even within a vortex pair, the individual vortices differed in size. This is in marked contrast to Reid's theory (12) which predicts uniform size and spacing. It is also contrary to the observations of Brewster (32).

Vortex pairs were observed in which the smaller vortex was only half the diameter of the larger one, as shown in Figure 19.b. Sizes of individual vortex cells ranged from a maximum of approximately 5/16 inch to a minimum of 1/8 inch. Based on the channel width, the nondimensional

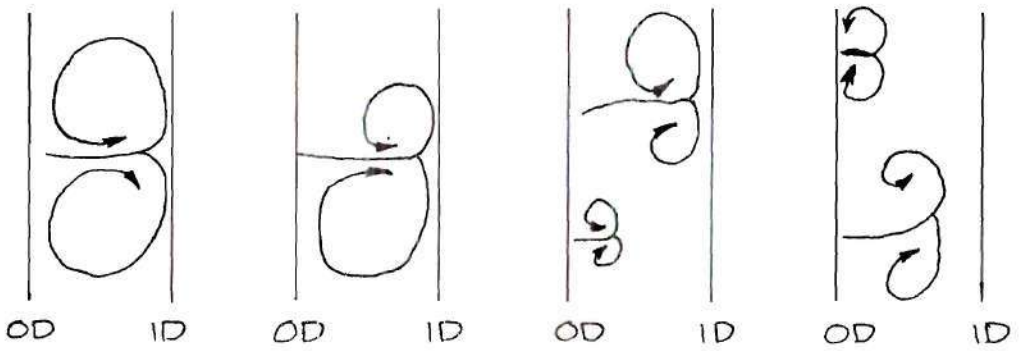

Figure 19. Typical Secondary Flow Patterns Observed.

vortex size R varied from 0.833 to 0.333; however the majority of the cells appeared near R = 0.5 or a diameter of 3/16 inch. Brewster (32) identified only one vortex size, R = 0.5, while Reid (12) shows R = 0.8. Neither of these workers mentions the possibility of size nonuniformity as illustrated by photographs in Figures 25.a, 26.a and 26.b.

The radial positions of the vortex cells, particularly the smaller ones had a wide variation as can be seen in Figures 28 and 29. Small vortices were observed in radial positions ranging from nearly tangent to the outer wall to within 0.1 d of the inner wall as well as at intermediate positions. The larger cells had much less latitude of movement and exhibited only small variations in radial position.

The bubbles mark particular fluid particles, those flowing directly across the H_2 electrode. The marked particles passing various points along the length of the wire, may ultimately constitute different relative parts of the vortex cells under observation. It is therefore possible that different radial positions, with respect to the vortex center, were made visible in one vortex as compared to another. If the bubbles

mark pockets of fluid that form the outer edge of one vortex and other bubbles identify fluid elements that form an intermediate radius of a second cell, two equal sized cells could appear different in size. This variation in marking may account for some of the differences in cell size observed but would not explain the variation in radial position. External perturbations and nonuniformity of the flow may also be responsible for some of the variations.

Figure 20 through 33, catalogued in Table 2, illustrate photographic results obtained in the visual study. Some of the photographs are difficult to interpret, others contain little usable information, while others give a very graphic illustration of the secondary flow patterns and the formation of streamwise vorticity. Many times two photographs of the same situation will reveal different points. This wide selection of photographs was included to illustrate the broad spectrum of visual patterns and type of results obtained. In general the best results were obtained from wire number 3, a 3 mil wire position on the outside wall, 5° into the bend. No reason was observed for the superior performance obtained from this wire location.

Kinematic-Kinetic Result Applied to Laminar Curved Channel Flow

The general results of both the secondary vorticity generation and the secondary velocity production can be specialized to apply to laminar flow. The turbulent flow results can be adapted to laminar flow simply by setting the Reynolds stress terms to zero.

The turbulent result for secondary vorticity generation along a streamline, equation 3.15, leads to:

Table 2. Schedule of Bubble Pattern Photographs

Figure No.	Page No.	Wire Ident. No.	Viewing Plane degrees from inlet	Average Velocity fpm
20.a,b	82	1	67°	6
20.c,d	82	1	100°	6
21.a,b	83	1	65°	16.5
21.c,d	83	1	110°	16.5
22.a,b	84	2	67°	6
22.c,d	84	2	110°	6
23.a	85	2	65°	16.5
23.b	85	2	90°	16.5
23.c,d	85	2	110°	16.5
24.a,b	86	3	67°	6
24.c,d	86	3	100°	6
25.a,b	87	3	65°	16.5
25.c,d	87	3	90°	16.5
26.a,b,c	88	3	110°	16.5
27.a,b	89	3	67° (closeup)	15
28.a,b	90	3	100° (closeup)	15
29.a,b	91	3	100° (closeup)	15
30.a	92	4	67°	6
30.b,c	92	4	100°	6
31.a,b	93	4	65°	16.5
31.c,d	93	4	70°	16.5
32.a,b	94	4	110°	16.5
33.a,b	94	4	100° (closeup)	15

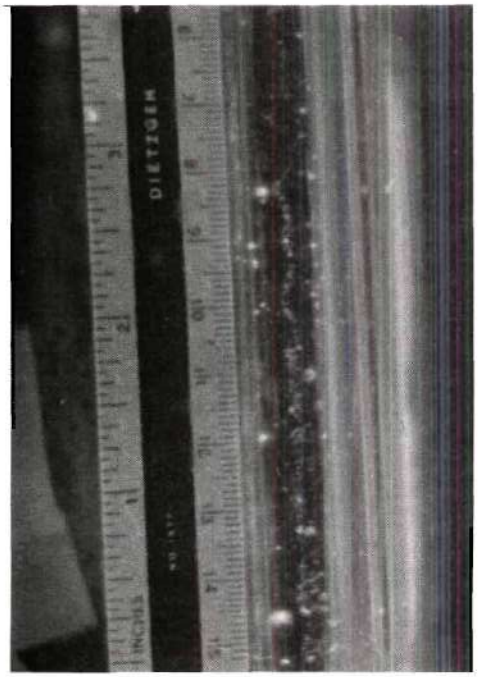

(a) $\theta_v = 67°$

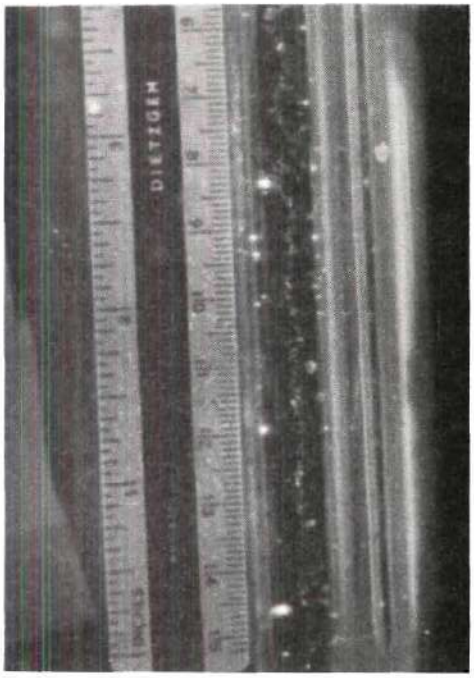

(b) $\theta_v = 67°$

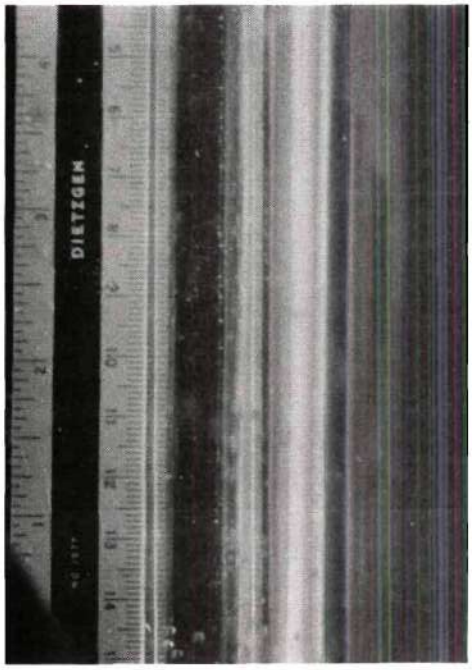

(c) $\theta_v = 100°$

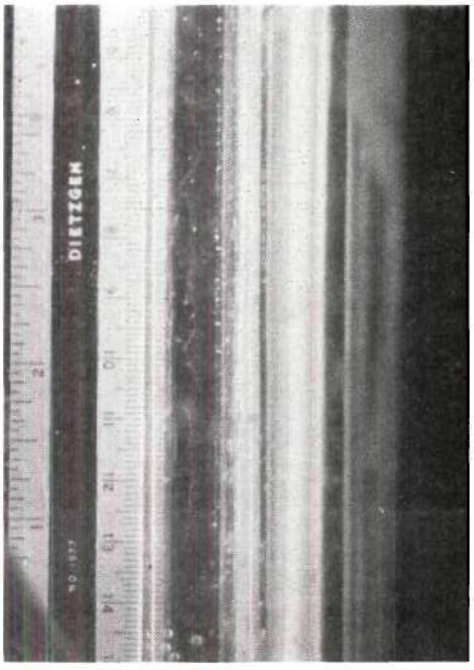

(d) $\theta_v = 100°$

Figure 20. Bubble Pattern from Wire No. 1, $V_{avg.} = 6$ ft/min.

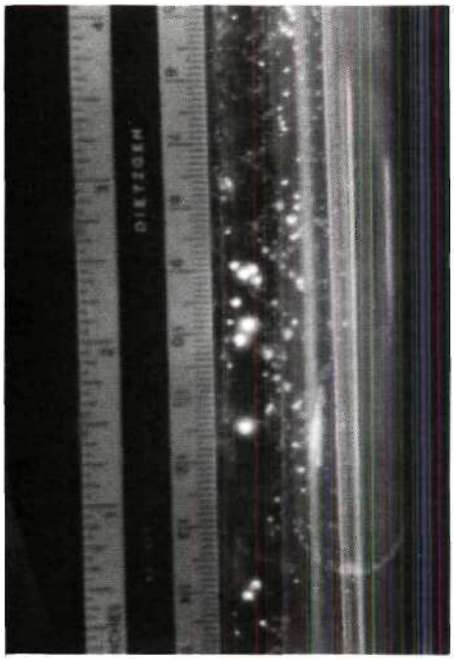

(a) $\theta_v = 65°$

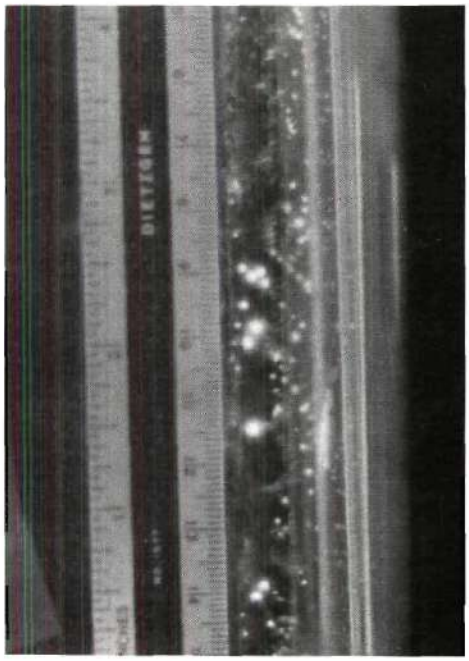

(b) = $\theta_v = 65°$

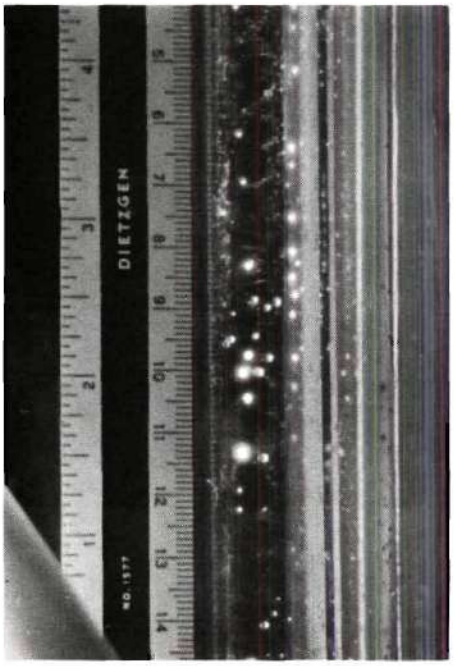

(c) $\theta_v = 110°$

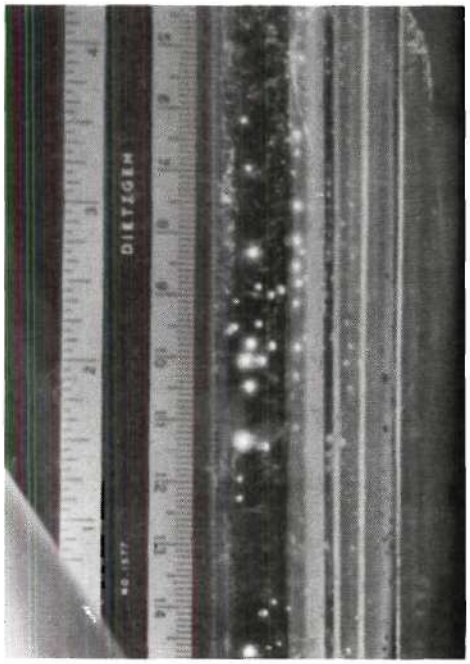

(d) $\theta_v = 110°$

Figure 21. Bubble Pattern from Wire No. 1, $V_{avg.} = 16\text{-}1/2$ ft/min.

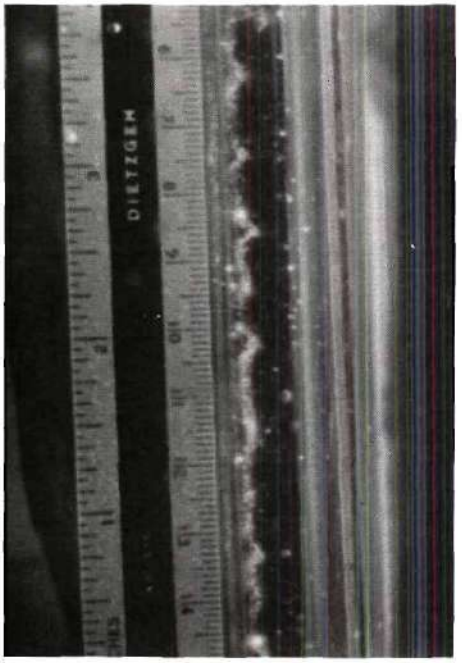

(a) $\theta_v = 67°$

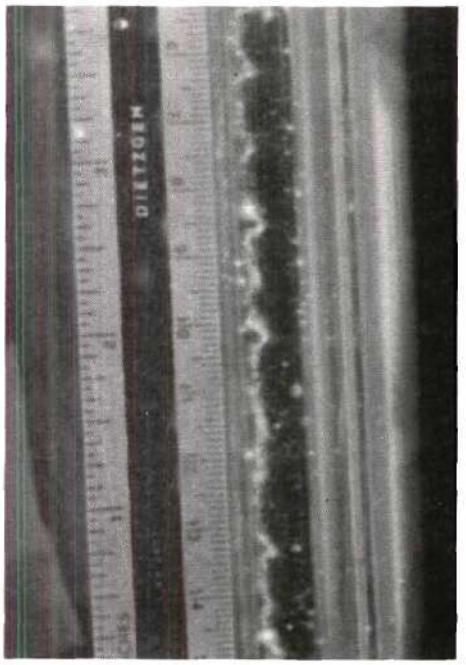

(b) $\theta_v = 67°$

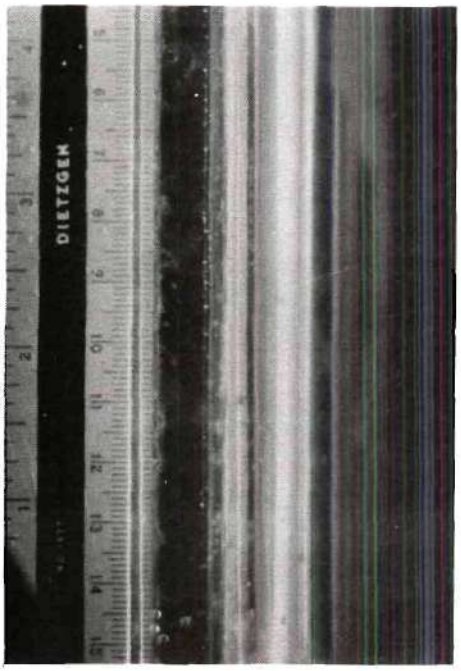

(c) $\theta_v = 100°$

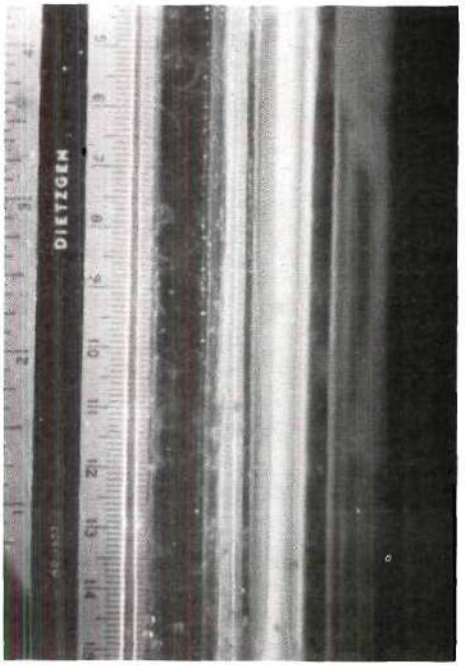

(d) $\theta_v = 100°$

Figure 22. Bubble Pattern from Wire No. 2, $V_{avg.} = 6$ ft/min.

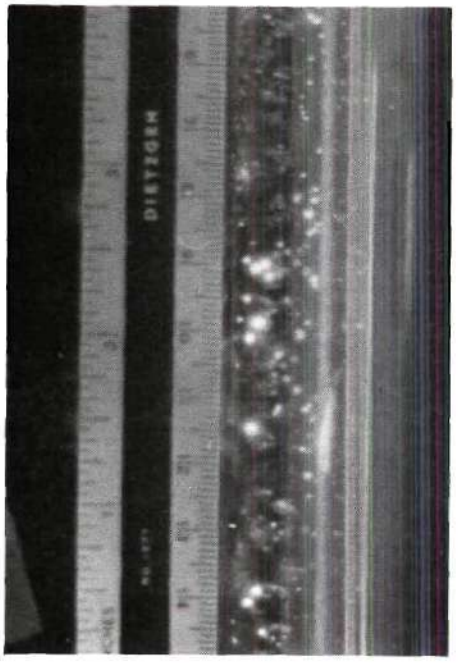

(a) $\theta_v = 65°$

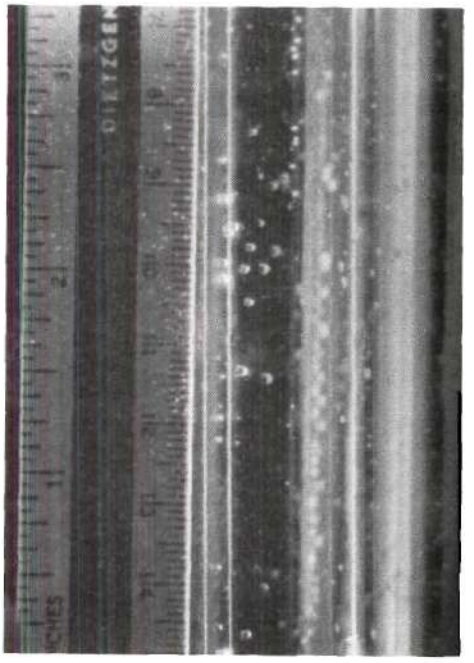

(b) $\theta_v = 90°$

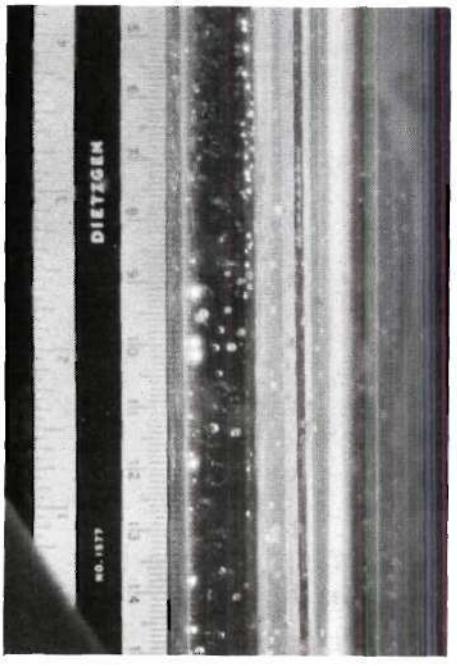

(c) $\theta_v = 110°$

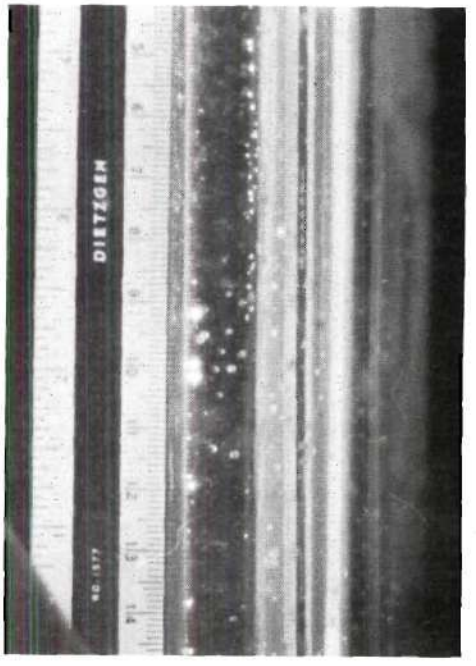

(d) $\theta_v = 110°$

Figure 23. Bubble Pattern from Wire No. 2, $V_{avg.}$ = 16-1/2 ft/min.

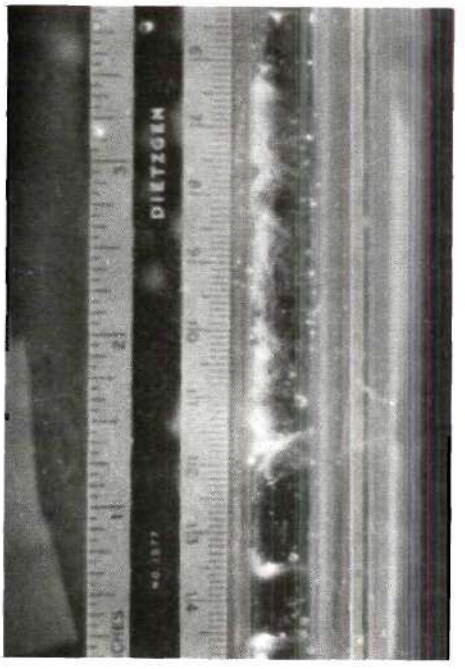

(a) $\theta_v = 67°$

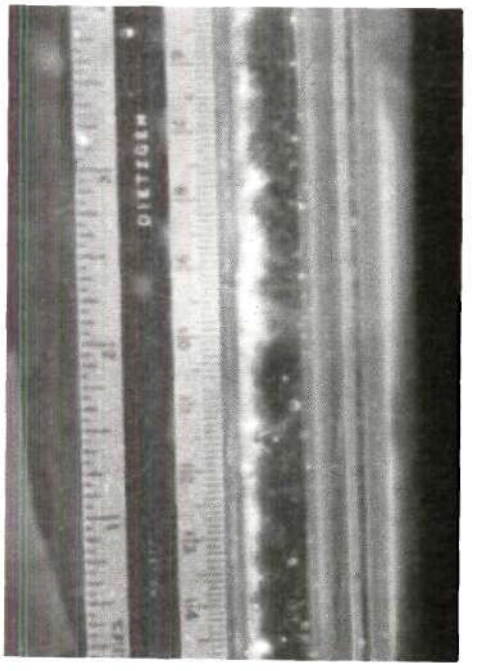

(b) $\theta_v = 67°$

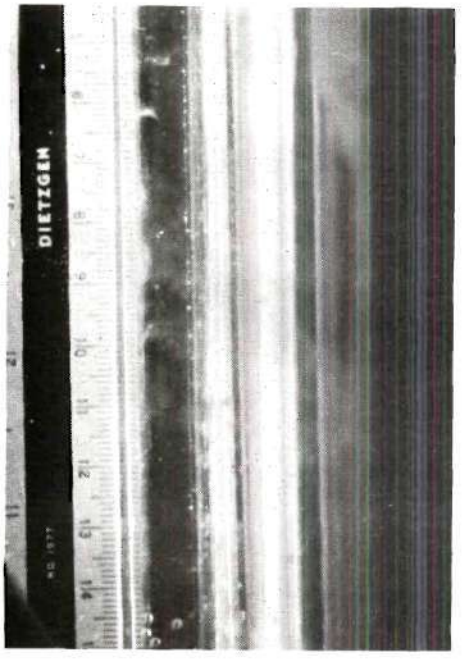

(c) $\theta_v = 100°$

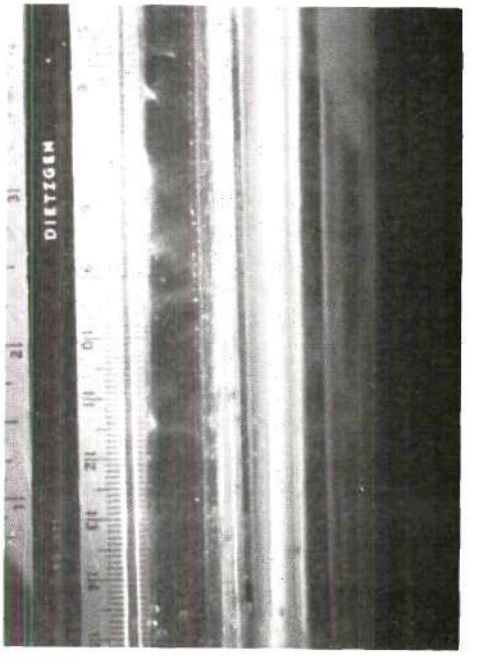

(d) $\theta_v = 100°$

Figure 24. Bubble Pattern from Wire No. 3, $V_{avg.} = 6$ ft/min.

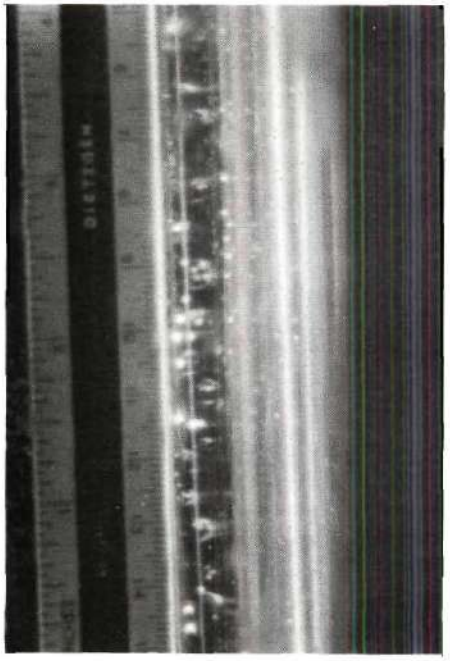

(a) $\theta_v = 65°$

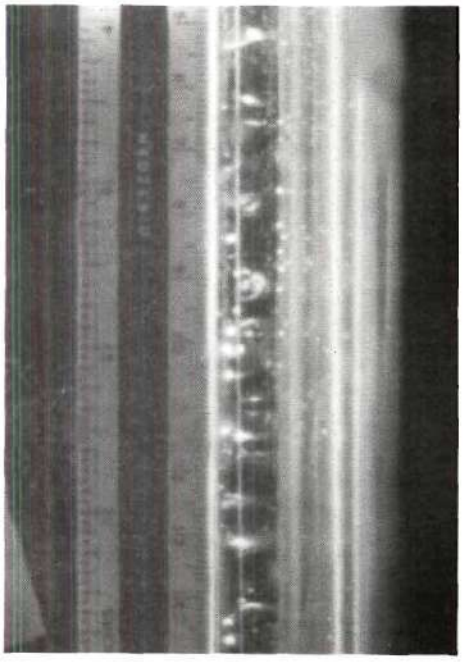

(b) $\theta_v = 65°$

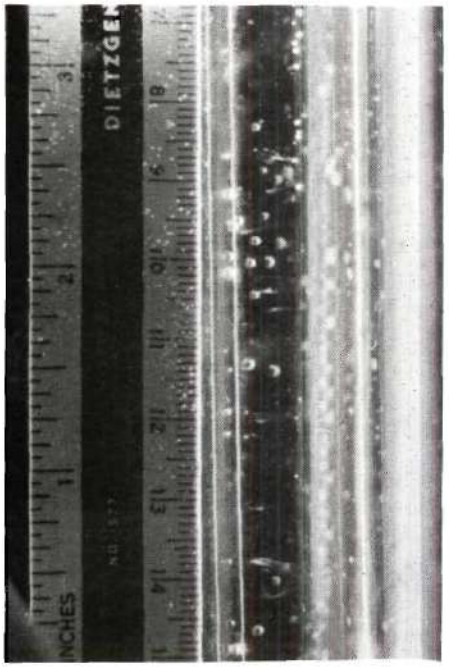

(c) $\theta_v = 90°$

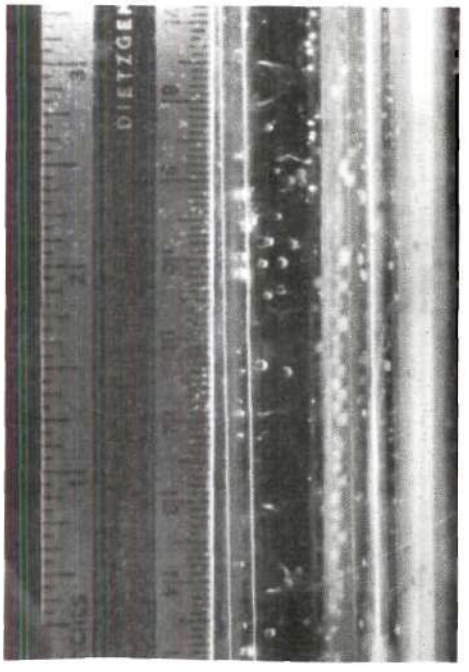

(d) $\theta_v = 90°$

Figure 25. Bubble Pattern from Wire No. 3, $V_{avg.}$ = 16-1/2 ft/min.

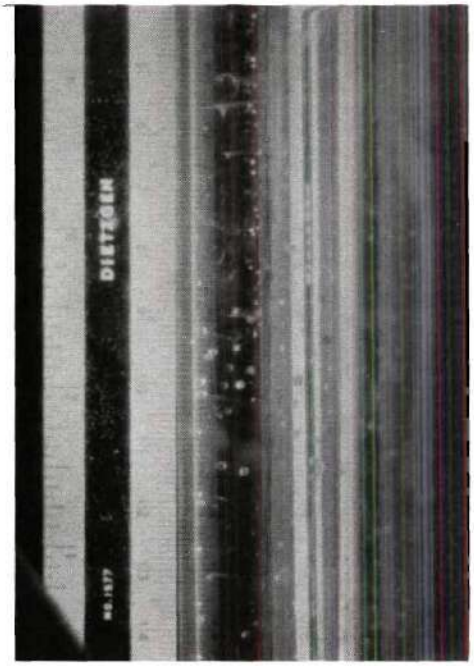

(a) $\theta_v = 110°$

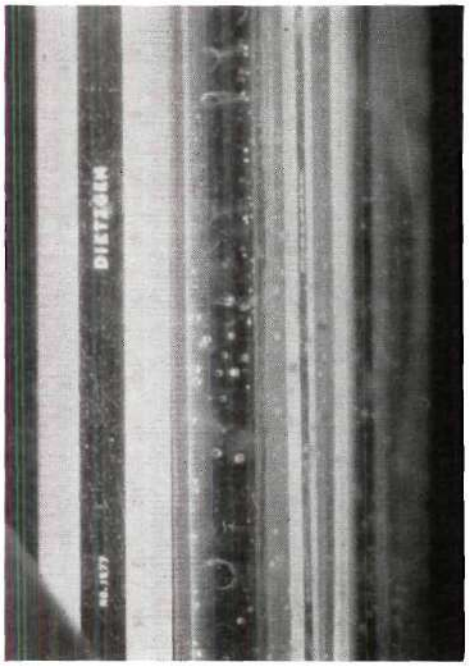

(b) $\theta_v = 110°$

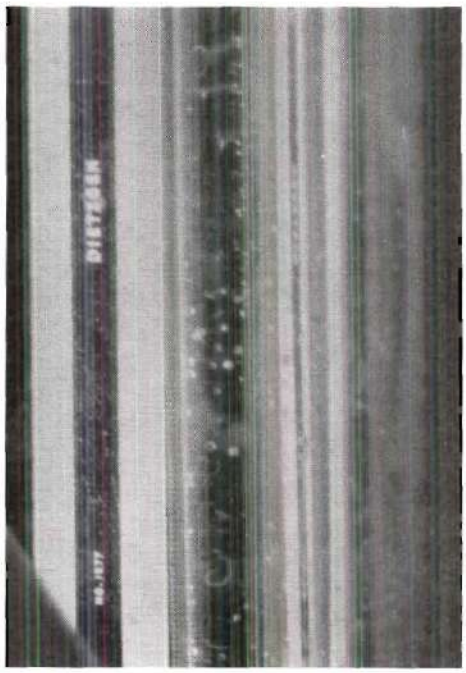

(c) $\theta_v = 110°$

Figure 26. Bubble Pattern from Wire No. 3, $V_{avg.} = 16\text{-}1/2$ ft/min.

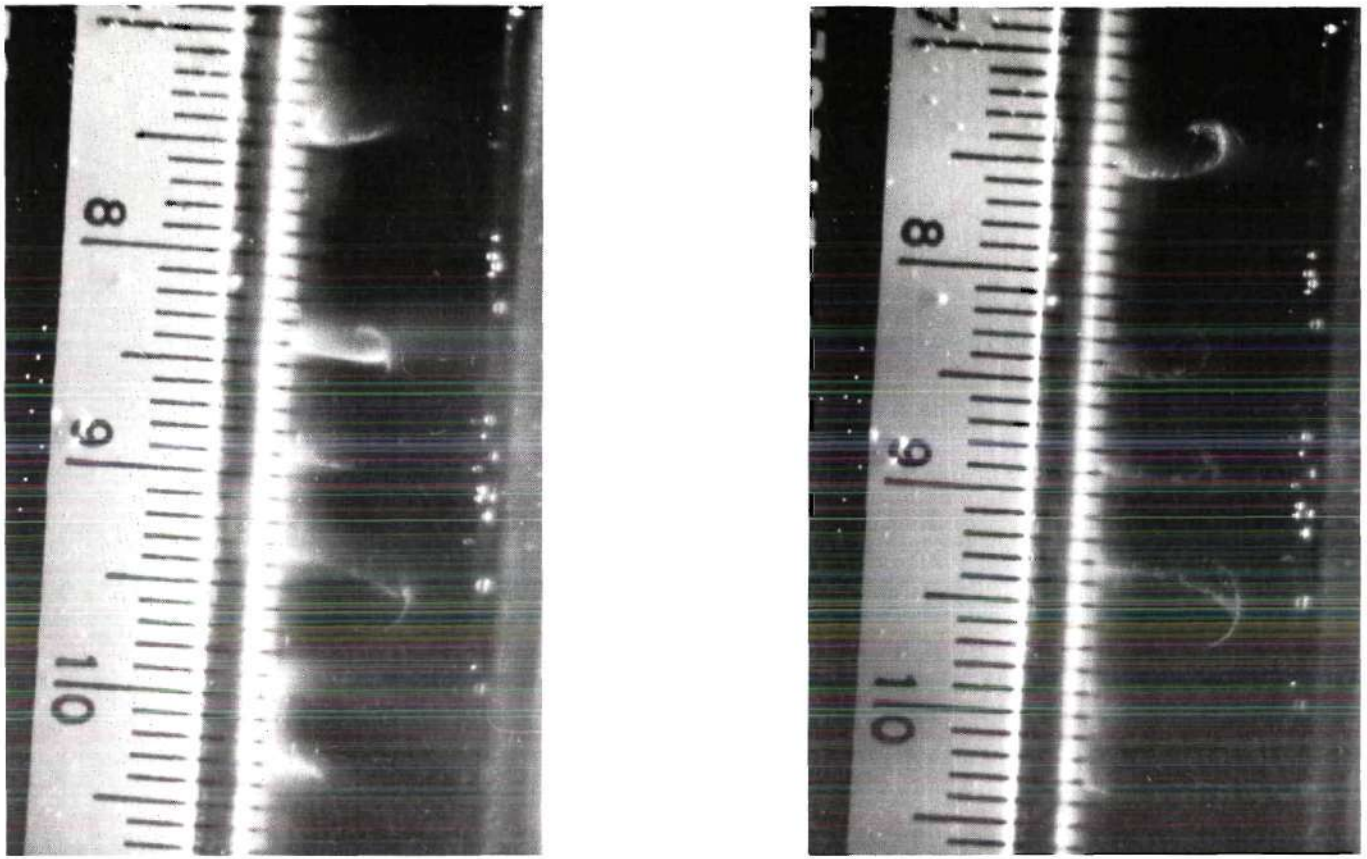

(a) (b)

Figure 27. Bubble Pattern from Wire No. 3, $V_{avg.}$ = 15 ft/min., θ_v = 67°.

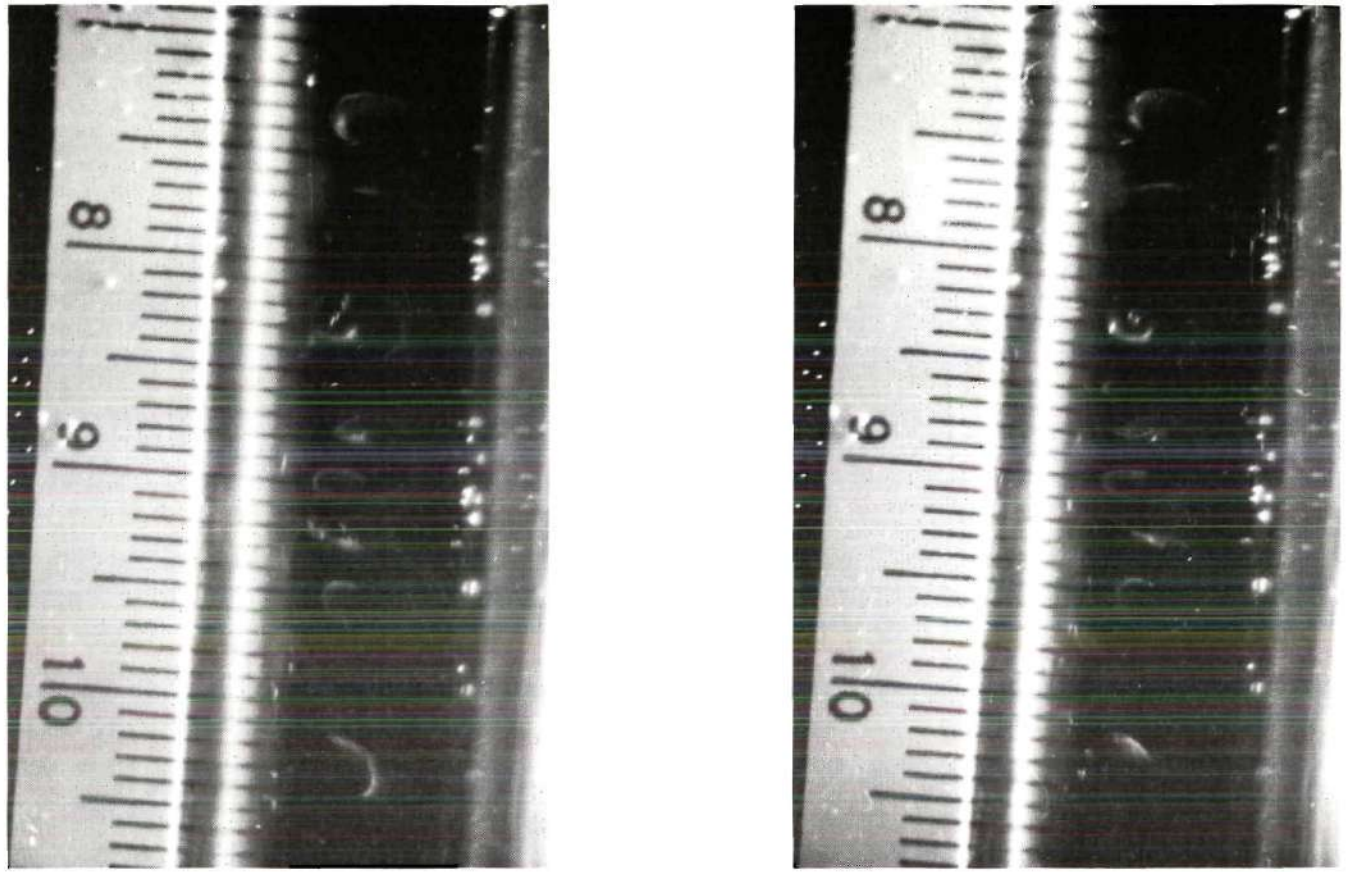

(a) (b)

Figure 28. Bubble Pattern from Wire No. 3, Enlarged, $V_{avg.}$ = 15 ft/min., θ_v = 100°.

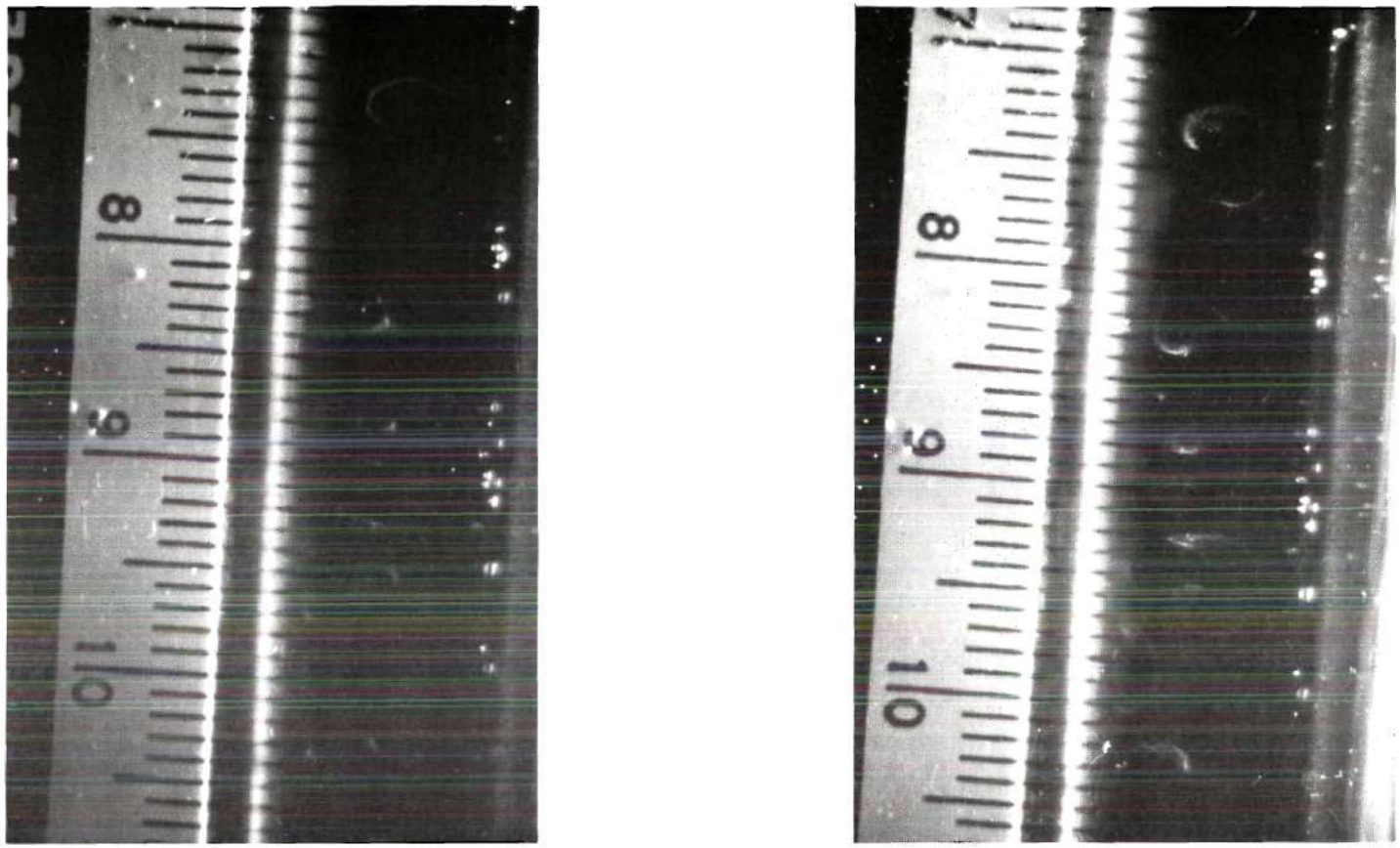

(a) (b)

Figure 29. Bubble Pattern from Wire No. 3, Enlarged
$V_{avg.}$ = 15 ft/min., θ_v = 100°.

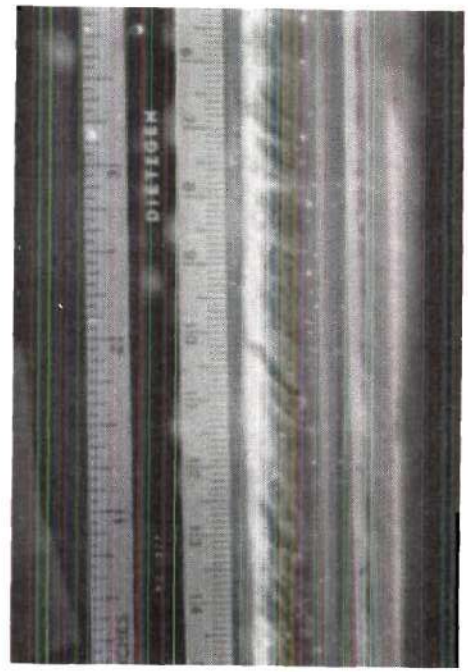

(a) $\theta_v = 67°$

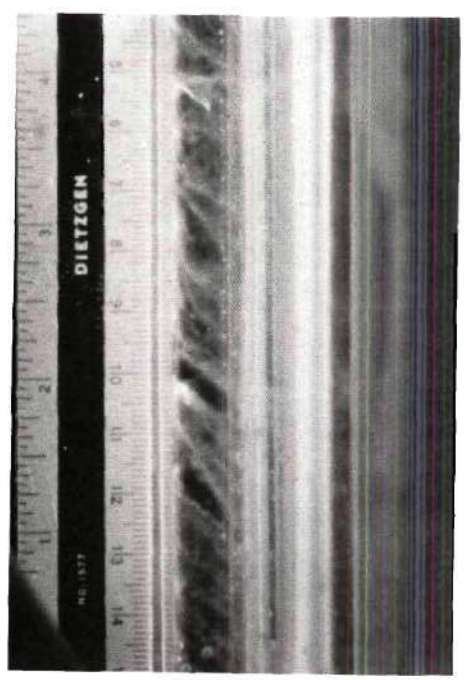

(b) $\theta_v = 100°$

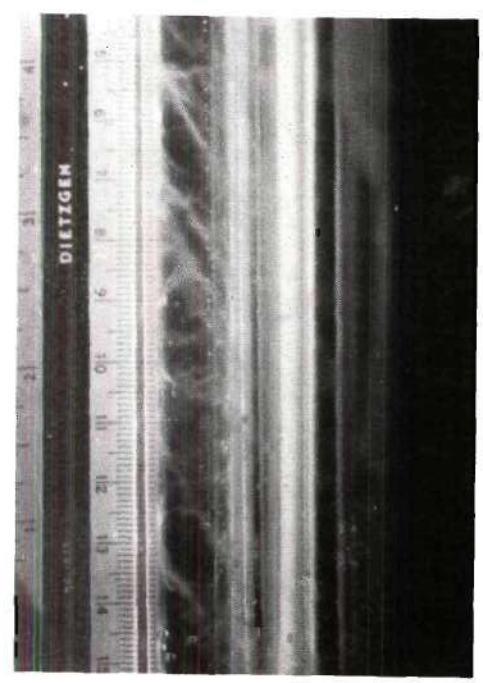

(c) $\theta_v = 100°$

Figure 30. Bubble Pattern from Wire No. 4, $V_{avg.} = 6$ ft/min.

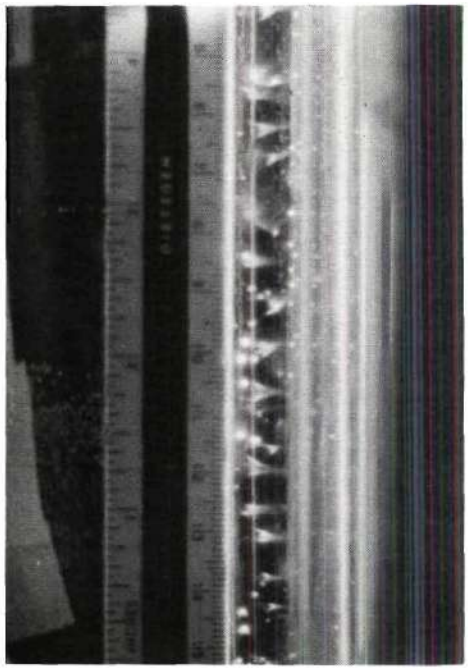

(a) $\theta_v = 65°$

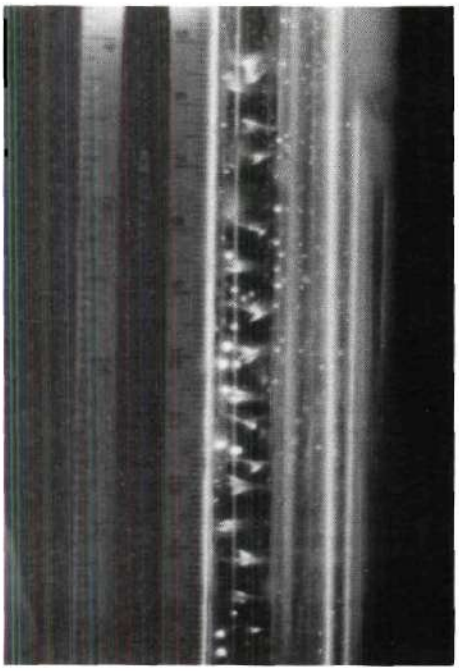

(b) $\theta_v = 65°$

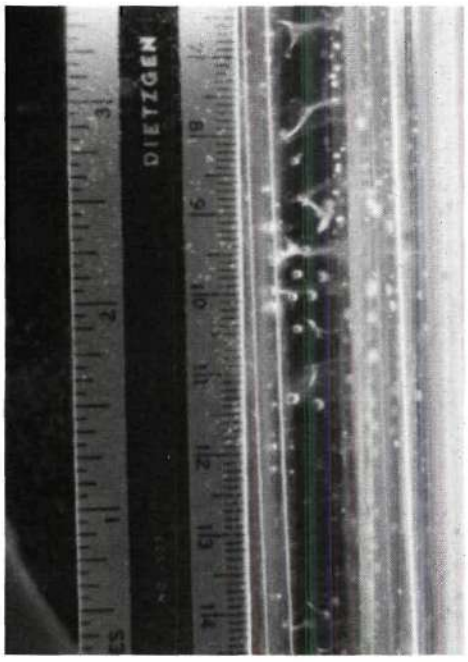

(c) $\theta_v = 90°$

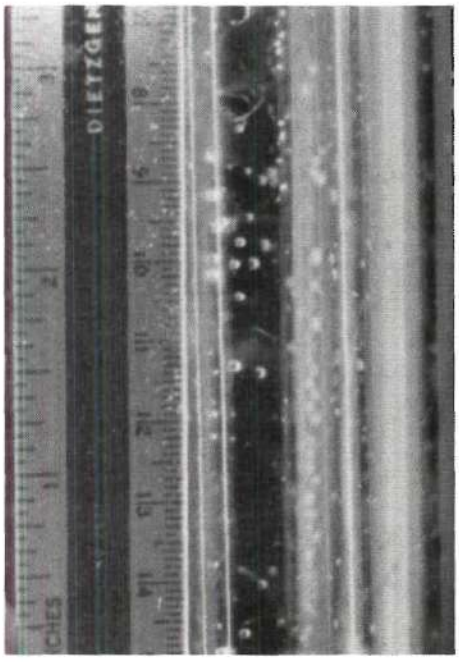

(d) $\theta_v = 90°$

Figure 31. Bubble Pattern from Wire No. 4, $V_{avg.}$ = 16-1/2 ft/min.

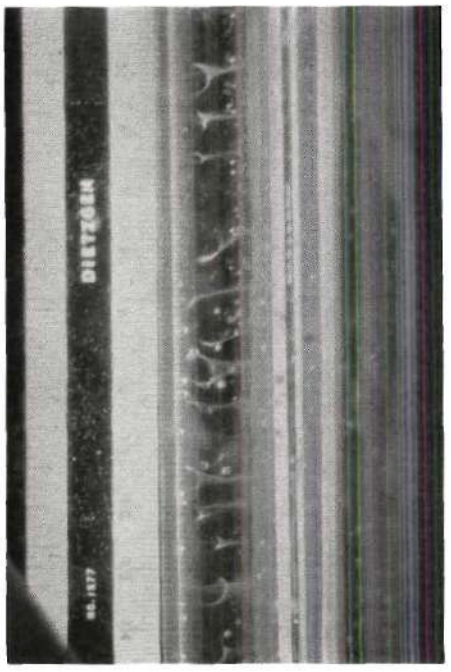

(a) $\theta_v = 110°$

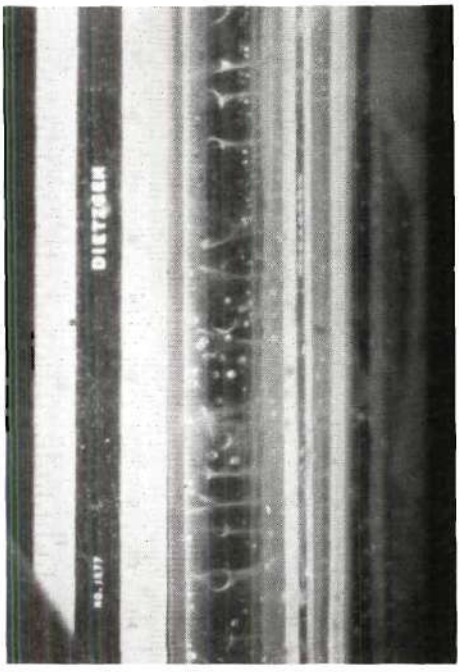

(b) $\theta_v = 110°$

Figure 32. Bubble Pattern from Wire No. 4, $V_{avg.}$ = 16-1/2 ft/min.

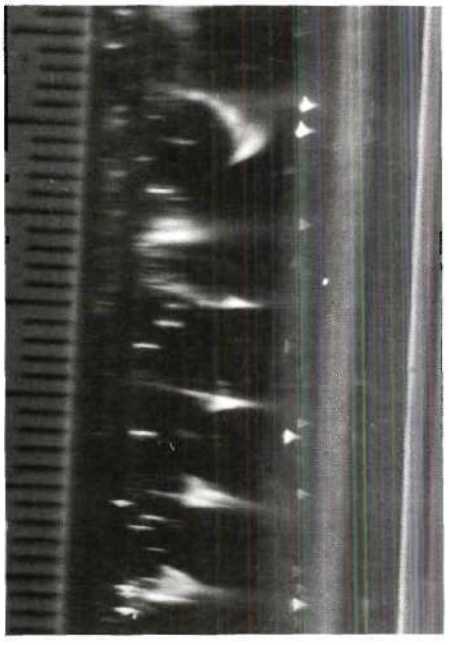

(c) $\theta_v = 100°$

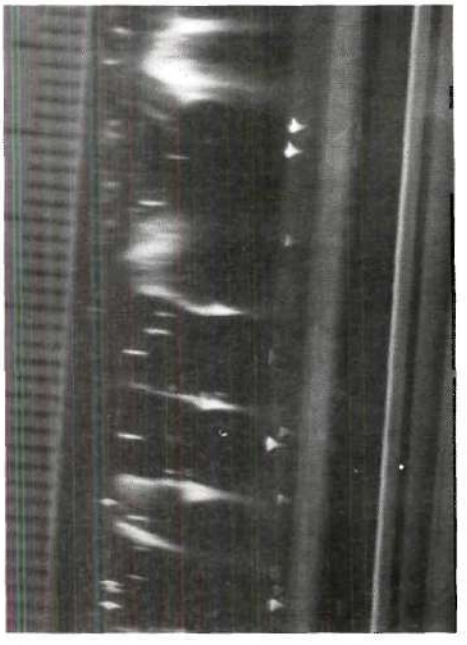

(d) $\theta_v = 100°$

Figure 33. Bubble Pattern from Wire No. 4, Enlarged, $V_{avg.}$ = 15 ft/min.

$$\frac{\partial}{\partial t}\left(\frac{\omega_t}{q}\right) = \frac{2}{q^2 r}\left[\frac{\partial U}{\partial b} - \nu \underset{\sim}{b} \cdot \nabla^2 \underset{\sim}{V}\right] + \frac{\underset{\sim}{t} \cdot \nu \nabla^2 \underset{\sim}{\Omega}}{q^2} \qquad (5.2)$$

a result derived directly for laminar flow by Marris (4).

Since viscosity acts on the fluid as a dissipative force, it can not directly initiate a secondary flow. The effects of viscosity can however lead to gradients in Bernoulli head that can generate secondary flow. Thus to study the direct effects on secondary flow, the viscous terms of equation 5.2 can be dropped, leaving

$$\frac{\partial}{\partial t}\left(\frac{\omega_t}{q}\right) = \frac{2}{q^2 r}\left[\frac{\partial U}{\partial b}\right] \qquad (5.3)$$

This equation reveals two necessary requirements for secondary vorticity generation to occur. The streamlines must be curved yielding a finite value for r, and concurrently the stream must have a gradient of Bernoulli head in the direction normal to the plane of streamline curvature. As the Bernoulli head U is the sum of pressure, velocity and potential, that is

$$U = \frac{p}{\rho} + \frac{q^2}{2} + \varphi \qquad (5.4)$$

A binormal gradient of any of these elements, either individually or in combination, could produce the necessary driving force for secondary flow development in a curved channel. Hawthorne (3) developed an analysis analytically, and demonstrated its validity experimentally, showing that a binormal gradient of velocity head did indeed produce secondary flow.

Equation 5.3 implies that secondary flow will not be generated

by direct action of the velocity gradient on the side walls of a curved channel, but rather due to the boundary layer on the end plates. As the secondary flow transports fluid elements, with their corresponding velocities, normal to the main flow, a streamwise component of vorticity generated at the end plates will move low velocity fluid from the side walls into the center of the stream creating a velocity depression in the flow. The secondary flow at the end plates thus can generate a binormal gradient in velocity in the adjoining fluid which in turn could produce a second vortex cell. The second cell would then lead to the establishment of a third and so on until the channel was filled with secondary flow cells.

If one cell triggered the next, one after another, as suggested above it should prove possible to detect secondary flow close to the end plates before it appears in the center of the stream.

The secondary flow in a curved channel can also be analyzed using the secondary velocity approach. This method, though it can not be used to follow the flow path appears to yield more specific information at a particular point in the flow. Reducing equation 3.29 to apply to steady laminar flow of an incompressible inviscid fluid yields the following

$$\frac{\partial V_1}{\partial x_1} = \frac{V_1}{\omega}\frac{\partial \omega}{\partial x_1} + \frac{1}{\omega^2}\left[\frac{\partial U}{\partial x_2}\frac{\partial \omega}{\partial x_3} - \frac{\partial U}{\partial x_3}\frac{\partial \omega}{\partial x_2}\right] - \frac{K}{\omega}\frac{\partial U}{\partial x_3} \qquad (5.5)$$

The intrinsic coordinates defined by the vortex lines in the curved channel system are illustrated in Figure 34. The variation of both Bernoulli head and vorticity will be due initially, without any secondary flow, to the viscous effects. Therefore the gradients in the

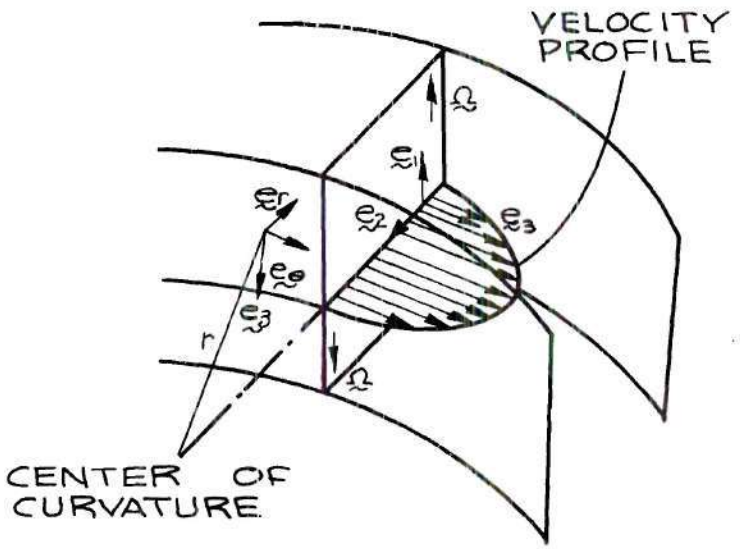

Figure 34. Laminar Flow in a Curved Channel.

x_2 or r direction should prove to be more important than those in x_3 or θ.

Using cylindrical coordinates, the vorticity can be expressed as

$$\underset{\sim}{\Omega} = \underset{\sim}{e}_r \left[\frac{1}{r}\frac{\partial V_z}{\partial \theta} - \frac{\partial V_\theta}{\partial z}\right] + \underset{\sim}{e}_\theta \left[\frac{\partial V_r}{\partial z} - \frac{\partial V_z}{\partial r}\right] + \underset{\sim}{e}_z \left[\frac{1}{r}\frac{\partial (r V_\theta)}{\partial r} - \frac{1}{r}\frac{\partial V_r}{\partial \theta}\right] \qquad (5.6)$$

The velocity vector, prior to the occurrence of secondary flow, is

$$\underset{\sim}{V} = V_\theta \, \underset{\sim}{e}_\theta \qquad (5.7)$$

Introducing this expression for velocity into 5.6, the expression for vorticity simplifies to

$$\underset{\sim}{\Omega} = \underset{\sim}{e}_r \left(-\frac{\partial V_\theta}{\partial z}\right) + \underset{\sim}{e}_z \left[\frac{V_\theta}{r} - \frac{\partial V_\theta}{\partial r}\right] \qquad (5.8)$$

On the end walls, the first term, containing $\frac{\partial V_\theta}{\partial z}$ will be dominant while on the side walls the second term, will be important.

Considering the secondary flow generation on the side walls, far removed from the end plates, where

$$\frac{\partial V_\theta}{\partial z} \simeq 0 \tag{5.9}$$

$$\underset{\sim}{\Omega} = \underset{\sim}{e}_z \left[\frac{V_\theta}{r} + \frac{\partial V_\theta}{\partial r} \right] \tag{5.10}$$

in this region, far from the end plates

$$U \approx U(r) \tag{5.11}$$

$$V_\theta \approx V_\theta(r) \tag{5.12}$$

and

$$\omega \approx \omega(r) \tag{5.13}$$

which, when introduced into equation 5.5 yields

$$\frac{\partial V_1}{\partial x_1} \simeq 0 \tag{5.14}$$

on the side walls. This is the same conclusion reached in applying the secondary vorticity equation, that secondary flow will not be generated solely due to side wall boundary layers in curved channel flow.

APPENDICES

APPENDIX A

DERIVATION OF SECONDARY VELOCITY ANALYSIS USING $\underset{\sim}{W}$ AND $\underset{\sim}{M}$

The resolution of the vector $\underset{\sim}{W}$ along and perpendicular to an m-line is expressed as (see Figure 1)

$$\underset{\sim}{W} = \frac{(\underset{\sim}{W} \times \underset{\sim}{M})\underset{\sim}{M}}{m^2} + \frac{\underset{\sim}{M} \times (\underset{\sim}{W} \times \underset{\sim}{M})}{m^2} \qquad (A.1)$$

Taking the divergence of equation A.1, one obtains

$$\nabla \cdot \left[\frac{(\underset{\sim}{W} \cdot \underset{\sim}{M})\underset{\sim}{M}}{m^2} \right] = \nabla \cdot \underset{\sim}{W} - \nabla \cdot \left[\frac{\underset{\sim}{M} \times (\underset{\sim}{W} \times \underset{\sim}{M})}{m^2} \right] \qquad (A.2)$$

Carrying out the vector operation, using the vector identity $\nabla \cdot (\psi \underset{\sim}{A}) = \underset{\sim}{A} \cdot \nabla\psi + \psi \nabla \cdot \underset{\sim}{A}$, and the fact $\nabla \cdot \underset{\sim}{M} = 0$, the left term of A.2 can be expressed as

$$\nabla \cdot \left[\frac{(\underset{\sim}{W} \cdot \underset{\sim}{M})\underset{\sim}{M}}{m^2} \right] = m \frac{\partial}{\partial S_1} \left(\frac{W_1}{m} \right) \qquad (A.3)$$

The second right hand term of equation A.2 can be rearranged with the aid of the vector identity $\nabla \cdot (\underset{\sim}{A} \times \underset{\sim}{B}) = \underset{\sim}{B} \cdot \nabla \times \underset{\sim}{A} - \underset{\sim}{A} \cdot \nabla \times \underset{\sim}{B}$ into

$$-\nabla \cdot \left[\frac{\underset{\sim}{M} \times (\underset{\sim}{W} \times \underset{\sim}{M})}{m^2} \right] = -(\underset{\sim}{W} \times \underset{\sim}{M}) \cdot \nabla \times \left(\frac{\underset{\sim}{M}}{m^2} \right) + \frac{\underset{\sim}{S}_1}{m} \cdot \nabla \times (\underset{\sim}{W} \times \underset{\sim}{M}) \qquad (A.4)$$

Substituting equations A.3 and A.4 into A.2 yields the folowwing expression

for the rate of change along an m line, of the ratio W_1/m

$$\frac{\partial}{\partial s_1}\left(\frac{W_1}{m}\right) = \frac{1}{m}\left[\frac{1}{m}\underset{\sim}{S}_1 \cdot \nabla \times (\underset{\sim}{W} \times \underset{\sim}{M}) - (\underset{\sim}{W} \times \underset{\sim}{M}) \cdot \nabla \times \left(\frac{\underset{\sim}{M}}{m^2}\right)\right] + \frac{\nabla \cdot \underset{\sim}{W}}{m} \tag{A.5}$$

The special case of $\underset{\sim}{W}$ being a solenoidal vector

$$\nabla \cdot \underset{\sim}{W} = 0 \tag{A.6}$$

reduces equation A.5 to

$$\frac{\partial}{\partial s_1}\left(\frac{W_1}{m}\right) = \frac{1}{m}\left[\frac{1}{m}\underset{\sim}{S}_1 \cdot \nabla \times (\underset{\sim}{W} \times \underset{\sim}{M}) - (\underset{\sim}{W} \times \underset{\sim}{M}) \cdot \nabla \times \left(\frac{\underset{\sim}{M}}{m^2}\right)\right] \tag{A.7}$$

APPENDIX B

EXPANSION OF $\nabla \cdot \underset{\approx}{\sigma}$ IN INTRINSIC COORDINATES

The vector expansion of the second order Reynolds stress tensor

$$\underset{\approx}{\sigma} = \sigma_{\alpha\beta}\, \underset{\sim}{i}_{\alpha}\, \underset{\sim}{i}_{\beta} \tag{B.1}$$

will be carried out in subscript notation and using the summation convention. A repeated index denotes summation over the index range i.e., 1,2, 3; t, n, b; or x, y, z. Thus in this convention

$$\sigma_{\alpha\beta,\alpha} = \sigma_{1\beta,1} + \sigma_{2\beta,2} + \sigma_{3\beta,3} \tag{B.2}$$

or

$$\underset{\sim}{i}_{\alpha}\, \underset{\sim}{i}_{\alpha} = \underset{\sim}{i}_{1}\, \underset{\sim}{i}_{1} + \underset{\sim}{i}_{2}\, \underset{\sim}{i}_{2} + \underset{\sim}{i}_{3}\, \underset{\sim}{i}_{3} \tag{B.3}$$

The comma will denote covariant differentiation, such that

$$\sigma_{1\beta,1} = \frac{\partial}{\partial x_1}\, \sigma_{1\beta} \tag{B.4}$$

The use of this notation will materially reduce the size of the expressions, but with no reduction of generality. After expansion, the resultant form may be written in any coordinate system one may wish to use.

The gradient operator, ∇, will be defined by

$$\nabla(\ \ ) \equiv \underset{\sim}{i}_{\alpha}\, \frac{\partial}{\partial x_{\alpha}}\, (\ \ ) = \underset{\sim}{i}_{\alpha} (\ \ )_{,\alpha} \tag{B.5}$$

from which one obtains the divergence operator

$$\nabla \cdot (\ ) \equiv \underset{\sim}{i}_\alpha \frac{\partial}{\partial x_\alpha} \cdot (\ ) = \underset{\sim}{i}_\alpha \cdot (\ )_{,\alpha} \tag{B.6}$$

and the curl operator

$$\nabla \times (\ ) \equiv \underset{\sim}{i}_\alpha \frac{\partial}{\partial x_\alpha} \times (\ ) = \underset{\sim}{i}_\alpha \times (\ )_{,\alpha} \tag{B.7}$$

Using these definitions,

$$\nabla \cdot \underset{\approx}{\sigma} = \underset{\sim}{i}_\alpha \cdot (\sigma_{\beta\varepsilon} i_\beta i_\varepsilon)_{,\alpha} \tag{B.8}$$

and applying the product rule for differentiation

$$\nabla \cdot \underset{\approx}{\sigma} = \underset{\sim}{i}_\alpha \cdot (\sigma_{\beta\varepsilon,\alpha} \underset{\sim}{i}_\beta \underset{\sim}{i}_\varepsilon + \sigma_{\beta\varepsilon} \underset{\sim}{i}_\beta \underset{\sim}{i}_{\varepsilon,\alpha} + \sigma_{\beta\varepsilon} \underset{\sim}{i}_{\beta,\alpha} \underset{\sim}{i}_\varepsilon) \tag{B.9a}$$

$$= \delta_{\alpha\beta}(\sigma_{\beta\varepsilon,\alpha} \underset{\sim}{i}_\varepsilon + \sigma_{\beta\varepsilon} \underset{\sim}{i}_{\varepsilon,\alpha}) + \underset{\sim}{i}_\alpha \cdot \underset{\sim}{i}_{\beta,\alpha} \sigma_{\beta\varepsilon} \underset{\sim}{i}_\varepsilon \tag{B.9b}$$

$$= (\sigma_{\alpha\varepsilon,\alpha} + \sigma_{\alpha\varepsilon} \nabla \cdot \underset{\sim}{i}_\alpha) \underset{\sim}{i}_\varepsilon + i_{\varepsilon,\alpha} \sigma_{\alpha\varepsilon} \tag{B.9c}$$

A more compact form for $\nabla \cdot \underset{\approx}{\sigma}$ can be obtained by recognizing

$$\underset{\sim}{i}_\varepsilon (\sigma_{\alpha\varepsilon,\alpha} + \sigma_{\alpha\varepsilon} \nabla \cdot \underset{\sim}{i}_\alpha) = \underset{\sim}{i}_\varepsilon (\nabla \cdot \underset{\sim}{\sigma}_\varepsilon) \tag{B.10}$$

where

$$\underset{\sim}{\sigma}_\varepsilon \equiv \underset{\sim}{i}_\varepsilon \cdot \underset{\approx}{\sigma} = \underset{\approx}{\sigma} \cdot \underset{\sim}{i}_\varepsilon = \sigma_{\varepsilon\alpha} \underset{\sim}{i}_\alpha \tag{B.11}$$

Since $\underset{\approx}{\sigma}$, expressed in matrix form, is symmetric, $\sigma_{\alpha\beta} = \sigma_{\beta\alpha}$

$$\underset{\approx}{\sigma} = \begin{bmatrix} \sigma_{11} & \sigma_{12} & \sigma_{13} \\ \sigma_{21} & \sigma_{22} & \sigma_{23} \\ \sigma_{31} & \sigma_{32} & \sigma_{33} \end{bmatrix} \tag{B.12}$$

either pre or post multiplication by $\underset{\sim}{i}_\varepsilon$, yields identical results. Thus one has

$$\nabla \cdot \underset{\sim}{\sigma}_\varepsilon = \underset{\sim}{i}_\alpha \cdot (\sigma_{\varepsilon\beta}\, \underset{\sim}{i}_\beta)_{,\alpha} \tag{B.13a}$$

$$= \underset{\sim}{i}_\alpha \cdot (\sigma_{\varepsilon\beta,\alpha}\, \underset{\sim}{i}_\beta + \sigma_{\varepsilon\beta}\, \underset{\sim}{i}_{\beta,\alpha}) \tag{B.13b}$$

$$= \delta_{\alpha\beta}\sigma_{\varepsilon\beta,\alpha} + \sigma_{\varepsilon\beta}\, \underset{\sim}{i}_\alpha \cdot \underset{\sim}{i}_{\beta,\alpha} \tag{B.13c}$$

$$= \sigma_{\varepsilon\alpha,\alpha} + \sigma_{\alpha\varepsilon}\, \nabla \cdot \underset{\sim}{i}_\alpha \tag{B.13d}$$

Therefore

$$\nabla \cdot \underset{\approx}{\sigma} = \underset{\sim}{i}_\varepsilon (\nabla \cdot \underset{\sim}{\sigma}_\varepsilon) + \underset{\sim}{\sigma}_\varepsilon \cdot \nabla \underset{\sim}{i}_\varepsilon \tag{B.14}$$

as

$$\underset{\sim}{\sigma}_\varepsilon \cdot \nabla \underset{\sim}{i}_\varepsilon = \underset{\sim}{\sigma}_\varepsilon \cdot (\nabla\, \underset{\sim}{i}_\varepsilon) = (\underset{\sim}{\sigma}_\varepsilon \cdot \nabla)\underset{\sim}{i}_\varepsilon \tag{B.15}$$

The expansion of $\nabla \cdot \underset{\approx}{\sigma}$ into, $\underset{\sim}{t}$, $\underset{\sim}{n}$, $\underset{\sim}{b}$ coordinate system can most readily be carried out using equation B.14. This expansion yields the following expression which can be applied equally well to either the streamline or the vortex line coordinate system:

$$\nabla \cdot \underset{\sim}{g} = (\sigma_{tt,t} + \sigma_{nt,n} + \sigma_{bt,b})\,\underset{\sim}{t}$$

$$+ (\sigma_{tn,t} + \sigma_{nn,n} + \sigma_{bn,b})\,\underset{\sim}{n}$$

$$+ (\sigma_{tb,t} + \sigma_{nb,n} + \sigma_{bb,b})\underset{\sim}{b}$$

$$+ (\sigma_{tt}\,\underset{\sim}{t} + \sigma_{tn}\,\underset{\sim}{n} + \sigma_{tb}\,\underset{\sim}{b})\,\nabla \cdot \underset{\sim}{t}$$

$$+ (\sigma_{nt}\,\underset{\sim}{t} + \sigma_{nn}\,\underset{\sim}{n} + \sigma_{nb}\,\underset{\sim}{b})\,\nabla \cdot \underset{\sim}{n}$$

$$+ (\sigma_{bt}\,\underset{\sim}{t} + \sigma_{bn}\,\underset{\sim}{n} + \sigma_{bb}\,\underset{\sim}{b})\,\nabla \cdot \underset{\sim}{b}$$

$$+ (\sigma_{tt}\frac{\partial \underset{\sim}{t}}{\partial t} + \sigma_{nt}\frac{\partial \underset{\sim}{t}}{\partial n} + \sigma_{bt}\frac{\partial \underset{\sim}{t}}{\partial b})$$

$$+ (\sigma_{tn}\frac{\partial \underset{\sim}{n}}{\partial t} + \sigma_{nn}\frac{\partial \underset{\sim}{n}}{\partial n} + \sigma_{bn}\frac{\partial \underset{\sim}{n}}{\partial b})$$

$$+ (\sigma_{tb}\frac{\partial \underset{\sim}{b}}{\partial t} + \sigma_{nb}\frac{\partial \underset{\sim}{b}}{\partial n} + \sigma_{bb}\frac{\partial \underset{\sim}{b}}{\partial b}) \qquad \text{(B.16)}$$

The three groups, of three terms each, on the right side of equation B.16 represent respectively:

1. The effect of the spatial rate of change of turbulent stress magnitude,

2. the effect of the nonparallel character of the coordinate system, and thus dependent on either the velocity or vorticity fields, and

3. the effect of the gradients of the unit vectors.

In using the above representations for $\nabla \cdot \underset{\sim}{g}$ to develop the equations for a particular coordinate system, i.e., cylindrical coordinates, one must account for coordinate scale changes through scale factors. These scale

factors, h_α, are related to the coordinate system variables χ_α through the increment of length ds such that

$$ds^2 = h_\alpha^2 \, d\chi_\alpha^2 \tag{B.17}$$

In general, the safest approach in applying these results to particular coordinate systems is to start with the vector equation and use the standard vector operators, as discussed in the introduction to Chapter IV.

In converting to cylindrical coordinates, using r, θ and z to replace t, n and b respectively one has

$$\underset{\sim}{e}_r = \underset{\sim}{t} \tag{B.18}$$

$$\underset{\sim}{e}_\theta = \underset{\sim}{n} \tag{B.19}$$

$$\underset{\sim}{e}_z = \underset{\sim}{b} \tag{B.20}$$

$$dr = dt \tag{B.21}$$

$$r d\theta = dn \tag{B.22}$$

$$dz = db \tag{B.23}$$

then

$$\frac{d}{dt} = \frac{d}{dr}\frac{dr}{dt} = \frac{d}{dr} \tag{B.24}$$

$$\frac{d}{dn} = \frac{d}{d\theta}\frac{d\theta}{dn} = \frac{1}{r}\frac{d}{d\theta} \tag{B.25}$$

$$\frac{d}{db} = \frac{d}{dz}\frac{dz}{db} = \frac{d}{dz} \tag{B.26}$$

and

$$\nabla \cdot \underset{\sim}{e}_r = \frac{1}{r} \tag{B.27}$$

$$\nabla \cdot \underset{\sim}{e}_\theta = 0 \tag{B.28}$$

$$\nabla \cdot \underset{\sim}{e}_z = 0 \tag{B.29}$$

$$\frac{d\underset{\sim}{e}_\alpha}{dr} = 0 \qquad \text{for } \alpha = r, \theta, z \tag{B.30, 31, 32}$$

$$\frac{1}{r}\frac{d\underset{\sim}{e}_r}{d\theta} = \frac{1}{r}\underset{\sim}{e}_\theta \tag{B.33}$$

$$\frac{d\underset{\sim}{e}_\theta}{d\theta} = -\underset{\sim}{e}_r \tag{B.34}$$

$$\frac{d\underset{\sim}{e}_z}{d\theta} = 0 \tag{B.35}$$

and

$$\frac{d\underset{\sim}{e}_\alpha}{dz} = 0 \qquad \text{for } \alpha = r, \theta, z \tag{B.36, 37, 38}$$

Using equation B.18 through B.38 to convert $\nabla \cdot \underset{\approx}{\sigma}$, and working from equation B.16, one obtains the following cylindrical coordinate expression:

$$\begin{aligned}\nabla \cdot \underset{\approx}{\sigma} = {} & (\sigma_{rr,r} + \frac{1}{r}\sigma_{\theta r,\theta} + \sigma_{zr,z} + \frac{1}{r}\sigma_{rr} - \frac{1}{r}\sigma_{\theta\theta})\underset{\sim}{e}_r \\ & + (\sigma_{r\theta,r} + \frac{1}{r}\sigma_{\theta\theta,\theta} + \sigma_{z\theta,z} + \frac{2}{r}\sigma_{r\theta})\underset{\sim}{e}_\theta \\ & + (\sigma_{rz,r} + \frac{1}{r}\sigma_{\theta z,\theta} + \sigma_{zz,z} + \frac{1}{r}\sigma_{rz})\underset{\sim}{e}_z \end{aligned} \tag{B.39}$$

This result is identical to that appearing in Goldstein (29) page 193.

APPENDIX C

REDUCTION OF SCALARS $\underset{\sim}{i}_{\alpha} \cdot (\nabla \cdot \underset{\approx}{\sigma})$

The magnitude of the vector $\nabla \cdot \underset{\approx}{\sigma}$ in a particular direction is obtained by scalar or dot multiplication of $\nabla \cdot \underset{\approx}{\sigma}$ with a unit vector in the desired direction. The derivation will be carried out in the $\underset{\sim}{t}$, $\underset{\sim}{n}$, $\underset{\sim}{b}$ coordinate system, as only a simple interchange of symbols is required to obtain the result in the $\underset{\sim}{e}_1$, $\underset{\sim}{e}_2$, $\underset{\sim}{e}_3$ coordinate system.

Using the form for $\nabla \cdot \underset{\approx}{\sigma}$ given in equation B.14,

$$\underset{\sim}{b} \cdot (\nabla \cdot \underset{\approx}{\sigma}) = \underset{\sim}{b} \cdot [\underset{\sim}{i}_{\varepsilon}(\nabla \cdot \underset{\sim}{\sigma}_{\varepsilon})] + \underset{\sim}{b} \cdot \underset{\sim}{\sigma}_{\varepsilon} \cdot \nabla \underset{\sim}{i}_{\varepsilon} \tag{C.1}$$

$$= \sigma_{b\alpha,\alpha} + \sigma_{b\alpha} \nabla \cdot \underset{\sim}{i}_{\alpha} + \underset{\sim}{b} \cdot [\underset{\sim}{\sigma}_t \cdot \nabla \underset{\sim}{t} + \underset{\sim}{\sigma}_n \cdot \nabla \underset{\sim}{n} + \underset{\sim}{\sigma}_b \cdot \nabla \underset{\sim}{b}] \tag{C.2}$$

which can be expanded into

$$\begin{aligned} \underset{\sim}{b} \cdot (\nabla \cdot \underset{\approx}{\sigma}) = {} & \sigma_{tb,t} + \sigma_{nb,n} + \sigma_{bb,b} + \sigma_{tb} \nabla \cdot \underset{\sim}{t} + \sigma_{nb} \nabla \cdot \underset{\sim}{n} \\ & + \sigma_{bb} \nabla \cdot \underset{\sim}{b} + \underset{\sim}{b} \cdot [\sigma_{tt} \underset{\sim}{t}_{,t} + \sigma_{tn} \underset{\sim}{t}_{,n} + \sigma_{tb} \underset{\sim}{t}_{,b} \\ & + \sigma_{tn} \underset{\sim}{n}_{,t} + \sigma_{nn} \underset{\sim}{n}_{,n} + \sigma_{bn} \underset{\sim}{n}_{,b} \\ & + \sigma_{tb} \underset{\sim}{b}_{,t} + \sigma_{nb} \underset{\sim}{b}_{,n} + \sigma_{bb} \underset{\sim}{b}_{,b}] \end{aligned} \tag{C.3}$$

The first set of six terms represents the influence of the divergence of the Reynolds stress vector $\underset{\sim}{\sigma}_b$. The remaining nine terms, in brackets, portrays the influence of the bending of the coordinate axes.

In general form, equation C.2 can be written as

$$\underset{\sim}{i}_\alpha \cdot (\nabla \cdot \underset{\sim}{\sigma}) = \nabla \cdot \underset{\sim}{\sigma}_\alpha + \underset{\sim}{i}_\alpha (\underset{\sim}{\sigma}_\beta \cdot \nabla \underset{\sim}{i}_\beta) \tag{C.4}$$

where

$$\nabla \cdot \underset{\sim}{\sigma}_\alpha = \sigma_{\alpha\gamma,\gamma} + \sigma_{\alpha\gamma} \nabla \cdot \underset{\sim}{i}_\gamma \tag{C.5}$$

and in the t, n, b system

$$\nabla \cdot \underset{\sim}{\sigma}_\alpha = \sigma_{\alpha t,t} + \sigma_{\alpha n,n} + \sigma_{\alpha b,b} + \sigma_{\alpha t} \nabla \cdot \underset{\sim}{t} + \sigma_{\alpha n} \nabla \cdot \underset{\sim}{n} + \sigma_{\alpha b} \nabla \cdot \underset{\sim}{b} \tag{C.6}$$

Equation C.4 is a convenient form to use in constructing $\underset{\sim}{e}_2 \cdot (\nabla \cdot \underset{\approx}{\sigma})$ and $\underset{\sim}{e}_3 \cdot (\nabla \cdot \underset{\approx}{\sigma})$ required in the secondary velocity development.

APPENDIX D

EXPANSION OF $\underset{\sim}{t} \cdot \text{curl (div } \underset{\approx}{\sigma})$ IN INTRINSIC COORDINATES

The development of the desired form for the scalar $\underset{\sim}{t} \cdot \text{curl (div } \underset{\approx}{\sigma})$ will start from Equation B.9c.

$$\nabla \cdot \underset{\approx}{\sigma} = \underset{\sim}{i}_\beta \, \sigma_{\alpha\beta,\alpha} + \sigma_{\alpha\beta} \, \underset{\sim}{i}_\beta \, \nabla \cdot \underset{\sim}{i}_\alpha + \underset{\sim}{\sigma}_\alpha \cdot \nabla \underset{\sim}{i}_\alpha \qquad (D.1)$$

The curl operator is defined by

$$\nabla x \equiv \underset{\sim}{i}_\alpha \times \frac{\partial}{\partial X_\alpha} \qquad (D.2)$$

The curl and then the $\underset{\sim}{t}$ component of the curl will be formed for each of the three right terms of div $\underset{\approx}{\sigma}$. For the first right hand term of D.1:

$$\nabla \times (\underset{\sim}{i}_\beta \, \sigma_{\gamma\beta,\gamma}) = \underset{\sim}{i}_\alpha \times \frac{\partial}{\partial X_\alpha} (\underset{\sim}{i}_\beta \, \sigma_{\gamma\beta,\gamma}) \qquad (D.3)$$

which expands into

$$\nabla \times (\underset{\sim}{i}_\beta \, \sigma_{\gamma\beta,\gamma}) = \sigma_{\gamma\beta,\gamma} \, \underset{\sim}{i}_\alpha \times \frac{\partial \underset{\sim}{i}_\beta}{\partial X_\alpha} - \underset{\sim}{i}_\beta \times \underset{\sim}{i}_\alpha \, \sigma_{\gamma\beta,\gamma\alpha} \qquad (D.4)$$

through use of the vector identity

$$\nabla \times (\varphi \, \underset{\sim}{A}) = \varphi \nabla \times \underset{\sim}{A} - A \times \nabla \varphi \qquad (D.5)$$

and the definition of gradient such that

$$i_\beta \times \nabla \, \sigma_{\gamma\beta,\gamma} = \underset{\sim}{i}_\beta \times \underset{\sim}{i}_\alpha \, \sigma_{\gamma\beta,\gamma\alpha} \qquad (D.6)$$

Taking the $\underset{\sim}{t}$ component of equation D-4 yields

$$\underset{\sim}{t} \cdot \nabla \times (\underset{\sim}{i}_\beta \, \sigma_{\gamma\beta,\gamma}) = \sigma_{\gamma\beta,\gamma}\left[\underset{\sim}{t} \cdot \underset{\sim}{i}_\alpha \times \frac{\partial \underset{\sim}{i}_\beta}{\partial x_\alpha}\right] - \left[\underset{\sim}{t} \cdot \underset{\sim}{i}_\beta \times \underset{\sim}{i}_\alpha\right]\sigma_{\gamma\beta,\gamma\alpha} \quad \text{(D.7)}$$

The above equation has a box or triple scalar product in each of the two right hand terms. As box products containing two parallel vectors are zero, $\underset{\sim}{i}_\alpha$ in the first term must be either $\underset{\sim}{n}$ or $\underset{\sim}{b}$ for a non zero product. In like manner the $\underset{\sim}{i}_\beta \times \underset{\sim}{i}_\alpha$ product of the second term is restricted to $\underset{\sim}{n} \times \underset{\sim}{b}$ or $\underset{\sim}{b} \times \underset{\sim}{n}$ and the scalar triple product $(\underset{\sim}{t} \cdot \underset{\sim}{i}_\beta \times \underset{\sim}{i}_\alpha)$ takes the values $+1$ if the cyclic order is preserved and -1 if not. Using the box product rule, equation D.7 becomes

$$\underset{\sim}{t} \cdot \nabla \times (\underset{\sim}{i}_\beta \, \sigma_{\gamma\beta,\gamma}) = \sigma_{\gamma\beta,\gamma}\left[\underset{\sim}{t} \times \underset{\sim}{n} \cdot \frac{\partial \underset{\sim}{i}_\beta}{\partial n} + \underset{\sim}{t} \times \underset{\sim}{b} \cdot \frac{\partial \underset{\sim}{i}_\beta}{\partial b}\right]$$

$$+ \sigma_{\gamma b,\gamma n} - \sigma_{\gamma n,\gamma b} \quad \text{(D.8)}$$

Since

$$\underset{\sim}{t} \times \underset{\sim}{n} = + \underset{\sim}{b} \quad \text{(D.9)}$$

and

$$\underset{\sim}{t} \times \underset{\sim}{b} = - \underset{\sim}{n} \quad \text{(D.10)}$$

$$\underset{\sim}{t} \cdot \nabla \times (\underset{\sim}{i}_\beta \, \sigma_{\gamma\beta,\gamma}) = \sigma_{\gamma\beta,\gamma}\left[\underset{\sim}{b} \cdot \frac{\partial \underset{\sim}{i}_\beta}{\partial n} - \underset{\sim}{n} \cdot \frac{\partial \underset{\sim}{i}_\beta}{\partial b}\right]$$

$$+ \sigma_{\gamma b,\gamma n} - \sigma_{\gamma n,\gamma b} \quad \text{(D.11)}$$

Using

$$\underset{\sim}{b} \cdot \frac{\partial \underset{\sim}{i}_\beta}{\partial n} - \underset{\sim}{n} \frac{\partial \underset{\sim}{i}_\beta}{\partial b} = \underset{\sim}{t} \cdot \nabla \times \underset{\sim}{i}_\beta \tag{D.12}$$

and applying the summation convention to the repeated suffixes yields the following expression for D.11.

$$\begin{aligned} \underset{\sim}{t} \cdot \nabla \times (\underset{\sim}{i}_\beta \sigma_{\gamma\beta,\gamma}) = {} & (\sigma_{bt,tn} + \sigma_{bn,nn} + \sigma_{bb,bn}) \\ & - (\sigma_{nt,tb} + \sigma_{nn,nb} + \sigma_{nb,bb}) \\ & + (\sigma_{tt,t} + \sigma_{nt,n} + \sigma_{bt,b})(\underset{\sim}{b} \cdot \frac{\partial \underset{\sim}{t}}{\partial n} - \underset{\sim}{n} \cdot \frac{\partial \underset{\sim}{t}}{\partial b}) \\ & + (\sigma_{tn,t} + \sigma_{nn,n} + \sigma_{bn,b})(\underset{\sim}{b} \cdot \frac{\partial \underset{\sim}{n}}{\partial n} - \underset{\sim}{n} \cdot \frac{\partial \underset{\sim}{n}}{\partial b}) \\ & + (\sigma_{tb,t} + \sigma_{nb,n} + \sigma_{bb,b})(\underset{\sim}{b} \cdot \frac{\partial \underset{\sim}{b}}{\partial n} - \underset{\sim}{n} \cdot \frac{\partial \underset{\sim}{b}}{\partial b}) \end{aligned} \tag{D.13}$$

Working now with the second term on the right side of equation D-1 yields

$$\underset{\sim}{t} \cdot \nabla \times (\sigma_{\alpha\beta} \underset{\sim}{i}_\beta \nabla \cdot \underset{\sim}{i}_\alpha) = \underset{\sim}{t} \cdot (\sigma_{\alpha\beta} \nabla \cdot \underset{\sim}{i}_\alpha \nabla \times \underset{\sim}{i}_\beta - \underset{\sim}{i}_\varepsilon \times \nabla(\sigma_{\alpha\varepsilon} \nabla \cdot \underset{\sim}{i}_\alpha) \tag{D.14}$$

$$t \cdot \sigma_{\alpha\beta} \underset{\sim}{i}_\alpha \times \frac{\partial \underset{\sim}{i}_\beta}{\partial x_\alpha} \nabla \cdot \underset{\sim}{i}_\alpha - \underset{\sim}{i}_\varepsilon \times \underset{\sim}{i}_\gamma (\sigma_{\alpha\varepsilon} \nabla \cdot \underset{\sim}{i}_\alpha)_{,\gamma} \tag{D.15}$$

and expanding on

$$\underset{\sim}{t} \cdot \nabla \times (\sigma_{\alpha\beta}\, \underset{\sim}{i}_\beta \nabla \cdot i_\alpha) = (\sigma_{\alpha t}\, \underset{\sim}{t} \cdot \underset{\sim}{i}_\gamma \times \frac{\partial \underset{\sim}{t}}{\partial x_\gamma} + \sigma_{\alpha n}\, \underset{\sim}{t} \cdot \underset{\sim}{i}_\gamma \times \frac{\partial \underset{\sim}{n}}{\partial x_\gamma} \qquad \text{(D.16)}$$

$$+ \sigma_{\alpha b}\, \underset{\sim}{t} \cdot \underset{\sim}{i}_\gamma \frac{\partial \underset{\sim}{b}}{\partial x_\gamma}) \nabla \cdot \underset{\sim}{i}_\alpha - \underset{\sim}{i}_\varepsilon \times \underset{\sim}{i}_\gamma \cdot \underset{\sim}{t} (\sigma_{\alpha\varepsilon} \nabla \cdot \underset{\sim}{i}_\alpha)_{,\gamma}$$

Using

$$\varepsilon_{\varepsilon\gamma t} = \underset{\sim}{i}_\varepsilon \times \underset{\sim}{i}_\gamma \cdot \underset{\sim}{t} \qquad \text{(D.17)}$$

which has a value of +1 when $\varepsilon = n$, $\gamma = b$, -1 for $\varepsilon = b$, $\gamma = n$ and 0 for all other permissible values.

$$\underset{\sim}{t} \cdot \nabla \times (\sigma_{\alpha\beta}\, \underset{\sim}{i}_\beta \nabla \cdot \underset{\sim}{i}_\alpha) = \underset{\sim}{t} \times \underset{\sim}{n} \cdot (\sigma_{\alpha t} \frac{\partial \underset{\sim}{t}}{\partial n} + \sigma_{\alpha n} \frac{\partial \underset{\sim}{n}}{\partial n} + \sigma_{\alpha b} \frac{\partial \underset{\sim}{b}}{\partial b}) \nabla \cdot \underset{\sim}{i}_\alpha$$

$$+ \underset{\sim}{t} \times \underset{\sim}{b} \cdot (\sigma_{\alpha t} \frac{\partial \underset{\sim}{t}}{\partial b} + \sigma_{\alpha n} \frac{\partial \underset{\sim}{n}}{\partial b} + \sigma_{\alpha b} \frac{\partial \underset{\sim}{b}}{\partial b}) \nabla \cdot i_\alpha$$

$$- \varepsilon_{\varepsilon\gamma t} (\sigma_{\alpha\varepsilon} \nabla \cdot \underset{\sim}{i}_\alpha)_{,\gamma} \qquad \text{(D.18)}$$

$$\underset{\sim}{t} \cdot \nabla \times (\sigma_{\alpha\beta}\, \underset{\sim}{i}_\beta \nabla \cdot \underset{\sim}{i}_\alpha) = \nabla \cdot \underset{\sim}{i}_\alpha \left[\underset{\sim}{b} \cdot (\sigma_\alpha \frac{\partial \underset{\sim}{t}}{\partial n} + \sigma_{\alpha n} \frac{\partial \underset{\sim}{n}}{\partial n} + \sigma_{\alpha b} \frac{\partial \underset{\sim}{b}}{\partial b}) \right.$$

$$\left. - \underset{\sim}{n} \cdot (\sigma_{\alpha t} \frac{\partial \underset{\sim}{t}}{\partial b} + \sigma_{\alpha n} \frac{\partial \underset{\sim}{n}}{\partial b} + \sigma_{\alpha b} \frac{\partial \underset{\sim}{b}}{\partial b}) \right]$$

$$+ (\sigma_{\alpha b} \nabla \cdot \underset{\sim}{i}_\alpha)_{,n} - (\sigma_{\alpha n} \nabla \cdot \underset{\sim}{i}_\alpha)_{,b} \qquad \text{(D.19)}$$

The expansion of the third right handed term of D.1 can be written as:

$$\underset{\sim}{t} \cdot \nabla \times \underset{\sim}{\sigma}_\alpha \cdot \nabla \underset{\sim}{i}_\alpha = \underset{\sim}{t} \cdot \nabla \times (\underset{\sim}{\sigma}_t \cdot \text{grad } \underset{\sim}{t} + \underset{\sim}{\sigma}_n \cdot \text{grad } \underset{\sim}{n} + \underset{\sim}{\sigma}_b \cdot \text{grad } \underset{\sim}{b}) \qquad \text{(D.20)}$$

Further manipulation of this relation does not appear worthwhile since it

involves the gradients of the unit vectors, $\underset{\sim}{t}$, $\underset{\sim}{n}$, and $\underset{\sim}{b}$, the form of which is unknown until the geometry of velocity field is specified. By adding the three terms making up the right hand side of D.1 the form of $\underset{\sim}{t} \cdot \text{curl}\ (\text{div}\ \underset{\approx}{\sigma})$ is available. As the expansions in $\underset{\sim}{t}$, $\underset{\sim}{n}$, and $\underset{\sim}{b}$ are lengthy and somewhat restricted in application, the combined result will be given in the more concise vector form. This relation is

$$\underset{\sim}{t} \cdot \nabla \times (\nabla \cdot \underset{\approx}{\sigma}) = (\underset{\sim}{t} \cdot \nabla \times \underset{\sim}{t})\ \nabla \cdot \underset{\sim}{\sigma}_t + (\underset{\sim}{t} \cdot \nabla \times \underset{\sim}{n})(\nabla \cdot \underset{\sim}{\sigma}_n)$$

$$+ (\underset{\sim}{t} \cdot \nabla \times \underset{\sim}{b})\ \nabla \cdot \underset{\sim}{\sigma}_b + \underset{\sim}{t} \cdot \nabla \times (\underset{\sim}{\sigma}_t \cdot \nabla \underset{\sim}{t} + \underset{\sim}{\sigma}_n \cdot \nabla \underset{\sim}{n} + \underset{\sim}{\sigma}_b \cdot \nabla \underset{\sim}{b})$$

$$+ (\underset{\sim}{n} \cdot \nabla)(\nabla \cdot \underset{\sim}{\sigma}_b) - (\underset{\sim}{b} \cdot \nabla)(\nabla \cdot \underset{\sim}{\sigma}_n) \qquad \text{(D.21)}$$

Replacing $\underset{\sim}{t}$, $\underset{\sim}{n}$ and $\underset{\sim}{b}$ respectively by $\underset{\sim}{e}_1$, $\underset{\sim}{e}_2$, and $\underset{\sim}{e}_3$ equation D.21, in streamline coordinates, may be translated into the vortex line components for use in the secondary velocity development.

APPENDIX E

GEOMETRIC CONDITIONS FOR PLANE CIRCULAR FLOW

The following vector operations, for cylindrical coordinates, are needed in reducing equation 4.16, page 50, together with the simplifications presented in equations 4.5 - 4.15.

$$\nabla = \underset{\sim}{e}_r \frac{\partial}{\partial r} + \frac{\underset{\sim}{e}_\theta}{r} \frac{\partial}{\partial \theta} + \underset{\sim}{e}_z \frac{\partial}{\partial z} \qquad \text{(E.1)}$$

$$\nabla \times \underset{\sim}{F} = \begin{vmatrix} \underset{\sim}{e}_r & r\underset{\sim}{e}_\theta & \underset{\sim}{e}_z \\ \frac{\partial}{\partial r} & \frac{\partial}{\partial \theta} & \frac{\partial}{\partial z} \\ f_r & f_\theta & f_z \end{vmatrix} \qquad \text{(E.2)}$$

$$\nabla \cdot \underset{\sim}{F} = \frac{\partial f_r}{\partial r} + \frac{f_r}{r} + \frac{1}{r} \frac{\partial f_\theta}{\partial \theta} + \frac{\partial f_z}{\partial z} \qquad \text{(E.3)}$$

where

$$\underset{\sim}{F} = f_r \underset{\sim}{e}_r + f_\theta \underset{\sim}{e}_\theta + f_z \underset{\sim}{e}_z \qquad \text{(E.4)}$$

and

$$\frac{\partial \underset{\sim}{e}_r}{\partial \theta} = \underset{\sim}{e}_\theta \quad , \qquad \frac{\partial \underset{\sim}{e}_\theta}{\partial \theta} = - \underset{\sim}{e}_r \qquad \text{(E.5, E.6)}$$

All other derivatives of the unit vectors $\underset{\sim}{e}_r$, $\underset{\sim}{e}_\theta$ and $\underset{\sim}{e}_z$, are zero. The equation to be simplified, 4.16, is rewritten here for convenience.

$$\frac{1}{r}\frac{\partial}{\partial\theta}\left(\frac{\Omega_\theta}{q}\right) = \frac{-2}{q^2 r}\left[\nabla\cdot\underset{\sim}{\sigma}_z + \underset{\sim}{e}_z\cdot\left(\underset{\sim}{\sigma}_\theta\frac{[-\underset{\sim}{e}_\theta\underset{\sim}{e}_r]}{r} - \underset{\sim}{\sigma}_r\frac{[-\underset{\sim}{e}_\theta\underset{\sim}{e}_\theta]}{r}\right)\right]$$

$$+\frac{1}{q^2}\left[\underset{\sim}{e}_\theta\cdot\nabla\times\left(\underset{\sim}{\sigma}_\theta\cdot\left\{\frac{-\underset{\sim}{e}_\theta\underset{\sim}{e}_r}{r}\right\} - \underset{\sim}{\sigma}_r\cdot\left\{\frac{-\underset{\sim}{e}_\theta\underset{\sim}{e}_\theta}{r}\right\}\right)\right.$$

$$\left. -\frac{\partial}{\partial r}(\nabla\cdot\underset{\sim}{\sigma}_z) + \frac{\partial}{\partial z}(\nabla\cdot\underset{\sim}{\sigma}_r)\right] \qquad \text{(E.7)}$$

The terms of the form $\nabla\cdot\underset{\sim}{\sigma}_\alpha$ can be reduced through

$$\nabla\cdot\underset{\sim}{\sigma}_\alpha = \nabla\cdot(\sigma_{\alpha r}\underset{\sim}{e}_r + \sigma_{\alpha\theta}\underset{\sim}{e}_\theta + \sigma_{\alpha z}\underset{\sim}{e}_z) \qquad \text{(E.8)}$$

$$= \sigma_{\alpha r,r} + \frac{1}{r}\sigma_{\alpha r} + \frac{1}{r}\sigma_{\alpha\theta,\theta} + \sigma_{\alpha z,z} \qquad \text{(E.9)}$$

thus

$$\nabla\cdot\underset{\sim}{\sigma}_z = \sigma_{zr,r} + \frac{1}{r}\sigma_{zr} + \frac{1}{r}\sigma_{z\theta,\theta} + \sigma_{zz,z} \qquad \text{(E.10)}$$

and

$$\frac{\partial}{\partial r}(\nabla\cdot\sigma_z) = \sigma_{zr,rr} + \frac{1}{r}\sigma_{zr,r} - \frac{1}{r^2}\sigma_{zr} - \frac{1}{r^2}\sigma_{z\theta,\theta} + \frac{1}{r}\sigma_{z\theta,\theta r} + \sigma_{zz,zr} \qquad \text{(E.11)}$$

The second term in the first bracket of equation E.5 is zero as

$$e_z\cdot\left[\underset{\sim}{\sigma}_\theta\cdot\left(\frac{-\underset{\sim}{e}_\theta\,\underset{\sim}{e}_\gamma}{\gamma}\right)\right] = -\underset{\sim}{e}_z\cdot\underset{\sim}{e}_\gamma\left[\underset{\sim}{\sigma}_\theta\cdot\frac{\underset{\sim}{e}_\theta}{\gamma}\right] \qquad \text{(E.12)}$$

A similar argument applies to the third term, first bracket of E.7

$$e_z \cdot [\underset{\sim}{\sigma}_r \cdot (\frac{-\underset{\sim}{e}_\theta \underset{\sim}{e}_\theta}{r})] = 0 \qquad (E.13)$$

Continuing onto the second bracket, and using

$$\underset{\sim}{e}_\theta \cdot \nabla \times \underset{\sim}{F} = r\left[\frac{\partial f_r}{\partial z} - \frac{\partial f_z}{\partial r}\right] \qquad (E.14)$$

$$\underset{\sim}{e}_\theta \cdot \nabla \times \left[\underset{\sim}{\sigma}_\theta \cdot (\frac{-\underset{\sim}{e}_\theta \underset{\sim}{e}_r}{r})\right] = \underset{\sim}{e}_\theta \cdot \nabla \times (-\sigma_{\theta\theta} \frac{\underset{\sim}{e}_r}{r}) \qquad (E.15)$$

$$= -r(\frac{\partial}{\partial z} \frac{\sigma_{\theta\theta}}{r}) = -\sigma_{\theta\theta,z} \qquad (E.16)$$

$$\underset{\sim}{e}_\theta \cdot \nabla \times \left[\underset{\sim}{\sigma}_r (\frac{\underset{\sim}{e}_\theta \underset{\sim}{e}_\theta}{r})\right] = \underset{\sim}{e}_\theta \cdot \nabla \times \left[\frac{\sigma_{r\theta}}{r} \underset{\sim}{e}_\theta\right] = 0 \qquad (E.17)$$

Using E.6

$$\nabla \cdot \underset{\sim}{\sigma}_r = \sigma_{rr,r} + \frac{1}{r}\sigma_{rr} + \frac{1}{r}\sigma_{r\theta,\theta} + \sigma_{rz,z} \qquad (E.18)$$

and the last term in the second bracket of E.7 becomes

$$\frac{\partial}{\partial z}(\nabla \cdot \underset{\sim}{\sigma}_r) = \sigma_{rr,z} + \frac{1}{r}\sigma_{rr,z} + \frac{1}{r}\sigma_{r\theta,\theta z} + \sigma_{rz,zz} \qquad (E.19)$$

Substituting E.10, E.12, E.13, E.16, E.17, E.11, and E.19 in that order, term by term, into E.7 yields

$$\frac{\partial}{\partial\theta}\left(\frac{\Omega_\theta}{q}\right) = -\frac{2}{q^2}\left[\left(\sigma_{zr,r} + \frac{1}{r}\sigma_{zr} + \frac{1}{r}\sigma_{z\theta,\theta} + \sigma_{zz,z}\right)\right]$$

$$+ \frac{r}{q^2}\left[\left(-\sigma_{\theta\theta,z}\right) - \left(\sigma_{zr,rr} + \frac{1}{r}\sigma_{zr,r} - \frac{1}{r^2}\sigma_{zr} - \frac{1}{r^2}\sigma_{z\theta,\theta}\right.\right.$$

$$+ \frac{1}{r}\sigma_{z\theta,\theta r} + \sigma_{zz,zr}\Big) + \left(\sigma_{rr,rz} + \frac{1}{r}\sigma_{rr,z} + \frac{1}{r}\sigma_{r\theta,\theta z}\right.$$

$$\left.\left. + \sigma_{rz,zz}\right)\right] \qquad \text{(E.20)}$$

APPENDIX F

CRITICAL VELOCITY IN CURVED CHANNEL

The critical velocity for laminar flow in a curved channel to develop a secondary flow was given by Reid (12). Upon reaching the critical velocity, the laminar flow should become unstable and a streamwise component of vorticity should appear. Reid's analysis has been verified by other theoretical predictions (13,30) and has received a tentative experimental confirmation (32). The critical velocity relation from Reid is:

$$\frac{V_c d}{\nu} = 36\sqrt{\frac{a}{d}}$$

where V_c = critical mean velocity

d = width of the channel

a = radius of curvature of inner wall

ν = kinematic viscosity

In the experimental apparatus used in this study, the parameters influencing the critical velocity are:

$$a = 2" = 1/6 \text{ ft}$$

$$d = 3/8" = \frac{3}{8 \times 12} = \frac{1}{32} \text{ ft}$$

$$\nu = 1.059 \times 10^{-5} \text{ ft}^2/\text{sec} \quad \text{(water at 70°F)}$$

and from which

$$V_c = \frac{1.059 \times 10^{-5} \frac{ft}{sec}}{1/32} 36\sqrt{\frac{2}{3/8}}$$

$$= 0.0282 \text{ fps} = 1.69 \text{ ft/min}$$

LITERATURE CITED

1. E. Brundrett and W. D. Baines, "The Production and Diffusion of Vorticity in Duct Flow," Journal of Fluid Mechanics, Vol. 19, (1964), p. 375.

2. H. B. Squire and K. G. Winter, "The Secondary Flow in a Cascade of Airfoils in a Nonuniform Stream," Journal of Aeronautical Science, Vol. 18, (1951), p. 271.

3. W. R. Hawthorne, "Secondary Circulation in Fluid Flow," Proceedings of The Royal Society, London, Series A, Vol. 206, (1951), p. 374.

4. A. W. Marris, "The Generation of Secondary Vorticity in an Incompressible Fluid," Transactions of the American Society of Mechanical Engineers, Series E, Vol. 30, (1964), p. 522.

5. R. S. Scorer and S. D. R. Wilson, "Secondary Instability in Steady Gravity Waves," Quarterly Journal of the Royal Meteorological Society, Vol. 89, no 382, (1963), p. 532-539.

6. L. Prandtl, Essentials of Fluid Dynamics, London: Blackie, (1952), p. 145-149.

7. S. Eskinazi and H. Yeh, "An Investigation on Fully Developed Turbulent Flows in a Curved Channel," Journal of the Aeronautical Sciences, Vol. 23, (1956), p. 23.

8. F. B. Gessner and J. B. Jones, "A Preliminary Study of Turbulence Characteristics of Flow Along a Corner," Transactions of the American Society of Mechanical Engineers, Series D, Vol. 83, (1961), p. 657-662.

9. J. W. Elder, "The Flow Past a Flat Plate of Finite Width," Journal of Fluid Mechanics, Vol. 9, (1960), p. 133.

10. C. Truesdell, The Kinematics of Vorticity, Bloomington: Indiana University Press, (1954), p. 13, 14.

11. C. C. Lin, The Theory of Hydrodynamic Stability, Cambridge: Cambridge University Press, (1955).

12. W. H. Reid, "On the Stability of Viscous Flow in a Curved Channel," Proceedings of the Royal Society, London, Series A, Vol. 244, (1958), p. 186.

13. R. C. DiPrima, "The Stability of Viscous Flow Between Rotating Concentric Cylinders With a Pressure Gradient Acting Round the Cylinders," Journal of Fluid Mechanics, Vol. 6, (1959), p. 462.

14. S. Chandrasekhar, Hydrodynamic and Hydromagnetic Stability, Oxford: The Clarendon Press, (1961).

15. A. W. Marris, "On the Generation of Secondary Velocity Along a Vortex Line," Transactions of the American Society of Mechanical Engineers, Series D, Vol. 86, (1964), p. 815.

16. P. M. Morse and H. Feshback, Methods of Theoretical Physics, New York: McGraw-Hill, (1953), Part I.

17. A. W. Marris, "Bending of Streamlines Toward Vortex Lines," Transactions of the American Society of Mechanical Engineers, Series E, Vol. 87, (1965), p. 203.

18. W. R. Hawthorne, "The Growth of Secondary Circulation in Frictionless Flow," Proceedings of Cambridge Phil. Society, Vol. 51, (1955), p. 737.

19. W. R. Hawthorne, "Engineering Aspects," Research Frontiers in Fluid Dynamics, Edited by R. J. Seager and G Temple, Interscience Publishers, (1965), Chp. 1, p. 1-28.

20. A. W. Marris, "The General Theory of Steady-State Generation of Secondary Vorticity," To be published.

21. A. G. Smith, "On the Generation of the Steamwise Component of Vorticity, for Flow in Rotating Channels," City and Guilds College, ASTIA Doucument, AD203581, (September 15, 1955).

22. G. O. Ellis, "A Study of Induced Vorticity in Centrifugal Compressors," Transactions of the American Society of Mechanical Engineers, Series A, Vol. 86, (1964), p. 63.

23. A. C. Eringen, Nonlinear Theory of Continuous Media, New York: McGraw-Hill, (1962).

24. O. Bjørgum, "On Beltrami Vector Fields and Flows," Part I, University Bergen Arbok, (1951), Naturv. Rekke No. 1, p. 1.

25. J. H. Preston, "A Simple Approach to the Theory of Secondary Flows," The Aeronautical Quarterly, Vol. V, (1954), p. 218.

26. P. S. Klebanoff, "Characteristics of Turbulence in a Boundary Layer with Zero Pressure Gradient," NACA Report 1247, (1955).

27. S. J. Kline and P. W. Runstadler, "Some Preliminary Results of Visual Studies of the Wall Layers of the Turbulent Boundary Layer," Transactions of the American Society of Mechanical Engineers, Series E, Vol. 81, (1959), p. 166.

28. K. A. Meyer and S. J. Kline, "A Visual Study of the Flow Model in the Later Stages of Laminar-Turbulent Transition on a Flat Plate," AFOSR-TN-1875, (1961).

29. S. Goldstein, Modern Developments in Fluid Dynamics, New York: Dover Publications, Inc., (1965), Vol. I.

30. W. R. Dean, "Fluid Motion in a Curved Channel" Proceedings of the Royal Society, London, Series A, Vol. 121, (1928), p. 402.

31. G. I. Taylor, "Stability of a Viscous Liquid Contained Between Two Rotating Cylinders," Phil. Transactions of the Royal Society, London, Series A, Vol. 223, (1923), p. 289.

32. Brewster, Grossberg and Nissan, "The Stability of Viscous Flow Between Horizontal Concentric Cylinders," Proceedings of the Royal Society, London, Series A, Vol. 251, (1959), p. 76.

33. E. W. Geller, "An Electrochemical Method of Visualizing the Boundary Layer," M. S. Thesis, Aeronautical Engineering Department, Mississippi State College, August, 1954.

34. D. W. Clutter and A. M. O. Smith, "Flow Visualization by Electrolysis of Water," Aerospace Engineering, Vol. 20, (1961), p. 24.

35. F. A. Schraub, S. J. Kline, J. Henry, P. W. Runstadler, Jr., A. Littell, "Use of Hydrogen Bubbles for Quantitative Determination of Time-Dependent Velocity Fields in Low-Speed Water Flows," Transactions of the American Society of Mechanical Engineers, Series D, Vol. 87, (1965).

VITA

William Baxter Swim was born in Stillwater, Oklahoma, on November 18, 1931. He attended elementary and high school in Stillwater and was graduated from Stillwater High School in 1949. He entered Oklahoma State University the same year. After completing the freshman year, he served 22 months in the Infantry from September 1950 to July 1952. He resumed his studies at Oklahoma State and was graduated in January 1955, receiving the degree of Bachelor of Science in Mechanical Engineering.

After graduation, Mr. Swim was employed by Pennsylvania State University as an Instructor in Mechanical Engineering from January 1955 to 1959. During this employment, he took part-time graduate study in Mechanical Engineering. In 1959 he accepted a position as Instructor in Engineering Research at Oklahoma State University. He held this position until he resumed his advanced studies at Georgia Institute of Technology in September, 1961. As a Ford Foundation Fellow, Mr. Swim majored in Mechanical Engineering. In 1964 he accepted his present position, Senior Research Engineer with the Trane Company.

Mr. Swim was married in 1954 to the former Mary Jeanette Wiley. They have two daughters and three sons.